Fluid Flow Phenomena in Materials Processing—The 2000 Freeman Scholar Lecture

Yogesh Jaluria
Fellow ASME,
Department of Mechanical
and Aerospace Engineering,
Rutgers, the State University of New Jersey,
New Brunswick, NJ 08903
e-mail: jaluria@jove.rutgers.edu

There has been an explosive growth in the development of new materials and processing techniques in recent years to meet the challenges posed by new applications arising in electronics, telecommunications, aerospace, transportation, and other new and traditional areas. Semiconductor and optical materials, composites, ceramics, biomaterials, advanced polymers, and specialized alloys are some of the materials that have seen intense interest and research activity over the last two decades. New approaches have been developed to improve product quality, reduce cost, and achieve essentially custom-made material properties. Current trends indicate continued research effort in materials processing as demand for specialized materials continues to increase. Fluid flow that arises in many materials processing applications is critical in the determination of the quality and characteristics of the final product and in the control, operation, and optimization of the system. This review is focused on the fluid flow phenomena underlying a wide variety of materials processing operations such as optical fiber manufacture, crystal growth for semiconductor fabrication, casting, thin film manufacture, and polymer processing. The review outlines the main aspects that must be considered in materials processing, the basic considerations that are common across fluid flow phenomena involved in different areas, the present state of the art in analytical, experimental and numerical techniques that may be employed to study the flow, and the effect of fluid flow on the process and the product. The main issues that distinguish flow in materials processing from that in other fields, as well as the similar aspects, are outlined. The complexities that are inherent in materials processing, such as large material property changes, complicated domains, multiple regions, combined mechanisms, and complex boundary conditions are discussed. The governing equations and boundary conditions for typical processes, along with important parameters, common simplifications and specialized methods employed to study these processes are outlined. The field is vast and it is not possible to consider all the different techniques employed for materials processing. Among the processes discussed in some detail are polymer extrusion, optical fiber drawing, casting, continuous processing, and chemical vapor deposition for the fabrication of thin films. Besides indicating the effect of fluid flow on the final product, these results illustrate the nature of the basic problems, solution strategies, and issues involved in the area. The review also discusses present trends in materials processing and suggests future research needs. Of particular importance are well-controlled and well-designed experiments that would provide inputs for model validation and for increased understanding of the underlying fluid flow mechanisms. Also, accurate material property data are very much needed to obtain accurate and repeatable results that can form the basis for design and optimization. There is need for the development of innovative numerical and experimental approaches to study the complex flows that commonly arise in materials processing. Materials processing techniques that are in particular need of further detailed work are listed. Finally, it is stessed that it is critical to understand the basic mechanisms that determine changes in the material, in addition to the fluid flow aspects, in order to impact on the overall field of materials processing. [DOI: 10.1115/1.1350563]

Introduction

One of the most crucial and active areas of research in fluids engineering today is that of materials processing. With growing international competition, it is imperative that the present processing techniques and systems are optimized and the quality of the final product is improved. In addition, new materials and processing methods are needed to meet the growing demand for special material properties in new and emerging applications related to diverse fields such as environment, energy, bioengineering, transportation, communications, and computers.

Fluids engineering is extremely important in a wide variety of materials processing systems such as crystal growing, casting, chemical vapor deposition, soldering, welding, extrusion of plastics, food and other polymeric materials, injection molding, spray coating, glass fiber drawing, and composite materials fabrication. The flows that arise in the molten material in crystal growing, for instance, strongly affect the quality of the crystal and, thus, of the semiconductors fabricated from the crystal. Therefore, it is important to understand these flows and obtain methods to minimize or control their effects. Similarly, the flow of molten metal in welding and soldering is often determined mainly by surface tension effects. On the other hand, the profile in the neck-down region of glass in an optical fiber drawing process is largely governed by the viscous flow of molten glass and by gravity. The buoyancy-driven flows generated in the liquid melt in casting processes strongly influence the microstructure of the casting and the shape, movement and other characteristics of the solid-liquid interface.

Contributed by the Fluids Engineering Division for publication in the JOURNAL OF FLUIDS ENGINEERING. Manuscript received by the Fluids Engineering Division Dec. 18, 2000. Associate Editor: Joseph Katz.

In chemical vapor deposition, the flow is of paramount importance in determining the deposition rate and uniformity, which in turn affect the quality of the thin film produced. The flows in furnaces and ovens used for heat treatment and drying strongly influence the transport rates and the migration of impurities that affect quality. The formation of metal droplets and the flow in sprays are important in rapid fabrication using spray deposition. Therefore, it is important to determine the nature, magnitude and behavior of the flows that arise in these processes, their effect on the transport and the ultimate effect on the product quality and system performance.

Because of the importance of fluid flow in materials processing, extensive work is presently being directed at this area. But what is missing is the link between the diverse processing techniques and the basic mechanisms that govern the flow. Much of the effort is concerned with specific manufacturing systems, problems and circumstances. It is important to extract the main underlying features, with respect to fluids engineering, from these studies in order to expand the applicability of the techniques developed and the results obtained. It is also important to couple the microscale mechanisms that determine material characteristics with the fluid flow that occurs at the macroscale level. Another aspect that is lacking in the literature is quantitative information on the dependence of product quality, process control and optimization on the fluid flow. It is critical to determine how fluid flow affects, for instance, the growth of defects in an optical fiber or in a crystal. It is necessary to establish the present state of the art in fluid flow phenomena in materials processing. It is also important to determine the research needs in this area so that future efforts may be directed at critical issues. The coupling between practical engineering systems and the basic fluid mechanics is another very important aspect that should be considered, so that the current and future practice of fluids engineering have a strong impact in an area that is of particular importance today.

This review paper is directed at these important issues, focusing on the fluid flow that is involved with materials processing and linking it with the characteristics of the product and with the system for a wide variety of important practical processes. A range of processes are considered in order to determine the basic aspects that arise and their effect on the processed material. Interest lies mainly in the basic fluid phenomena, rather than in the complexities of the different processes. Because of the importance of this field today and in the future, a summary of the state of the art on this topic will make a very significant and timely contribution to the current and future efforts in materials processing, an area which encompasses a wide range of real problems of fluids-engineering interest.

The three main aspects that are considered in this paper are:

1 Basic fluid flow phenomena underlying materials processing, including non-Newtonian flows, free surface flows, surface tension driven flows, flows with phase change and chemical reactions, flow in sprays, flows under microgravity conditions, and other specialized flows that are of particular interest in this field.

2 Influence of fluid flow on the characteristics of the final product, in terms of consistency, uniformity, defect formation and concentration, and other relevant measures, as well as the rate of fabrication.

3 Coupling between fluid flow and the operation, design and optimization of the system, considering a range of practical and important processes for the fabrication of traditional and advanced materials.

Materials Processing

In the last two decades, there has been a tremendous growth in new materials with a wide variety of properties and characteristics. Such advanced and new materials include composites, ceramics, different types of polymers and glass, coatings, and many specialized alloys and semiconductor materials. By an appropriate combination and processing of materials, a very wide range of desired material characteristics can be obtained. The choice or, in many cases, design of an appropriate material for a given application has become a very important consideration in the design and optimization of processes and systems, as discussed by Jaluria [1]. Thus, new techniques have been developed and are used along with the classical techniques of materials processing, such as heat treatment, forming and casting, to obtain the desired properties in the chosen material. Consequently, a consideration of the processing of traditional, as well as advanced and emerging, materials involves both classical and new procedures, with a strong emphasis on the link between the resulting material properties and the process used.

Table 1 Different types of materials processing operations, along with examples of commonly used processes

1.	Processes With Phase Change casting, continuous casting, crystal growing, drying
2.	Heat Treatment annealing, hardening, tempering, surface treatment, curing, baking
3.	Forming Operations hot rolling, wire drawing, metal forming, extrusion, forging
4.	Cutting laser and gas cutting, fluid jet cutting, grinding, machining
5.	Bonding Processes soldering, welding, explosive bonding, chemical bonding
6.	Polymer Processing extrusion, injection molding, thermoforming
7.	Reactive Processing chemical vapor deposition, food processing
8.	Powder Processing powder metallurgy, sintering, sputtering
9.	Glass Processing optical fiber drawing, glass blowing, annealing
10.	Coating thermal spray coating, polymer coating
11.	Other Processes composite materials processing, microgravity materials processing

Fluid flow considerations are important in a wide variety of manufacturing processes. Some of the ways in which the flow affects the process are

1 Effect on the underlying transport mechanisms
2 Generation and distribution of impurities and defects
3 Mixing of different components in the material
4 Time spent by the material in the system
5 Process instability and feasibility
6 Shape of processed material
7 Properties and characteristics of the final product
8 Rate of fabrication
9 Product quality

A few important processes in which fluid flow plays a very important role are summarized in Table 1. Several manufacturing processes, in which the flow is of particular importance, are also sketched in Fig. 1. These include the optical glass fiber drawing process in which a specially fabricated glass preform is heated and drawn into a fiber, continuous casting which involves solidification of a liquid over an essentially stationary interface, mold casting in an enclosed region with time-dependent liquid-solid interface location, and screw extrusion in which materials such as plastics are melted and forced through an appropriate die to obtain specific dimensions and shape. Figure 2 shows a few common materials processing techniques used in the fabrication of electronic devices. The processes shown include Czochralski crystal growing in which molten material such as silicon is allowed to solidify across an interface as a seed crystal is withdrawn, the floating-zone method in which a molten zone is established between a polycrystalline charge rod and a crystalline rod, soldering to form solder coating or solder joints, and thin film fabrication by chemical vapor deposition (CVD). In all these processes, the quality and characteristics of the final product and the rate of fabrication are strong functions of the underlying fluid flow.

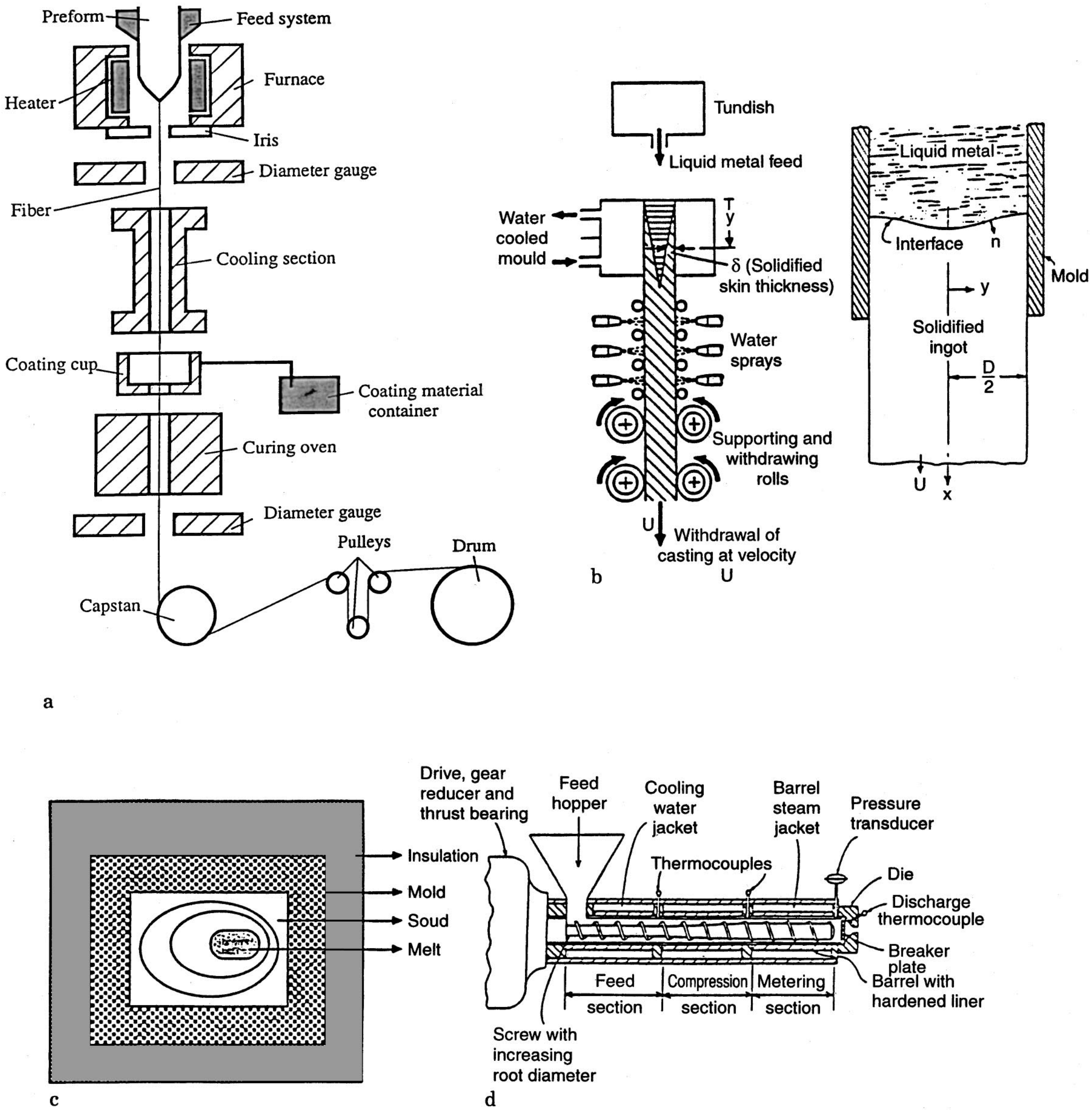

Fig. 1 Sketches of a few common manufacturing processes that involve the flow of the material being processed. (*a*) optical fiber drawing; (*b*) continuous casting; (*c*) mold casting; (*d*) plastic screw extrusion

Because of the importance of materials processing, considerable research effort has been directed in recent years at the transport phenomena in such processes. Many books concerned with the area of manufacturing and materials processing are available. However, most of these discuss important practical considerations and manufacturing systems relevant to the various processes, without considering in detail the underlying transport and fluid flow. See, for instance, the books by Doyle et al. [2], Schey [3] and Kalpakjian [4]. A few books have been directed at the fundamental transport mechanisms in materials processing, for instance, the books by Szekely [5] and by Ghosh and Mallik [6]. The former considers fluid flow in metals processing and presents both the fundamental and applied aspects in this area. Some other books consider specific manufacturing processes from a fundamental standpoint, see the books by Avitzur [7], Altan et al. [8], Fenner [9] and Easterling [10]. In addition, there are several review articles and symposia volumes on fluid flow and thermal transport in materials processing. Examples of these are the books edited by Hughel and Bolling [11], Kuhn and Lawley [12], Chen et al. [13], Li [14], and Poulikakos [15], and the review article by Viskanta [16].

Many important considerations arise when dealing with the mathematical and numerical modeling of the fluid flow and the associated transport in the processing of materials, as presented in Table 2. Many of the relevant processes are time-dependent, since the material must often undergo a given variation with time of the temperature, pressure, shear and other such variables in order to attain desired characteristics. Sometimes, a transformation of the variables in the problem can be used to convert a time-dependent problem to a steady one. Most manufacturing processes involve combined modes of transport. Conjugate conditions usually arise due to the coupling between transport in the solid material and-fluid flow. Thermal radiation is frequently important in these processes. The material properties are often strongly dependent on temperature, concentration, and pressure, giving rise to strong nonlinearity in the governing equations [17,18]. Also, the material

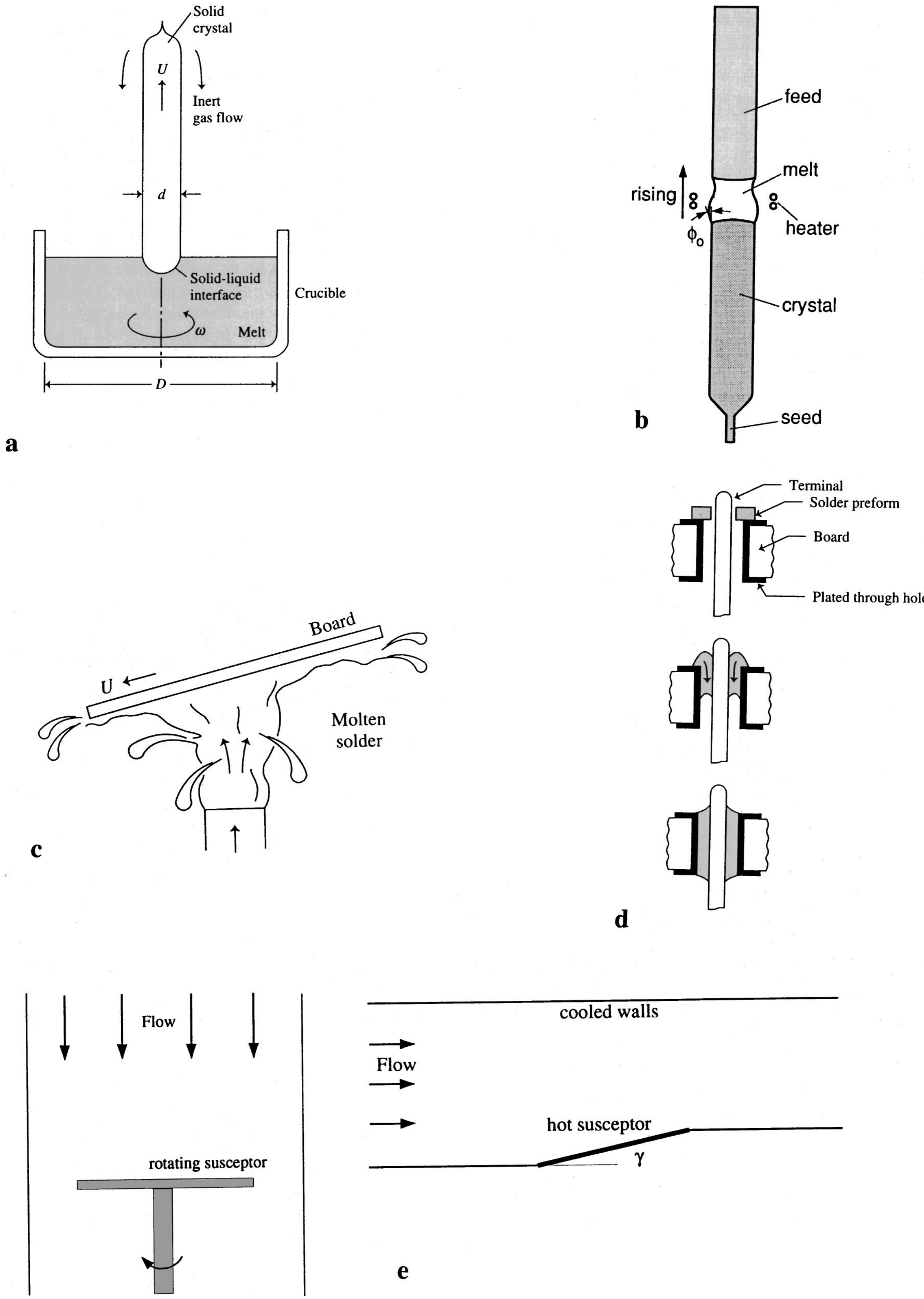

Fig. 2 Sketches of a few processes used for the manufacture of electronic devices. (*a*) Czochralski crystal growing; (*b*) floating-zone method for crystal growth; (*c*) wave soldering; (*d*) solder joint formation; (*e*) chemical vapor deposition

properties may depend on the shear rate, as is the case for polymeric materials which are generally non-Newtonian [9,19]. The material properties affect the transport processes and are, in turn, affected by the transport. This aspect often leads to considerable complexity in the mathematical modeling, as well as in the numerical simulation. The material undergoing the transport process may be moving, as in hot rolling or extrusion [20], or the energy or mass source itself may be moving, as in laser cutting or welding. Additional mechanisms such as surface tension and chemical reactions are important in many cases. Complex geometry and

Table 2 Some of the important considerations in fluid flow associated with materials processing

1. Coupling of Transport With Material Characteristics different materials, properties, behavior, material structure
2. Variable Material Properties strong variation with temperature, pressure and concentration
3. Complex Geometries complicated domains, multiple regions
4. Complicated Boundary Conditions conjugate conditions, combined modes
5. Interaction Between Different Mechanisms surface tension, heat and mass transfer, chemical reactions, phase change
6. Micro-Macro Coupling micro-structure changes, mechanisms operating at different length and time scales
7. Complex Flows non-Newtonian flows, free surface flows, powder and particle transport
8. Inverse Problems non-unique multiple solutions, iterative solution
9. Different Energy Sources laser, chemical, electrical, gas, fluid jet, heat
10. System Optimization and Control link between flow and system

boundary conditions are commonly encountered. Multiple, coupled, regions with different material properties arise in many cases. Frequently, an inverse problem is to be solved to obtain the conditions that result in a desired flow or temperature variation with time and space. Finally, the process is linked with the manufacturing system design, control, and optimization.

All these considerations make the mathematical and numerical modeling of materials processing very involved and challenging. Special procedures and techniques are often needed to satisfactorily simulate the relevant boundary conditions and material property variations. The results obtained are important and interesting, since these are generally not available in the existing fluid mechanics and heat and mass transfer literature. The results from the simulation provide appropriate inputs for the design and optimization of the relevant system. Experimental techniques and results are also closely linked with the mathematical modeling in order to simplify the experiments and obtain characteristic results in terms of important dimensionless parameters. Also, experimental results are of critical value in validating mathematical and numerical models, as well as in providing the physical insight needed for model development.

It must be noted that even though research on the fluid flow phenomena associated with materials processing can be used to provide important inputs to the area, it is necessary for researchers working in fluids engineering to thoroughly understand the concerns, intricacies and basic considerations that characterize materials processing in order to make a significant impact on the field. Otherwise, basic research serves only in a supporting capacity in this important field. The dependence of the characteristics of the final product on the flow must be properly understood and characterized so that analysis or experimentation can be used to design processes to achieve desired product characteristics and production rates. This is the only way research on fluid flow can stay at the cutting edge of technology in materials processing and significantly affect the future developments in this field.

This paper is concerned with fluid flow phenomena in materials processing. The basic flows that commonly arise in this area are first outlined. The main aspects that are common to many of these processes are outlined next, followed by a discussion of some of the major complexities, and common approaches to obtain the solution, using analytical, numerical and experimental methods. Typical results for several common processing methods for advanced and new materials, as well as for traditional materials, are then presented. These examples serve to indicate common features and considerations in different materials processing techniques. Experimental results are discussed at various stages as a means to validate the models, to provide insight into the underlying phenomena, and to provide inputs on material characteristics, properties and other aspects. Let us first consider the basic flows, followed by a discussion of the conservation principles and the appropriate governing equations for these processes.

Basic Flows

Materials processing involves a very wide range of problems in which fluids engineering is of particular interest. It is very important that a review of this area cover this diversity and extract the basic fluid flow phenomena that arise and affect the final product and the design of the relevant system. This is a fairly involved task because of different types of processes employed and the intrinsic complexity of each process. However, fluid flow mechanisms are similar in many cases and the basic techniques that apply in one case may be applied to another.

Some of the basic flows that arise in materials processing, along with the important considerations that are involved, are listed below:

1 Buoyancy-Driven Flows. This involves a consideration of the magnitude and nature of the buoyancy-induced flow, such as that in the melt regions sketched in Figs. 1(*c*) and 2(*a*). The dependence of this flow on the parameters of the problem such as material properties, boundary conditions and geometry must be determined. The effect of this flow on the rate of phase change, on the characteristics of the solid-liquid interface, and on the migration of impurities is important in casting and crystal growing. The modeling of the mushy (liquid-solid mixture) region is of interest for alloy and mixture solidification. Similarly, buoyancy effects arise in other materials processing techniques such as chemical vapor deposition, soldering, welding, and laser melting.

2 Non-Newtonian Flows. These flows, in which the viscosity of the fluid is dependent on the flow through the shear rate, are particularly important in the processing of plastics and other polymeric materials in processes such as extrusion, sketched in Fig. 1(*d*), and injection molding. Non-Newtonian behavior substantially complicates the solution for the flow. Additional complexities arise due to strong temperature dependence of properties, phase and structural changes, and viscous dissipation effects due to the typically large viscosities of these fluids. An important element in these processes is the nature of fluid mixing that arises due to shear and possible chaotic behavior of the flow.

3 Surface Tension Driven Flows. These flows are relevant to many materials processing techniques. The flow of molten metal in welding and soldering is largely driven by surface tension, see Fig. 2(*d*). Under microgravity conditions, such as those in space applications, surface tension effects become particularly important in processes such as crystal growing and solidification due to the reduction in the buoyancy force. Marangoni convection, that arises due to the variation of surface tension with temperature and concentration, is of particular interest in these circumstances. Materials processing in space is an important research area today because of the need to improve the quality of materials such as crystals by reducing the buoyancy-induced flow and its effects.

4 Particulate Flows. Many materials processing circumstances involve particle motion, for instance, spray coating and chemical vapor deposition, sketched in Fig. 2(*e*). Also, the characteristics of mixing and of impurity migration involve particle motion. The particles are driven by the flow and particle trajectories are obtained, often by the use of a Lagrangian approach, to characterize the process. An example of this consideration is the behavior of impurities in a solidifying material. Similarly, mixing in food extrusion is a very important consideration in the determination of the quality of the extruded product.

5 Flow of Powdery Materials. This is an important aspect in many materials processing applications, ranging from powder metallurgy to the processing of food and pharmaceutical materials. Powders are conveyed along channels in these processes with compaction arising due to the rise in pressure and heating due to friction. The flow of such materials and the compaction process are not very well understood at the present time, though some recent work has been directed at this problem due to its practical importance.

6 Flows With Combined Transport Mechanisms. In many cases, the flow is driven or influenced by combined effects of heat and mass transfer and this flow, in turn, affects the resulting transport rates. Reactive polymers involve chemical reactions, which affect the concentration and impart energy changes to the system. Similarly, moisture transport is very important in food processing since the moisture concentration substantially affects the properties of the fluid. Drying processes also involve combined transport mechanisms. The quality and productivity of thin films fabricated by chemical vapor deposition are determined by the interaction between the flow and the chemical reactions at the surface and in the gases. Therefore, such multi-species and multimode transport processes must be studied in order to understand the basic mechanisms involved and to determine the flow and transport in practical circumstances.

7 Fluid Flow in Coating Processes. An important materials processing technique is coating. Optical fibers are coated by polymers to impart strength to the fiber. Surfaces are commonly coated to increase their resistance to corrosive environments. A wide variety of materials, ranging from polymers to metals, are used for coating processes. The quality of the coating, particularly trapped bubbles and other imperfections, as well as its thickness are determined by the flow occurring in the coating die and applicator. It is important to understand the basic flow mechanisms involved in this process so that high quality coatings may be achieved at relatively large speeds of the coated material. The problem involves highly viscous flow in complicated channels, as well as menisci on either side of the coating region. Also important is spray coating, which involves droplet formation and the flow in sprays leading to deposition or etching.

8 Flows With Coupling of Micro/Macro Mechanisms. The characteristics and quality of the material being processed are often determined by the microscale transport processes occurring in the material, for instance at the solid-liquid interface in casting or at sites where defects are formed in an optical fiber. However, experiments, modeling and analysis usually consider the macroscale, with practical dimensions, typical physical geometries and appropriate boundaries. It is crucial to link the two approaches so that the appropriate boundary conditions for a desired microstructure can be imposed in a physically realistic system. A considerable interest exists today in this aspect of materials processing, particularly with respect to the underlying fluid mechanics.

9 Other Flows. Several other flows are of interest and importance in materials processing. These include flows with large property variations. This is a very important consideration since it applies to most problems of practical interest, such as those dealing with plastics, glass and ceramics. The temperature, pressure and concentration ranges are often large enough to affect the flow and transport processes very substantially due to strong property variations. Interfacial phenomena are important in continuous casting, crystal growing, among others. Similarly, free surface flows arise in material emerging from an extrusion process, wire and fiber drawing through a neck-down region, and use of fluid jets for cutting or heating. Another important area is that of radiation-correction coupled flows. Such flows arise, for instance, in furnaces and substantially affect the relevant processing techniques. Many of these flows are considered in greater detail in the following sections.

The preceding list indicates the wide range of flows that typically arise in materials processing. However, in most manufacturing processes, a combination of different flows is encountered making the analysis and simulation very complicated. This is illustrated by taking various examples of important practical manufacturing systems later in the review.

Basic Considerations and Governing Equations

General Equations. The governing equations for fluid flow and the associated heat transfer in materials processing are derived from the basic conservation principles for mass, momentum and energy. For a pure viscous fluid, these equations may be written as

$$\frac{D\rho}{Dt}+\rho\nabla.\overline{V}=0 \tag{1}$$

$$\rho\frac{D\overline{V}}{Dt}=\overline{F}+\nabla.\underline{\underline{\tau}} \tag{2}$$

$$\rho\, Cp\frac{DT}{Dt}=\nabla.(k\nabla T)+\dot{Q}+\beta T\frac{Dp}{Dt}+\mu\Phi \tag{3}$$

Here, D/Dt is the substantial or particle derivative, given in terms of the local derivatives in the flow field by $D/Dt=\partial/\partial t+\overline{V}.\nabla$. The other variables are defined in the Nomenclature.

For a solid, the energy equation is written as

$$\rho\, C\frac{DT}{Dt}=\frac{\partial T}{\partial t}+\overline{V}.\nabla T=\nabla.(k\nabla T)+\dot{Q} \tag{4}$$

where C is the specific heat of the solid material, the specific heat at constant pressure and at constant volume being essentially the same. For a stationary solid, the convection term drops out and the particle derivative is replaced by the transient term $\partial/\partial t$. In a deforming solid, as in wire drawing, extrusion or fiber drawing, the material is treated as a fluid, with an appropriate constitutive equation, and the additional terms due to pressure work and viscous heating are generally included. In the preceding equations, the material is taken as isotropic, with the properties assumed to be the same in all directions. For certain materials such as composites, the nonisotropic behavior must be taken into account.

The stress tensor in Eq. (2) can be written in terms of the velocity $\overline{V}$ if the material characteristics are known. For instance, if μ is taken as constant for a Newtonian fluid, the relationship between the shear stresses and the shear rates, given by Stokes, are employed to yield

$$\rho\frac{D\overline{V}}{Dt}=\overline{F}-\nabla p+\mu\nabla^2\overline{V}+\frac{\mu}{3}\nabla(\nabla.\overline{V}) \tag{5}$$

Here, the bulk viscosity $K=\lambda+(2/3)\mu$ is taken as zero. For an incompressible fluid, ρ is constant, which gives $\nabla\cdot\overline{V}=0$ from Eq. (1). Then, the last term in Eq. (5) drops out.

Buoyancy Effects. The body force $\overline{F}$ is also important in many manufacturing processes, such as crystal growing and casting where it gives rise to the thermal or solutal buoyancy term. The governing momentum equation is obtained from Eq. (5), when thermal buoyancy is included, as

$$\rho\frac{D\overline{V}}{Dt}=-\overline{e}g\rho\beta(T-T_a)-\nabla p_d+\mu\nabla^2\overline{V} \tag{6}$$

where p_d is the dynamic pressure, obtained after subtracting out the hydrostatic pressure p_a. Therefore, p_d is the component due to fluid motion, as discussed by Jaluria [21] and Gebhart et al. [22]. Boussinesq approximations, that neglect the effect of the density variation in the continuity equation and assume a linear variation of density with temperature, are employed here. However, in many practical cases, these approximations cannot be used and the solution is more involved. If the x coordinate axis is taken as vertical, the buoyancy term appears only in the x component of the momentum equation. The governing equations are coupled because of the buoyancy term in Eq. (6) and must be solved simultaneously. This differs from the forced convection problem with constant fluid properties, for which the flow is independent of the temperature and may be solved independently before solving the energy equation [23].

Viscous Dissipation. The viscous dissipation term $\mu\Phi$ in Eq. (3) represents the irreversible part of the energy transfer due to the stress. Therefore, viscous dissipation gives rise to a thermal source in the flow and is always positive. For a Cartesian coordinate system, Φ is given by the expression

$$\Phi = 2\left[\left(\frac{\partial u}{\partial x}\right)^2 + \left(\frac{\partial v}{\partial y}\right)^2 + \left(\frac{\partial w}{\partial z}\right)^2\right] + \left(\frac{\partial v}{\partial x} + \frac{\partial u}{\partial y}\right)^2 + \left(\frac{\partial w}{\partial y} + \frac{\partial v}{\partial z}\right)^2 + \left(\frac{\partial u}{\partial z} + \frac{\partial w}{\partial x}\right)^2 - \frac{2}{3}(\nabla.\overline{V})^2 \quad (7)$$

Similarly, expressions for other coordinate systems may be obtained. This term becomes important for very viscous fluids and at high speeds. The former circumstance is of particular interest in the processing of glass, plastics, food, and other polymeric materials.

Processes With Phase Change. Many material processing techniques involve a phase change. Examples of such processes are crystal growing, casting, and welding. For such problems, there are two main approaches for numerical simulation. The first one treats the two phases as separate, with their own properties and characteristics. The interface between the two phases must be determined so that conservation principles may be applied there and appropriate discretization of the two regions may be carried out [15,24]. This becomes fairly involved since the interface location and shape must be determined for each time step or iteration. The governing equations are the same as those given earlier for the solid and the liquid.

In the second approach, the conservation of energy is considered in terms of the enthalpy H, yielding the governing energy equation as

$$\rho\frac{DH}{Dt} = \rho\frac{\partial H}{\partial t} + \rho\overline{V}.\nabla H = \nabla.(k\nabla T) \quad (8)$$

where each of the phase enthalpies H_i is defined as

$$H_i = \int_0^T C_i dT + H_i^0 \quad (9)$$

C_i being the corresponding specific heat and H_i^0 the enthalpy at 0 K. Then, the solid and liquid enthalpies are given by, respectively,

$$H_s = C_s T \quad H_1 = C_1 T + [(C_s - C_1)T_m + L_h] \quad (10)$$

where L_h is the latent heat of fusion and T_m the melting point. The continuum enthalpy and thermal conductivity are given, respectively, as

$$H = H_s + f_1(H_1 - H_s) \quad k = k_s + f_1(k_1 - k_s) \quad (11)$$

where f_1 is the liquid mass fraction, obtained from equilibrium thermodynamic considerations. The dynamic viscosity μ is expressed as the harmonic mean of the phase viscosities, employing the limit $\mu_s \to \infty$, i.e., $\mu = \mu_1/f_1$. This model smears out the discrete phase transition in a pure material. But the numerical modeling is much simpler since the same equations are employed over the entire computational domain and there is no need to keep track of the interface between the two phases [25–27]. In addition, impure materials, mixtures and alloys can be treated very easily by this approach. Figure 3 shows examples of the two approaches outlined here for numerical modeling, indicating a single domain for the enthalpy method and the interface between the two regions for the two-phase approach.

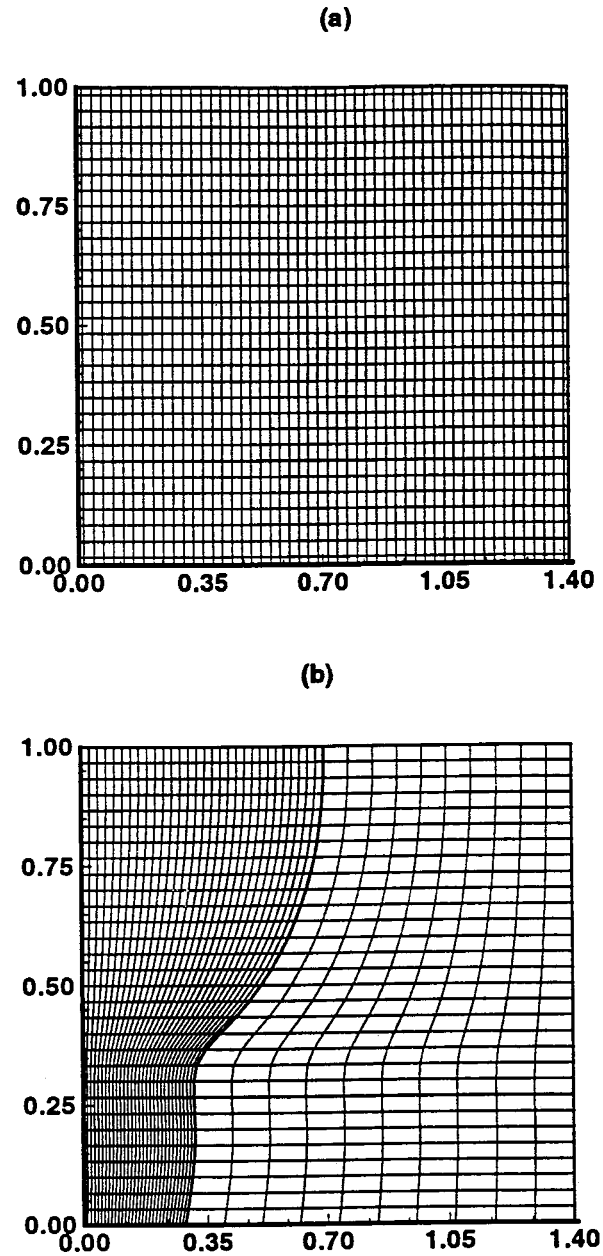

Fig. 3 Numerical grids used for the (*a*) enthalpy method (single region) and (*b*) the two-phase (two region) method

Chemically Reactive Flows. Combined thermal and mass transport mechanisms are important in many materials processing circumstances, such as chemical vapor deposition and processing of food, reactive polymers, and several other materials with multiple species. Extrusion is an important manufacturing technique for thermal processing of food materials, particularly snacks, cereals, pasta, and bread substitutes. Various starches, wheat, rice flour and other materials, along with a chosen amount of water, are fed into the hopper and cooked through the input of shear and heat to obtain different extruded products, see Harper [28] and Kokini et al. [29]. Chemical reactions occur in food materials and other chemically reactive materials to substantially alter the structure and characteristics of the product. Chemical reactions and conversion are also important in the curing of polymers, for example, in surface coating and chemical bonding.

A simple approach to model the chemical conversion process in reactive materials, such as food, in order to determine the nature and characteristics of the extruded material is outlined here. The governing equation for chemical conversion may be given as [30]

$$\frac{d}{dt}[(1-\tilde{X}]=-K(1-\tilde{X})^m \tag{12}$$

where $\tilde{X}$ is the degree of conversion, defined as,

$$\tilde{X}=\frac{M_i-M_t}{M_i-M_f} \tag{13}$$

Here M_i is the initial amount of unconverted material, taken as starch here, M_f is the final amount of unconverted starch and M_t is the amount of unconverted starch at time t. The order of the reaction is m and K is the reaction rate.

The order of the reaction m in Eq. (12) has been shown to be zero for starches and the rate of the reaction K given as a combination of thermal and shear driven convection as [30]

$$K=K_T+K_S \tag{14}$$

where

$$K_T=K_{T0}\exp(-E_T/RT) \quad K_S=K_{S0}\exp(-E_S/\tau\eta) \tag{15}$$

Here, E_τ and E_S are the corresponding activation energies, K_{T0} and K_{S0} are constants, τ is the shear stress, and η is a constant which is obtained experimentally for the material, along with other constants in the equation. A simple approximation may be applied to model the degree of conversion defined in Eq. (12), as given by [31,32]

$$w\frac{d\tilde{X}}{dZ}=K \tag{16}$$

Here, w is the velocity in the down-channel direction Z in an extruder. Thus, numerical results on conversion are obtained by integrating this equation.

Similarly, chemical kinetics play a critical role in the deposition of material from the gas phase in chemical vapor deposition systems [33,34]. The concentrations of the chemical species in the reactor affect the chemical kinetics, which in turn affect the deposition. In many cases, the process is chemical kinetics limited, implying that the transport processes are quite vigorous and the deposition is restricted largely by the kinetics. The chemical kinetics for several materials are available in the literature. For instance, the chemical kinetics for the deposition of Silicon from Silane (SiH_4) with Hydrogen as the carrier gas in a CVD reactor is given by the expression [35]

$$K=\frac{K_0 p_{\mathrm{SiH4}}}{1+K_1 p_{H2}+K_2 p_{\mathrm{SiH4}}} \tag{17}$$

where the surface reaction rate K is in mole of Si/m^{2}s, $K_0=A\exp(-E/RT)$, E being the activation energy, and A, K_1, and K_2 are constants which are obtained experimentally. The p's are the partial pressures of the two species in the reactor.

Material Property Considerations

Variable Properties. The properties of the material undergoing thermal processing play a very important role in the mathematical and numerical modeling of the process, as well as in the interpretation of experimental results. As mentioned earlier, the ranges of the process variables, such as pressure, concentration and temperature, are usually large enough to make it necessary to consider material property variations. The governing equations are Eqs. (1)–(4), which are written for variable properties. Usually, the dependence of the properties on temperature T is the most important effect. Numerical curve fitting may be employed to obtain a given material property as a function of T, as say, $k(T)=k_r[1+a(T-T_r)+b(T-T_r)^2]$, where T_r is a reference temperature at which $k=k_r$. Thus, a continuous function $k(T)$ replaces the discrete data on k at different temperatures [36]. This gives rise to nonlinearity since

$$\frac{\partial}{\partial x}\left[k(T)\frac{\partial T}{\partial x}\right]=\frac{\partial k}{\partial x}\frac{\partial T}{\partial x}+k\frac{\partial^2 T}{\partial x^2}=\frac{\partial k}{\partial T}\left(\frac{\partial T}{\partial x}\right)^2+k(T)\frac{\partial^2 T}{\partial x^2} \tag{18}$$

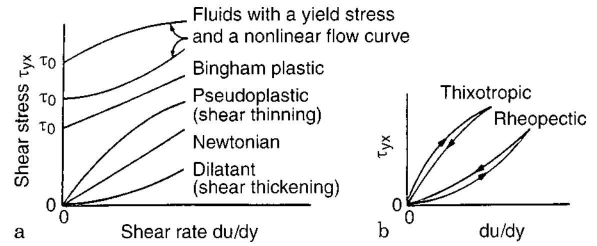

Fig. 4 Plots of shear stress versus shear rate for viscoinelastic non-Newtonian fluids. (*a*) Time-independent, and (*b*) time-dependent fluids.

Similarly, the data for other material properties may be represented by appropriate curve fits. Because of the resulting additional nonlinearity, the solution of the equations and the interpretation of experimental results become more involved than for constant property circumstances. Iterative numerical procedures are often required to deal with such nonlinear problems, as discussed by Jaluria and Torrance [23]. Due to these complexities, average constant property values at different reference conditions are frequently employed to simplify the solution [37]. Similar approaches are used to interpret and characterize experimental data. However, such an approach is satisfactory only for small ranges of the process variables. Most manufacturing processes require the solution of the full variable-property problem for accurate predictions of the resulting transport.

Viscosity Variation. The variation of dynamic viscosity μ requires special consideration for materials such as plastics, polymers, food materials and several oils, that are of interest in a variety of manufacturing processes. Most of these materials are non-Newtonian in behavior, implying that the shear stress is not proportional to the shear rate. The viscosity μ is a function of the shear rate and, therefore, of the velocity field. Figure 4 shows the variation of the shear stress τ_{yx} with the shear rate du/dy for a shear flow such as the flow between two parallel plates with one plate moving at a given speed and the other held stationary. The viscosity is independent of the shear rate for Newtonian fluids like air and water, but increases or decreases with the shear rate for shear thickening or thinning fluids, respectively. These are viscoinelastic (purely viscous) fluids, which may be time-independent or time-dependent, the shear rate being a function of both the magnitude and the duration of shear in the latter case. Viscoelastic fluids show partial elastic recovery on the removal of a deforming shear stress. Food materials are often viscoelastic in nature.

Various models are employed to represent the viscous or rheological behavior of fluids of practical interest. Frequently, the fluid is treated as a Generalized Newtonian Fluid (GNF) with the non-Newtonian viscosity function given in terms of the shear rate which is related to the second invariant of the rate of strain tensor. For instance, time-independent viscoinelastic fluids without a yield stress are often represented by the power-law model, given by [38]

$$\tau_{yx}=K_c\left|\frac{du}{dy}\right|^{n-1}\frac{du}{dy} \tag{19}$$

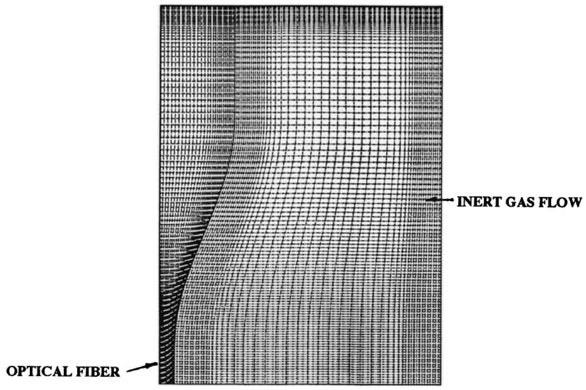

Fig. 5 Grid for the numerical modeling of the two regions, consisting of glass and inert gases, in optical fiber drawing

where K_c is the consistency index and n the power law fluid index. Note that $n=1$ represents a Newtonian fluid. For $n<1$, the behavior is pseudoplastic (shear thinning) and for $n>1$, it is dilatant (shear thickening). The viscosity variation may be written as [38]

$$\mu=\mu_0\left(\frac{\dot{\gamma}}{\dot{\gamma}_0}\right)^{n-1}e^{-b(T-T_0)} \tag{20}$$

where

$$\dot{\gamma}=\left[\left(\frac{\partial u}{\partial y}\right)^2+\left(\frac{\partial w}{\partial y}\right)^2\right]^{1/2}, \text{ with } \tau_{yx}=\mu\frac{\partial u}{\partial y}, \quad \tau_{yz}=\mu\frac{\partial w}{\partial y} \tag{21}$$

for a two-dimensional flow, with u and w varying only with y. Similarly, expressions for other two- and three-dimensional flows may be written. Here $\dot{\gamma}$ is the shear strain rate, the subscript o denotes reference conditions and b is the temperature coefficient of viscosity. Other expressions for the viscosity may be used to consider other reactive and non-reactive polymeric materials.

For food materials, the viscosity is also a strong function of the moisture concentration c_m and is often represented as

$$\mu=\mu_0\left(\frac{\dot{x}}{\dot{\gamma}_0}\right)^{n-1}e^{-b(T-T_0)}e^{-b_m(c_m-c_{m0})} \tag{22}$$

The temperature dependence is also often represented more accurately by an Arrhenius type of variation, i.e.,

$$\mu=\mu_0\left(\frac{\dot{\gamma}}{\dot{\gamma}_0}\right)^{n-1}e^{B/T} \tag{23}$$

In addition, chemical changes, that typically occur at the microscale level in the material, affect the viscosity and other properties. Other models, besides the power-law model, are also employed to represent different materials [19,38–40].

The non-Newtonian behavior of the material complicates the viscous terms in the momentum and the energy equations. For instance, the viscous dissipation term Φ_v for the two-dimensional flow considered earlier for Eq. (21) is

$$\Phi_v=\tau_{yx}\frac{\partial u}{\partial y}+\tau_{yz}\frac{\partial w}{\partial y} \tag{24}$$

where the variation of μ with $\dot{\gamma}$ and, therefore, with the velocity field is taken into account. Similarly, the viscous force term in the momentum equation yields $\partial(\tau_{yx})/\partial y$ in the x-direction, requiring the inclusion of the non-Newtonian behavior of the fluid [40]. Similarly, other flow circumstances may be considered for the flow of non-Newtonian fluids. Viscous dissipation effects are generally not negligible in these flows because of the large viscosity of the fluid.

Glass is another very important, though complicated, material. It is a supercooled liquid at room temperature. The viscosity varies almost exponentially with temperature. In optical fiber drawing, for instance, the viscosity changes through several orders of magnitude in a relatively short distance. This makes it necessary to employ very fine grids and specialized numerical techniques. Figure 5 shows the grid in glass, as well as in the inert gases flowing outside the fiber in a fiber-drawing furnace. Even a change of a few degrees in temperature in the vicinity of the softening point, which is around 1600°C for fused silica, can cause substantial changes in viscosity and thus in the flow field and the neck-down profile in optical fiber drawing. This can lead to a significant effect on defect generation in the fiber and thus on fiber quality [17,18,41].

Other Aspects. There are several other important considerations related to material properties. Constraints on the temperature level in the material, as well as on the spatial and temporal gradients, arise due to the characteristics of the material. In thermoforming, for instance, the material has to be raised to a given temperature level, above a minimum value $T_{\min}$, for material flow to occur in order for the process to be carried out. However, the maximum temperature $T_{\max}$ must not be exceeded to avoid damage to the material. In polymeric materials, $T_{\max}-T_{\min}$ is relatively small and the thermal conductivity k is also small, making it difficult to design a process which restricts the temperature to $T_{\max}$ while raising the entire material to above $T_{\min}$ for material flow to occur. An example of this process is the manufacturing of plastic-insulated wires, as considered by Jaluria [42]. Similarly, constraints on $\partial T/\partial t$, $\partial T/\partial x$, etc., arise due to thermal stresses in the material undergoing thermal processing. Such constraints are particularly critical for brittle materials such as glass and ceramics. The design of the manufacturing system is then governed by the material constraints.

In several circumstances, the material properties are not the same in all the directions because of the nature of the material or because of the configuration. For anisotropic materials, such as wood, asbestos, composite materials, cork, etc., the conduction flux vector $\overline{q}$ may be written as $\overline{q}=-\underline{\underline{k}}\nabla T$, where $\underline{\underline{k}}$ is the conductivity tensor, with nine components k_{ij}, obtained by varying i and j from 1 to 3 to represent the three directions. For orthotropic materials, the coordinate axes coincide with the principal axes of the conductivity tensor and the energy equation for a stationary material, in the Cartesian coordinate system, is

$$\rho C\frac{\partial T}{\partial t}=\frac{\partial}{\partial x}\left(k_x\frac{\partial T}{\partial x}\right)+\frac{\partial}{\partial y}\left(k_y\frac{\partial T}{\partial y}\right)+\frac{\partial}{\partial z}\left(k_z\frac{\partial T}{\partial z}\right)+\dot{Q} \tag{25}$$

Similarly, the equations for other coordinate systems may be written. In the annealing of coiled steel sheets, the thermal conductivity k_r in the radial direction is often much smaller than k_z in the axial direction, due to gaps within the coils and the governing conduction equation may be written taking this effect into account [43]. This affects the underlying fluid flow and the overall transport.

The preceding discussion brings out the importance of material properties in a satisfactory mathematical and numerical modeling of thermal manufacturing processes, as well as for accurate interpretation of experimental results. The properties of the material undergoing thermal processing must be known and appropriately modeled to accurately predict the resulting flow and transport, as well as the characteristics of the final product. However, this is an area in which there is acute lack of data and critical work is needed in the future.

Boundary Conditions and Simplifications

Many of the boundary and initial conditions are the usual no-slip conditions for velocity and the appropriate thermal or mass transfer conditions at the boundaries. However, a few special considerations arise for the various processes considered earlier. Some of these are discussed here.

Free Surfaces and Openings. At a free surface, the shear stress is often specified as zero, yielding a Neumann condition of the form $\partial \overline{V}/\partial n = 0$, where n is normal to the surface, if negligible shear is applied on the surface. If the shear stress exerted by the ambient fluid is significant, it replaces the zero in this equation. Basically, a balance of all the forces acting at the surface is used to obtain the interface. As considered in detail by Roy Choudhury et al. [41] and as presented later, the free surface may be determined numerically by iterating from an initial profile and using the imbalance of the forces for correcting the profile at intermediate steps, finally yielding a converged profile such as the one shown in Fig. 5.

In a stationary ambient medium, far from the solid boundaries, the velocity and temperature may be given as $\overline{V} \to 0$, $T \to T_a$ as $n \to \infty$. However, frequently the condition $\partial \overline{V}/\partial n \to 0$ is used, instead, in order to allow for entrainment into the flow. The use of this gradient, or Neumann, condition generally allows the use of a much smaller computational domain, than that needed for a given value, or Dirichlet condition, imposed on the velocity $\overline{V}$ [20]. The gradient conditions allow the flow to adjust to ambient conditions more easily, without forcing it to take on the imposed values at a chosen boundary. This consideration is very important for simulating openings in enclosures, where gradient conditions at the opening allow the flow to adjust gradually to the conditions outside the enclosure. Such conditions are commonly encountered in furnaces and ovens with openings to allow material and gas flow.

Phase Change. If a change of phase occurs at the boundary, the energy absorbed or released due to the change of phase must be taken into account. Thus, the boundary conditions at the moving interface between the two phases (Fig. 1(*c*)) must be given if a two-zone model is being used. This is not needed in the enthalpy model given by Eqs. (8)–(11). For one-dimensional solidification, this boundary condition is given by the equation

$$k_s \frac{\partial T_s}{\partial y} - k_1 \frac{\partial T_1}{\partial y} = \rho L_h \frac{d\delta}{dt} \tag{26}$$

where $y = \delta$ is the location of the interface. This implies that the energy released due to solidification is conveyed by conduction in the two regions. Similarly, for two-dimensional solidification, the boundary condition is written as [24]

$$\left(k_s \frac{\partial T_s}{\partial y} - k_1 \frac{\partial T_1}{\partial y} \right) \left[1 + \left(\frac{\partial \delta}{\partial x} \right)^2 \right] = \rho L_h \frac{d\delta}{dt} \tag{27}$$

For a stationary interface, as shown in Fig. 1(*b*), the boundary condition is [44,45]

$$\left(-k \frac{\partial T}{\partial n} \right)_1 + \rho U L_h \frac{dy}{ds} = \left(-k \frac{\partial T}{\partial n} \right)_s \tag{28}$$

where ds is a differential distance along the interface and n is distance normal to it. Also, the temperature at the interface in all these cases is T_m.

Surface Tension Effects. Surface tension effects are important in many materials processing flows where a free surface arises. Examples include flows in welding, Czochralski and the floating-zone crystal growing methods, wave soldering, and continuous casting. Surface tension affects the force balance on a free surface and can affect, for instance, the equilibrium shape of a solder joint, such as the one shown in Fig. 2(*d*) [46]. Similarly, the profile of material emerging from a die or a roller can be affected by the surface tension, the relative significance of this effect being determined by other forces acting on the surface.

Surface tension can also have a significant effect on the flow near the free surface, which represents the interface between a liquid and a gas in many cases, and on the shape, stability and other characteristics of the interface. Large surface tension gradients can arise along the interface due to temperature T and concentration c_m gradients and the variation of surface tension σ with these variables. Such surface tension gradients can generate significant shear stresses and resulting flow along the interface. This flow, known as thermocapillary or Marangoni convection, is important in many material processing flows [47]. There has been growing interest in Marangoni convection in recent years because of materials processing under microgravity conditions in space where other more dominant effects, such as buoyancy, are considerably reduced, making thermocapillary convection particularly significant.

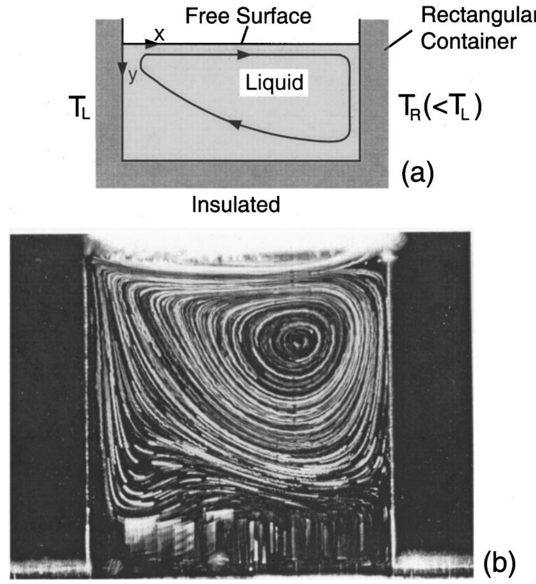

Fig. 6 Thermocapillary convection in a rectangular container: (*a*) schematic sketch and (*b*) flow in a $NaNO_3$ melt [47]

Consider a rectangular container with its left wall at temperature T_L and the right wall at a lower temperature T_R. The bottom is insulated, as shown in Fig. 6. Then the boundary condition at the free surface is

$$-\mu \frac{\partial u}{\partial y} = \frac{\partial \sigma}{\partial T} \frac{\partial T}{\partial x} + \frac{\partial \sigma}{\partial c_m} \frac{\partial c_m}{\partial x} \tag{29}$$

where u is the velocity component along the coordinate axis x. For most pure materials, σ decreases with T, i.e., $\partial \sigma/\partial T < 0$, and since $\partial T/\partial x < 0$ in this case, the fluid is pulled from the left to the right at the surface, resulting in a clockwise circulation, as shown. The flow pattern in a melt of $NaNO_3$ is also shown, indicating the dominance of thermocapillary convection and the vertical flow near the vertical wall due to thermal buoyancy. Similarly, boundary conditions may be written for other geometries.

Conjugate and Initial Conditions. Several other boundary conditions that typically arise in materials processing may be mentioned here. The normal gradients at an axis or plane of symmetry are zero, simplifying the problem by reducing the flow domain. The temperature and heat flux continuity must be maintained in going from one homogeneous region to another, such as the regions shown in Figs. 3 and 5. This results in the thermal conductivity at the interface being approximated numerically as the harmonic mean of the conductivities in the two adjacent regions for one-dimensional transport [23]. The conjugate conditions that arise at a solid surface in heat exchange with an adjacent fluid are

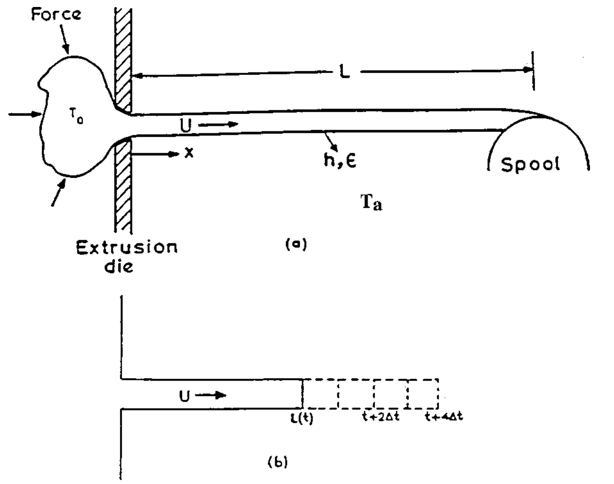

Fig. 7 (*a*) Sketch of the extrusion process for a heated material, (*b*) moving material at different time intervals

$$T_s = T_f; \quad \left(-k\frac{\partial T}{\partial n}\right)_s = \left(-k\frac{\partial T}{\partial n}\right)_f \tag{30}$$

where the subscripts s and f refer to the solid and the fluid, respectively.

The initial conditions are generally taken as the no-flow circumstance at the ambient temperature, representing the situation before the onset of the process. However, if a given process precedes another, the conditions obtained at the end of the first process are employed as the initial conditions for the next one. For periodic processes, the initial conditions are arbitrary.

Moving Material or Source. In the case of material flow in a moving cylindrical rod for extrusion or hot rolling, as sketched in Fig. 7, the temperature T is a function of time and location if a Lagrangian approach is used to follow a material element. However, by placing the coordinate system outside the moving material, a steady problem is obtained if the edge of the rod is far from the inlet, $x=0$, i.e., for large time, and if the boundary conditions are steady. Transient problems arise for small lengths of the rod, short times following onset of the process, and for boundary conditions varying with time [48,49]. For many practical cases, the temperature T may be taken as a function of time and only the downstream distance x, assuming it to be uniform at each cross-section. Such an assumption can be made if the Biot number Bi_R based on the radius R of the rod is small, i.e., $Bi_R = hR/k \ll 1.0$, h being the convective heat transfer coefficient. Thus, for a thin rod of high thermal conductivity material, such an assumption would be valid. The governing energy equation is

$$\rho C\left(\frac{\partial T}{\partial t} + U\frac{\partial T}{\partial x}\right) = k\frac{\partial^2 T}{\partial x^2} - \frac{hP}{A}(T - T_a) \tag{31}$$

where P is the perimeter of the rod, A its area of cross-section and T_a the ambient temperature.

For a long, continuous, moving rod or plate, the problem may be considered as steady for many problems of practical interest. Then, the three-dimensional temperature distribution $T(x,y,z)$ in a moving plate is governed by the convection-conduction equation

$$\rho CU\frac{\partial T}{\partial x} = k\left(\frac{\partial^2 T}{\partial x^2} + \frac{\partial^2 T}{\partial y^2} + \frac{\partial^2 T}{\partial z^2}\right) \tag{32}$$

The boundary conditions in x may be taken as $T(0,y,z) = T_0$ and $T(\infty,y,z) = T_a$. For lumping in the y and z directions, an ordinary differential equation (ODE) is obtained from Eq. (31) by dropping the transient term. Similar considerations apply for the flow in such forming processes.

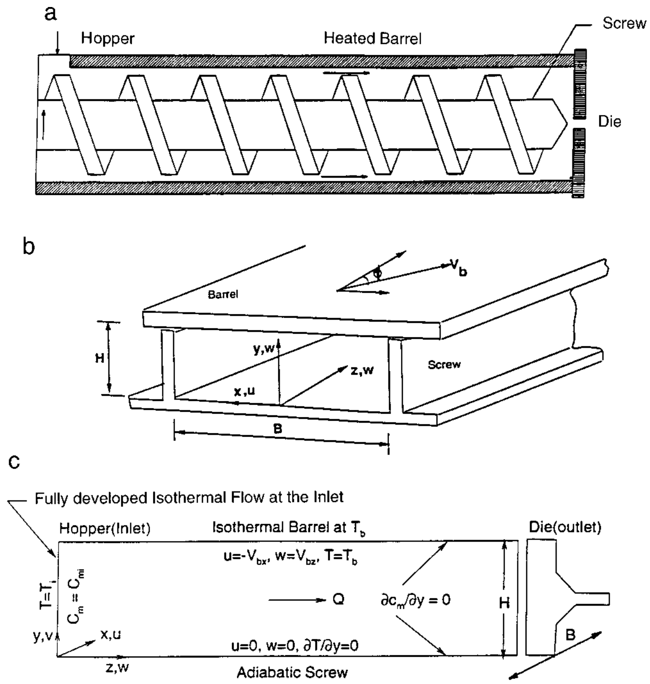

Fig. 8 Screw channel and simplified computational domain for a single-screw extruder

Similarly, coordinate transformations can be employed to convert transient problems to steady state ones in other circumstances. For instance, a moving thermal source at the surface of an extensive material gives rise to a transient circumstance if the coordinate system is fixed to the material. However, a steady state situation is obtained by fixing the origin of the coordinate system at the source. If x is measured in the direction of the source movement from a coordinate system fixed on the material surface and U is the location of the point source, the transformation used is $\xi = x - Ut$, which yields the governing equation

$$\frac{\partial^2 T}{\partial \xi^2} + \frac{\partial^2 T}{\partial y^2} + \frac{\partial^2 T}{\partial z^2} = -\frac{U}{\alpha}\frac{\partial T}{\partial \xi} \tag{33}$$

This transformation applies to processes such as welding and laser cutting. This equation is solved and the transformation is used to yield the time-dependent results.

In some manufacturing systems, the transient response of a particular component is much slower than the response of the others. The thermal behavior of this component may then be treated as quasi-steady, i.e., as a sequence of steady state circumstances. For instance, in a heat treatment furnace, the walls and the insulation are often relatively slow in their response to the transport processes, as compared to the flow. Consequently, these may be assumed to be at steady state at a given time, with different steady-states arising at different time intervals whose length is chosen on the basis of the transient response [43].

Very Viscous Flow. This circumstance usually gives rise to very small Reynolds numbers, for which the creeping flow approximation is often employed. For instance, the Reynolds number Re is generally much smaller than 1.0 for plastic and food flow in a single screw extruder and the inertia terms are usually dropped. Assuming the flow to be developed in the down-channel, z, direction and lumping across the flights, i.e., velocity varying only with distance y from the screw root towards the barrel, see Fig. 8, the governing momentum equations become [40]

$$\frac{\partial p}{\partial x} = \frac{\partial \tau_{yx}}{\partial y}, \quad \frac{\partial p}{\partial y} = 0, \quad \frac{\partial p}{\partial z} = \frac{\partial \tau_{yz}}{\partial y} \tag{34}$$

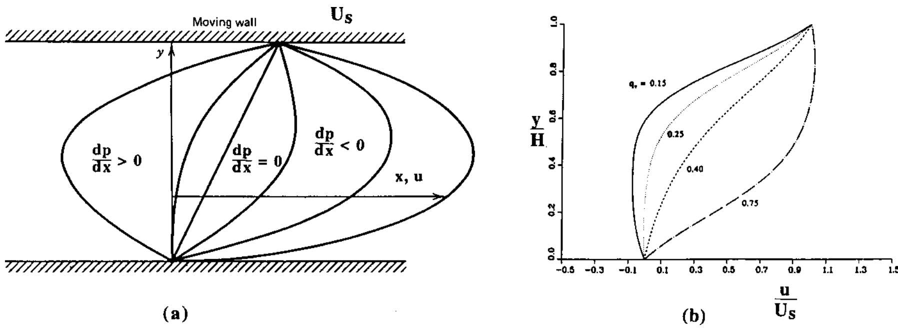

Fig. 9 Velocity profiles for developed flow in a channel of height H with combined shear due to a wall moving at velocity U_S and an imposed pressure gradient. (*a*) Newtonian fluid; (*b*) non-Newtonian fluid with $n=0.5$ at different q_v.

where the pressure terms balance the viscous forces. The coordinate system is generally fixed to the rotating screw and the channel straightened out mathematically, ignoring the effects of curvature. Then the complicated flow in the extruder is replaced by a pressure and shear driven channel flow, with shear arising due to the barrel moving at the pitch angle over a stationary screw, as shown in Fig. 8. This is similar to the shear and pressure driven channel flow available in the literature. Therefore, this approximation substantially simplifies the mathematical/numerical model.

Other Simplifications. The basic nature of the underlying physical processes and the simplifications that may be obtained under various circumstances can be best understood in terms of dimensionless variables that arise when the governing equations and the boundary conditions are nondimensionalized. The commonly encountered governing dimensionless parameters are the Strouhal number Sr, the Reynolds number Re, the Grashof number Gr, the Prandtl number Pr and the Eckert number Ec. These are defined as

$$\mathrm{Sr}=\frac{L}{V_c t_c},\quad \mathrm{Re}=\frac{V_c L}{\nu},\quad \mathrm{Gr}=\frac{g\,\beta(T_s-T_a)L^3}{\nu^2},\quad \mathrm{Pr}=\frac{\nu}{\alpha},$$

$$\mathrm{Ec}=\frac{V_c^2}{C_p(T_s-T_a)} \tag{35}$$

where V_c is a characteristic speed, L a characteristic dimension, and t_c a characteristic time. It is often convenient to apply different nondimensionalization to the solid and fluid regions.

The dimensionless equations may be used to determine the various regimes over which certain simplifications can be made. For instance, at small values of the Reynolds number Re, the convection terms are small, compared to the diffusion terms, and may be neglected. This approximation is applied to the flow of highly viscous fluids such as plastics and food materials, as mentioned earlier. At large Re, boundary layer approximations can be made to simplify the problem. At very small Prandtl number Pr, the thermal diffusion terms are relatively large and yield the conduction-dominated circumstance, which is often applied to the flow of liquid metals in casting, soldering and welding. A small value of $\mathrm{Gr}/\mathrm{Re}^2$ implies negligible buoyancy effects, for instance, in continuous casting where the effect of buoyancy on the transport in the melt region may be neglected. A small value of the Eckert number Ec similarly implies negligible pressure work effects and a small value of Ec/Re can be used to neglect viscous dissipation. Finally, a small value of the Strouhal number Sr indicates a very slow transient, which can be treated as a quasi-steady circumstance. Therefore, the expected range of the governing parameters such as Re, Gr, Pr, Sr, and Ec can be employed to determine the relative importance of various physical mechanisms underlying the transport process. This information can then be used to simplify the relevant governing equations and the corresponding modeling. Similarly, Marangoni number Ma $=(\partial\sigma/\partial T)L\Delta T/\mu\alpha$, where ΔT is the total temperature difference, arises in thermocapillary flow, and Weber number We $=\rho V_c^2 L/\sigma$ arises in flows with surface tension effects such as the one shown in Fig. 2(*d*).

Several other such simplifications and approximations are commonly made to reduce the computational effort in the numerical simulation of thermal manufacturing processes. For instance, dy/ds may be taken as unity in Eq. (28) for many continuous casting processes that use an insulated mold, which gives rise to a fairly planar interface. Also, for slow withdrawal rates, the heat transfer due to convection is small compared to that due to conduction within the moving material and may be neglected. If the extent of the material undergoing, say, thermal processing at the surface, is large, it may often be assumed to be semi-infinite, simplifying both the analysis and the numerical simulation [1]. Similarly, the boundaries are often approximated as planar to simplify the imposition of the boundary conditions there. Clearly, the preceding discussion is not exhaustive and presents only a few common approximations and simplifications.

Solution Techniques

Analytical. It is obvious from the complexity of the governing equations, boundary conditions, and the underlying mechanisms that analytical methods can be used to obtain the solution in very few practical circumstances. However, though numerical approaches are extensively used to obtain the flow and associated transport in most materials processing systems, analytical solutions are very valuable since they provide

1. Results that can be used for validating numerical models
2. Physical insight into the basic mechanisms and expected trends
3. Limiting or asymptotic conditions
4. Quantitative results for certain simple components

The validation of the numerical models, expected physical characteristics of the process, and limitations on important variables are all very important in the development of a numerical or experimental approach to study the process. Also, certain components or processes can be simplified and idealized to allow analytical solutions to be obtained.

A few examples of analytical solutions may be mentioned here. The complex flow in a screw extruder, such as the one shown in Fig. 1(*d*), was simplified to shear and pressure driven flow in a channel, as seen in Fig. 8(*c*). The simplest case is that of fully developed flow for which the velocity field is assumed to remain unchanged downstream. Analytical solutions can be obtained for such channel flows driven by pressure and shear, as shown in Fig. 9(*a*) for Newtonian fluids. When the pressure gradient is zero, the flow is only due to the viscous effect of the wall moving at ve-

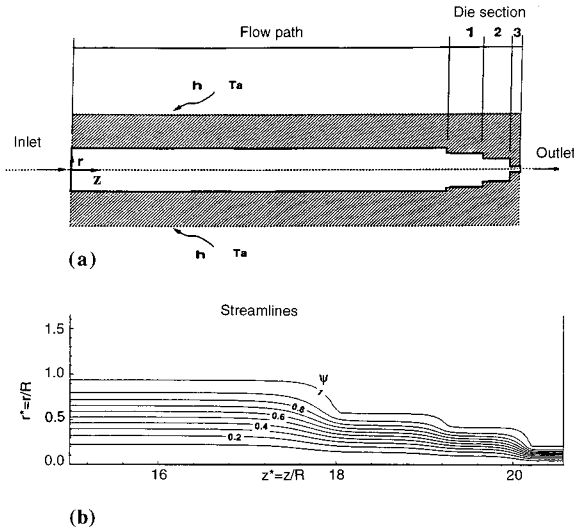

Fig. 10 Geometry of a practical extrusion die, with R as the inlet radius, along with the calculated streamlines for a non-Newtonian material for typical operating conditions

locity U_s and is termed drag flow. For Newtonian flow, the velocity profile is linear and the dimensionless flow rate, or throughput, q_v, which is the flow rate divided by the product of wall speed and cross-sectional area, is simply 0.5. For a favorable pressure gradient, the throughput exceeds 0.5 and for an adverse pressure gradient it is less. Similar trends are expected for non-Newtonian fluids though the profiles and the q_v value for drag flow would be different. Numerical results have confirmed this behavior and have used the analytical results to validate the model as well as to characterize different flow regimes, as shown in Fig. 9(*b*).

Another analytical solution that has been used to model the extrusion process is that of flow in a die. The relationship between the pressure drop Δp across a cylindrical region of length L and radius R, with mass flow rate $\dot{m}$ for a non-Newtonian fluid, was obtained by Kwon et al. [50] by assuming developed flow. The expression given is

$$\Delta p = \frac{2L}{R}\hat{C}(T)\left[\frac{3n+1}{4n}\,\frac{4\dot{m}}{\rho\pi R^3}\right]^n \tag{36}$$

where $\hat{C}(T)$ is a temperature dependent coefficient in the viscosity expression, which is given as $\mu=\hat{C}(T)(\dot{\gamma})^{1-n}$, $\dot{\gamma}$ being the shear rate, defined earlier. This expression would apply for the flat portions of a typical die, such as the one shown in Fig. 10. But the flow is not developed, as seen from the calculated streamlines shown in Fig. 10. However, the expression can be used without significant error for long cylindrical regions, such as the portion on the left of the die shown here [51]. Similarly, expressions for a conical die and for an orifice were given by Kwon et al. [50].

Numerical

The governing equations given earlier are the ones usually encountered in fluid flow and heat and mass transfer. Though additional complexities due to the geometry, boundary conditions, material property variations, combined mechanisms, etc., arise in materials processing, as mentioned earlier, the numerical solution of the governing equations is based on the extensive literature on computational fluid dynamics. Among the most commonly employed techniques for solving these equations is the SIMPLER algorithm, given by Patankar [52], and the several variations of this approach. This method employs the finite volume formulation with a staggered grid, so that the value of each scalar quantity, such as pressure, concentration and temperature, is associated with the grid node and the vector quantities like velocity are displaced in space relative to the scalar quantities and generally located on the faces of the control volume. This grid system has an advantage in solving the velocity field since the pressure gradients that drive the flow are easy to evaluate and the velocity components are conveniently located for the calculation of the convective fluxes. A pressure correction equation is used during the iteration or time marching to converge to the solution. Also, the pressure at any arbitrary point is chosen at a reference value and separate boundary conditions are not needed for pressure.

For two-dimensional and axisymmetric problems, the governing equations are often cast in terms of the vorticity and streamfunction by eliminating the pressure from the two components of the momentum equation and by defining a streamfunction to take care of the continuity equation [23]. This reduces the number of equations by one and pressure is eliminated as a variable, though it can be calculated after the solution is obtained. The solution yields the streamfunction, which is used for obtaining the velocity field and plotting streamlines, the temperature, which is used for plotting the isotherms and calculating heat transfer rates, and the vorticity. Because the streamfunction is specified on the boundaries, convergence of the streamfunction equation is usually quite fast. Thus, this approach is generally advantageous, as compared to the methods based on the primitive variables of velocity, pressure and temperature, for two-dimensional and axisymmetric flows. The latter approach is more appropriate for three-dimensional circumstances.

Both transient and steady state solutions are of interest, depending on the process under consideration. In the former case, time marching is used with convergence at each time step to obtain the time-dependent variation of the flow, temperature field, heat and mass transfer rates, chemical conversion, etc. For steady problems also, time marching may be used to obtain the desired results at large time. However, the problem can also be solved by iteration or by using false transients with large time steps [53]. Though central differences are desirable for all the approximations, numerical instability with the convection terms is often avoided by the use of upwind, exponential or power-law differencing schemes [52]. Because of the inaccuracy due to false diffusion, second-order upwind differencing and third-order QUICK schemes have become quite popular for discretizing the convection terms [54]. Under-relaxation is generally needed for convergence due to the strong nonlinearities that arise in these equations mainly due to property variations. Several methods are available to solve the vorticity transport and energy equations. The Alternating Direction Implicit (ADI) method of Peaceman and Rachford [55], as well as modifications of this time-splitting method, are particularly efficient for two-dimensional problems. Similarly, cyclic reduction, successive over relaxation and other standard methods may be used for the streamfunction or the pressure equation. Solution-adaptive methods have been developed in recent years to address many of the complexities that arise in heat transfer and fluid flow problems, as reviewed by Acharya [56].

As mentioned earlier, major difficulties arise in material processing simulations due to the complexity of the computational domain as well as that of the boundary conditions. Finite element and boundary element methods have been used advantageously to simulate a wide variety of material processing systems. Several of these cases are outlined later in the paper. Finite difference and finite volume methods have also been used with coordinate transformations employed to convert the complex domains into much simpler forms so that the discretization is simplified and accurate results are obtained. A few cases based on such transformations are also presented later.

Experimental

Experimental work is extremely important in a study of fluid phenomena in materials processing. The main contributions of experimental investigations are

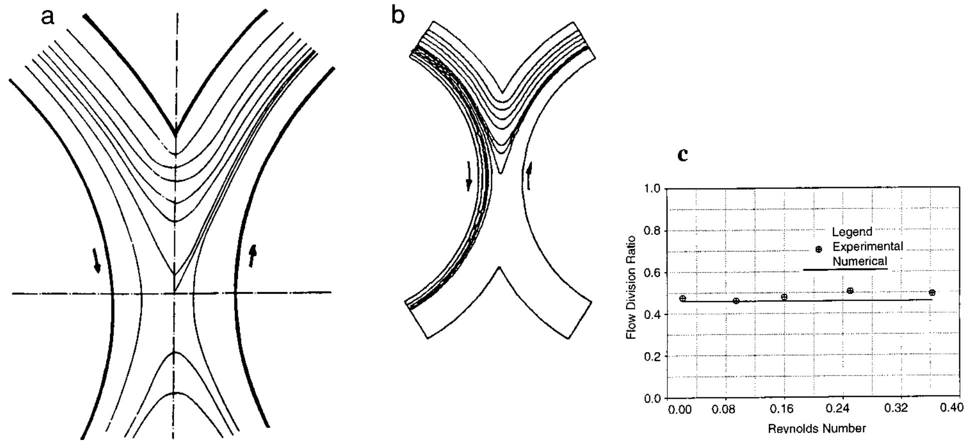

Fig. 11 Streamlines in the region between two rotating cylinders for CMC solution at 16 rpm. (*a*) Experimental results; (*b*) numerical predictions for flow entering the region over one cylinder; (*c*) comparison of flow division ratio x_f obtained from experimental and numerical results [57].

1 Enhancing the basic understanding of the flow and associated transport
2 Providing insight that can be used in the development of mathematical and numerical models, particularly for determining important aspects and variables
3 Providing results that can be used for validation of the models
4 Yielding quantitative results that can be used to characterize processes and components in the absence of accurate and dependable models

Though validation of models is often considered as the main reason for experimentation, there are many complex flows where experimental results guide the development of the model and also generate quantitative data that can be used as empirical inputs if accurate modeling is not available. Flow visualization is particularly important in studying the nature of the flow. However, many practical materials are opaque and must be substituted by simpler transparent materials for optical methods to visualize the flow. The same considerations apply for optical measurement techniques like laser Doppler anemometry and particle image velocimetry.

As an example, let us consider the fluid flow in the region between two rotating screws in mixers and extruders. This flow, as well as the nature of the resulting mixing process, are not very well understood. Sastrohartono et al. [57] carried out an experimental study of the flow in this region. Two rotating plexiglas cylinders were driven by a variable speed motor and the flow in the region between the two cylinders was observed. Corn syrup and carboxy-methyl-cellulose (CMC) solutions were used as the fluids, the former being Newtonian and the latter non-Newtonian. Air bubbles and dyes were used for visualization.

Figure 11 shows the experimentally obtained streamlines in the region between the two cylinders, along with the predictions from a numerical model. Clearly, good agreement is seen between the two. It is also seen that some of the fluid flowing adjacent the left cylinder continues to flow adjacent to it while the remaining goes to the other cylinder. This process is similar to the movement of fluid from one screw channel to the other in a tangential twin screw extruder. A flow division ratio x_f may be defined as the fraction of the mass flow that crosses over from one channel to the other. A dividing streamline that separates the two fluid streams was determined from the path lines and used to determine the flow division ratio. A comparison between experimental and numerical results is shown, indicating good agreement at small Reynolds numbers. A deviation between numerical and experimental results was observed for Reynolds numbers greater than around 1.0, mainly because of negligible inertia terms assumed in the mathematical model. These experiments indicate the basic features of the mixing process in the intermeshing region, even though only cylinders are considered. The flow division ratio may be taken as a measure of mixing.

Results for a Few Important Processes

The preceding sections have presented the basic considerations that arise in a study of fluid flow phenomena in materials processing. The important basic flows, governing equations and boundary conditions were outlined. The analytical, numerical and experimental approaches to investigate various types of flows were discussed. Several important processes were mentioned and briefly discussed. The common aspects that link different processes are seen in terms of the underlying mechanisms and governing equations and parameters. However, major differences exist between various materials processing techniques and demand specialized treatment. The desired results from numerical or experimental investigations are also usually quite different. It is not possible to discuss all the major aspects that characterize different processes and the available results in these areas. However, a few important processes are considered in greater detail in the following to illustrate the approaches used to obtain the desired solution as well as the characteristic results.

Polymer Extrusion. An important manufacturing process which has been mentioned in the preceding sections is plastic screw extrusion, sketched in Figs. 1(*d*) and 8. The viscosity expression and the governing equations for a relatively simple two-dimensional model were given earlier. This is a fairly complicated problem because of the strong shear rate and temperature dependence of the viscosity, complex geometry, large viscous dissipation, and the resulting coupling between the energy and momentum equations. Interest lies in control and prediction of the flow in order to improve mixing and modify physical and chemical changes undergone by the material.

Figure 12 shows typical computed velocity and temperature fields in an extruder channel. Large temperature differences are seen to arise across the channel height because of the relatively small thermal conductivity of plastics. The flow is well-layered, with little bulk mixing, due to the high viscosity of these fluids, the typical viscosity being more than a million times that of water at room temperature. Many approaches such as reverse screw elements and sudden changes in the screw have been used to disrupt the well-layered flow and promote mixing. Viscous dissipation causes the temperature to rise beyond the imposed barrel tempera-

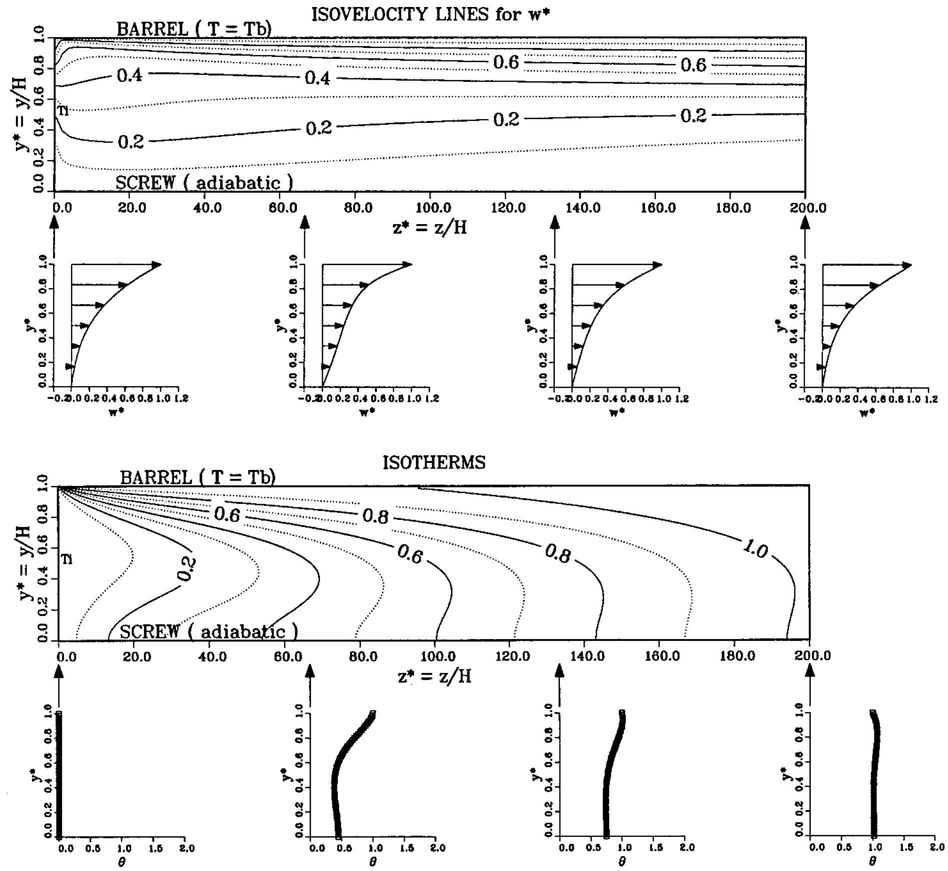

Fig. 12 Calculated velocity and temperature fields in the channel of a single screw extruder at n=0.5 and dimensionless throughput q_v=0.3, for typical operating conditions

ture. A lot of work has been done on this problem because of its importance to industry, as reviewed by Tadmor and Gogos [38] and Jaluria [19].

An important consideration in the extrusion process is the residence time distribution (RTD). The residence time is the amount of time spent by a fluid particle in the extruder from the hopper to the die. If the material spends an excessive amount of time, it may be over-processed, over-cooked, if it is food, or degraded. Similarly, too small a time may lead to under-processing. The final product is, therefore, strongly dependent on the residence time distribution since structural changes due to thermal processing and chemical reactions are usually time-dependent. The residence time distribution is largely a function of the flow field. It is experimentally obtained by releasing a fixed amount of color dye or tracer in the material at the hopper and measuring the flow rate of the dye material as it emerges from the extruder at the other end. The time it takes for the dye to first appear is the minimum residence time and relates to the fastest moving fluid. Similarly, an average residence time may be defined.

The experimental determination of residence time may be numerically simulated by considering the flow of a slab of a dye as it moves from the hopper to the die, as sketched in Fig. 13(a). If the velocity field is known from the solution of the governing equations, a fluid particle may be numerically traced by integrating the velocity over time. The axial component of the velocity is used to trace the particles. As expected, the particles near the barrel and the screw take a very long time to come out, as compared to the particles near the middle portion of the screw channel. This yields the amount of color dye emerging from the extruder as a function of time and may be used to obtain the minimum, average and the spatial distribution of the residence time. Figure 13(b) shows these results in terms of the dye flow rate, normalized by the total flow rate. Clearly, in this case, most of the dye emerges over a short time interval, with the extended regions representing fluid near the barrel and the screw root. The calculated cumulative function $F(t)$, which indicates the cumulative fraction of the total amount of dye emerging up to time t, is defined as

$$F(t)=\int_0^t f(t)dt \tag{37}$$

where $f(t)dt$ is the amount of material that has a residence time between t and $t+dt$. The average residence time $\bar{t}$ is given by V_e/Q_e, where V_e is the total internal volume of the extruder and Q_e the volume flow rate. $F(t)$ is plotted as a function of time in Fig. 13(c), along with the distributions for a few other flows. It is seen that, though the basic trends are similar, the RTD is affected by the nature of the fluid and the flow configuration. It is found to be only slightly affected by the barrel temperature. It is mainly affected by the flow rate, or throughput, which substantially influences the flow field. Results at different operating conditions have been obtained in the literature and used for selecting the appropriate conditions for a given material or thermal process.

Mixing. An important consideration is the fluid mixing inside the screw channel since it determines the homogeneity of the material being processed. A simple experiment as well as some results on mixing, as given by the flow division ratio for flow between two rotating cylinders, were discussed earlier. The flow undergone by the material particles as the fluid moves downstream may be considered for a better understanding of the mixing process. Based on the calculated three-dimensional velocity field, one can introduce particles inside the screw channel and follow

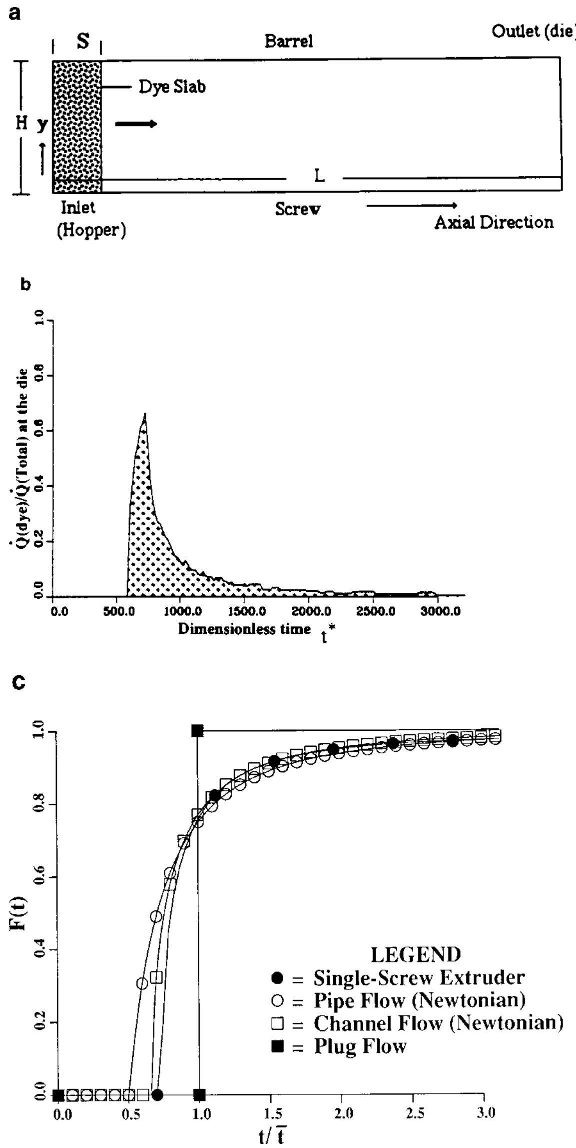

Fig. 13 Residence time distribution (RTD) calculations. (*a*) Schematic diagram showing the dye slab and the computational domain for RTD calculations; (*b*) variation of the dye flow rate, normalized by the total flow rate, with time for typical operating conditions; (*c*) variation of the cumulative distribution function F(t) for different flow configurations, with $\bar{t}$ as the average residence time.

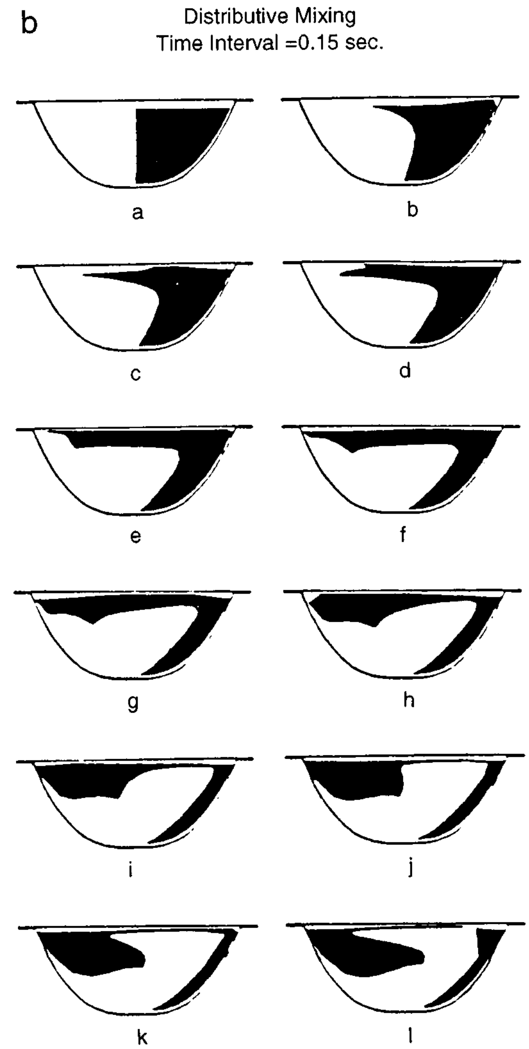

Fig. 14 Mixing characteristics in a single screw extruder channel shown in terms of time sequence of distributive mixing of two different materials inside the screw channel [58]

the movement of these particles along the channel [58]. The particles undergo spiral movements, except those near the barrel surface which go straight across the flight gap into the adjacent channel. The spiral movement of the particles inside the screw channel promotes mixing within the single screw extruder. This recirculating flow is not captured by the simpler two-dimensional model discussed earlier.

The distributive mixing inside the channel may be represented in terms of mixing between two different types of materials, shown as white and black portions in Fig. 14 with each initially occupying one half of the channel. These materials are followed with time as the fluid moves in the channel. Clearly, the process is a slow one, though the materials are eventually mixed with each other as time elapses. Several other measures of mixing have been considered in the literature. Kwon et al. [59] studied kinematics and deformation to characterize mixing. Substantial work has also been done on mixing in twin screw extruders, including the use of chaos introduced by changes in the geometry and the boundary conditions [60].

Experimental Results. Experimentation on fluid flow in the extruder channel is involved because of the complex domain and generally opaque nature of the typical materials. However, extensive experimental data on the overall characteristics of the extrusion process are available in the literature. Most of these concern the practical issues in extrusion such as temperature and pressure at the die, residence time distribution, total heat input, characteristics of the extrudate, total torque exerted on the screw, and flow rate. Much of this information is reviewed in books such as those by Tadmor and Gogos [38], Harper [28], and Rauwendaal [61]. However, very few studies have focused on the fluid flow in the channel. Over the last decade, Sernas and co-workers [62,63] have carried out well-designed, accurate, controlled and innovative experiments on single- and twin screw extruders. These results have been used for the validation of the analytical and numerical models presented here, as well as for providing a better understanding of the basic fluid flow and heat transfer processes associated with extrusion.

A specially designed single screw extruder is used for these experiments. A plexiglas window can be fitted at any one of the measuring ports to provide optical access to the flow to observe

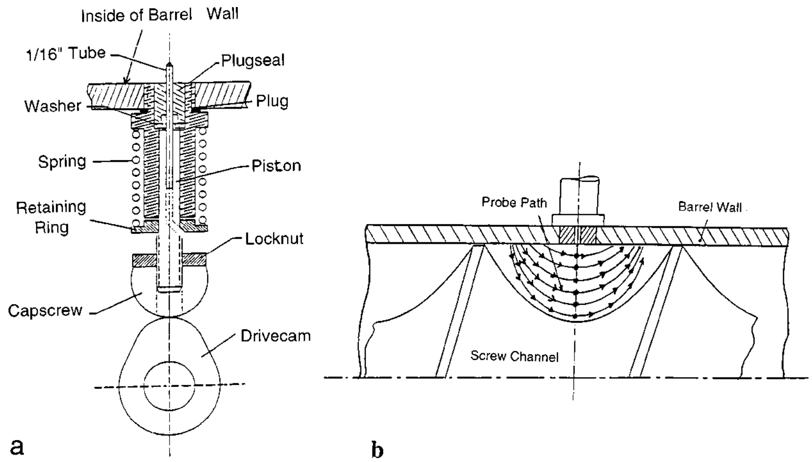

Fig. 15 (*a*) Cam-driven thermocouple for temperature measurements in the screw channel; (*b*) representation of the loci of points where temperature data are collected [62,63]

the extent of fill of the screw channel. The barrel is subdivided into three sections which can be maintained at different uniform temperatures by the use of circulating water jackets. The pressure and temperature are measured at various locations. The measurement of the temperature profile in the screw channel is complicated because of the rotating screw. A cam-driven thermocouple system, as shown in Fig. 15(*a*), is installed on the extruder to allow the thermocouple probe to travel in and out of the channel in a synchronized motion linked to the screw rotation. The probe moves into the channel to a preset distance while the flights traverse due to screw rotation. The loci of points where data are taken are sketched in Fig. 15(*b*). As expected, considerable amount of care is involved in extracting the appropriate data for the temperature profile [62,63].

Some characteristic experimental results for Viscasil-300M, which is a non-Newtonian fluid, are shown in Fig. 16, along with numerical results from two-dimensional finite difference and three-dimensional finite element calculations [40,64]. The effect of recirculation in the screw channel is seen in terms of the temperature near the screw root being closer to that near the barrel, than that predicted by the two-dimensional model. Clearly, a three-dimensional model is needed to capture this recirculation. It is interesting to note that these observations led to the development of the three-dimensional model for flow in the screw channel. A close agreement between the experimental and numerical results, in terms of pressure and temperature measured at the die, was also observed, providing strong support to the model. It was found that, for a given die, the die pressure rises with the flow rate which is increased by raising the screw speed. Also, as expected, the pressure increases as the fluid moves from the inlet towards the die.

Twin-Screw Extrusion. Twin screw extruders are used extensively in the processing of polymeric materials and in operations which include pumping, polymer blending, and distribution of pigments and reinforcing materials in molten polymers. The main advantages of twin-screw extruders, over single-screw extruders, are better stability, control and mixing characteristics. In twin screw extruders, two screws lie adjacent to each other in a barrel casing whose cross section is in a figure of eight pattern, see Fig. 17. Twin screw extruders are of many types, such as, intermeshing, non-intermeshing, co-rotating, counter-rotating, to name a few. When the screws rotate in the same direction they are called co-rotating and when they rotate in opposite directions, they are known as counter-rotating twin screw extruders. Depending upon the separation between the axes of the two screws, twin screw extruders are classified as intermeshing or non-intermeshing extruders. If the distance between the screw axes is less than the diameter at the tip of the screw flight, then one screw intermeshes with the other and thus yields an intermeshing twin screw extruder. Otherwise, it is known as a non-intermeshing twin screw extruder. When the distance between the screw axes is equal to twice the radius at the screw root and the flights of one screw wipe the root of the other screw, then the extruder is known as a fully intermeshing and self wiping twin screw extruder.

The flow domain of a twin-screw extruder is a complicated one and the simulation of the entire region is very involved and challenging [65]. In order to simplify the numerical simulation of the problem, the flow is divided into two regions: the translation, or T

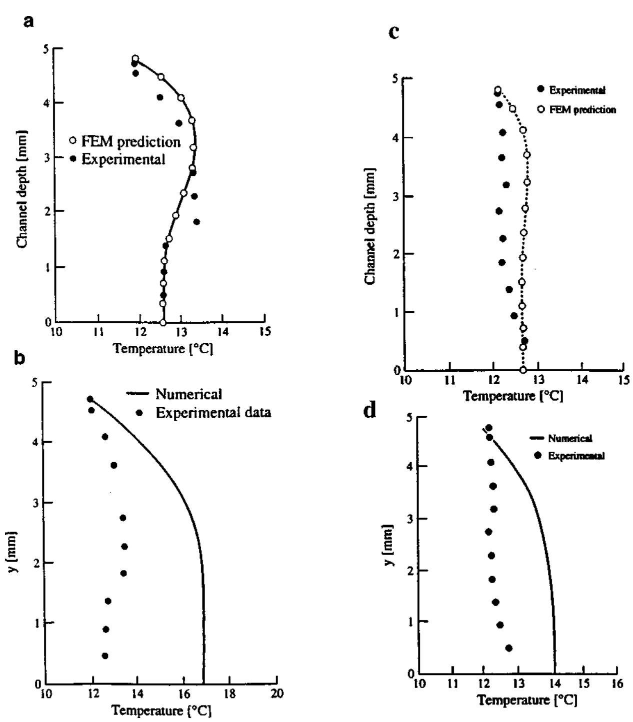

Fig. 16 Comparisons between numerical and experimental results on temperature profiles for Viscasil-300M, with (*a*) and (*c*) from the 3D (FEM) model and (*b*) and (*d*) from the 2D (FDM) model. For (*a*) and (*b*): $T_i=20.3°C$, $T_b=12.2°C$, $N=20$. For (*c*) and (*d*): $T_i=18.8°C$, $T_b=22.3°C$, $N=35$.

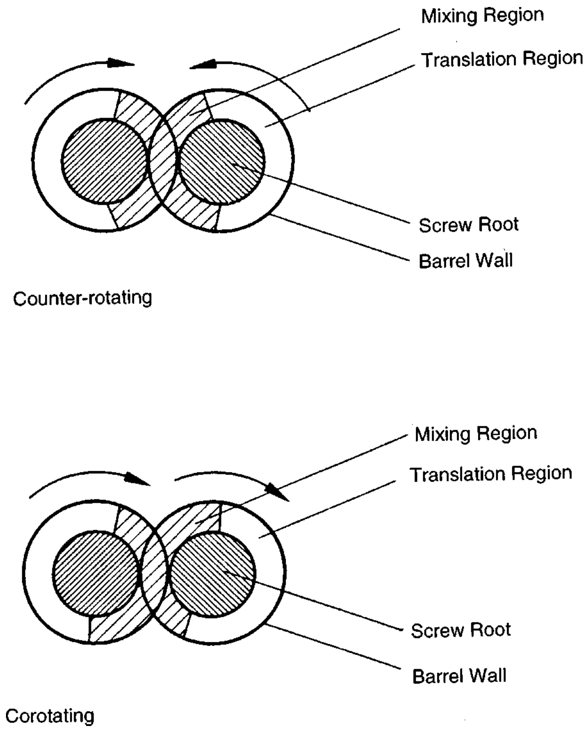

Fig. 17 Schematic diagram of the cross-section of a tangential twin screw extruder, showing the translation (T) and intermeshing, or mixing (M), regions

region, and the intermeshing, or *M* region, as sketched in Fig. 17. This figure schematically shows a section taken normal to the screw axis of a tangential co-rotating twin screw extruder and the two regions. The counter-rotating case is also shown. Due to the nature of the flow and geometric similarity, the flow in the translation region is analyzed in a manner identical to that for a single screw extruder. Therefore, this region is approximated by a channel flow. The intermeshing, or mixing, region is represented by the geometrically complex central portion of the extruder, between the two screws. The two regions are separated by a hypothetical boundary used for numerical calculations only. For further details on this model for the twin screw extruder and on the numerical scheme, see [60,65–67]. The finite-element method is particularly well suited to the complex domains that arise in twin-screw extruders. Figure 18 shows the finite element mesh used and some typical results on the transport in the mixing or nip region of the extruder. It is seen that large gradients in pressure, velocity and shear rate arise in the nip region, resulting in substantial fluid mixing, unlike the small recirculation in single-screw extruders.

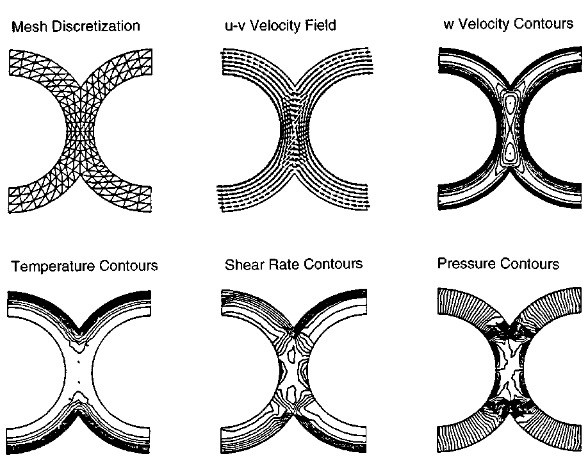

Fig. 18 Mesh discretization for the mixing region in a co-rotating tangential twin screw extruder, along with typical computed results for low density polyethylene (LDPE) at $n=0.48$, $T_b=320°C$, $T_i=220°C$, $N=60$ rpm, $q_v=0.3$

Chiruvella et al. [68] approximated the intermeshing region of a self-wiping co-rotating twin screw extruder to develop a control-volume based numerical scheme similar to the SIMPLER algorithm [52]. Figure 19(*a*) shows a cut-away view of the extruder considered. The flow in the intermeshing region is three-dimensional with the flow shifting by the flight width as it goes from one channel to the other. Solutions are obtained for the translation and intermeshing regions and linked at the interface, or overlapping region. The screw channels are assumed to be completely filled and leakage across the flights is neglected [68]. Figure 19(*b*) shows the pressure and temperature rise when the translation and intermeshing regions are coupled. A good agreement with earlier finite-element results is observed. Additional results at different operating conditions and materials were obtained [68,69]. Viscous dissipation was found to increase the temperature in the fluid above the barrel temperature for typical operating conditions. This model is much simpler than the finite element model, requiring much less storage space and computational time, thus making it attractive in modeling practical problems and in design for industrial applications.

Velocity measurements are quite involved because of the complex geometry and rotating screws. Karwe and Sernas [70] and Bakalis and Karwe [71] have carried out measurements of the fluid velocity field for heavy corn syrup which is transparent. A plexiglas window was used for visual access to the twin screws in the extruder. A two-component Laser Doppler Anemometer (LDA) in the back-scatter mode was used to measure the local velocities in the extruder, as shown in Fig. 20(*a*). As expected, the flow was found to be very complicated and three-dimensional. The flow field in the translation region could be compared with the numerical prediction and is shown in Fig. 20(*b*). A fairly good agreement is observed, lending support to the model and the experimental procedure. Tangential and axial velocity components were also measured in the intermeshing region and compared with numerical predictions, yielding good agreement. Leakage across the flights was found to be significant and the three-dimensional nature of the flow field was evident in the results.

Chemical Conversion. Typical results on the conversion of amioca, which is a pure form of starch, at constant screw speed and throughput, are presented in Fig. 21. The degree of conversion depends upon the velocity field and the reaction rate constant *K* which varies with the local temperature of the extrudate, as mentioned earlier. For smaller velocities, the degree of conversion up to a given axial location is higher. This is clear in the region near the screw root in all of the conversion contours. As the temperature increases along the down-channel direction, the degree of conversion increases, though the down-channel velocity does not change much. At a barrel temperature of 150°C, the local temperature is much higher than that at 115°C. Since the reaction rate constant is higher when the local temperature is higher, the material gets converted in a shorter distance than that in the case where the temperature is lower. Several other results were obtained under different temperature levels and throughputs [32]. This figure shows the typical trends observed. With increasing flow rate, the degree of conversion decreases since the residence time is smaller allowing less time for the chemical reactions to occur. A comparison with experimental results also showed good agreement. However, in these cases the screw is not filled with a rheological fluid throughout. Only a fraction of the channel length, as given in the figure, is completely filled, with the remaining portion either par-

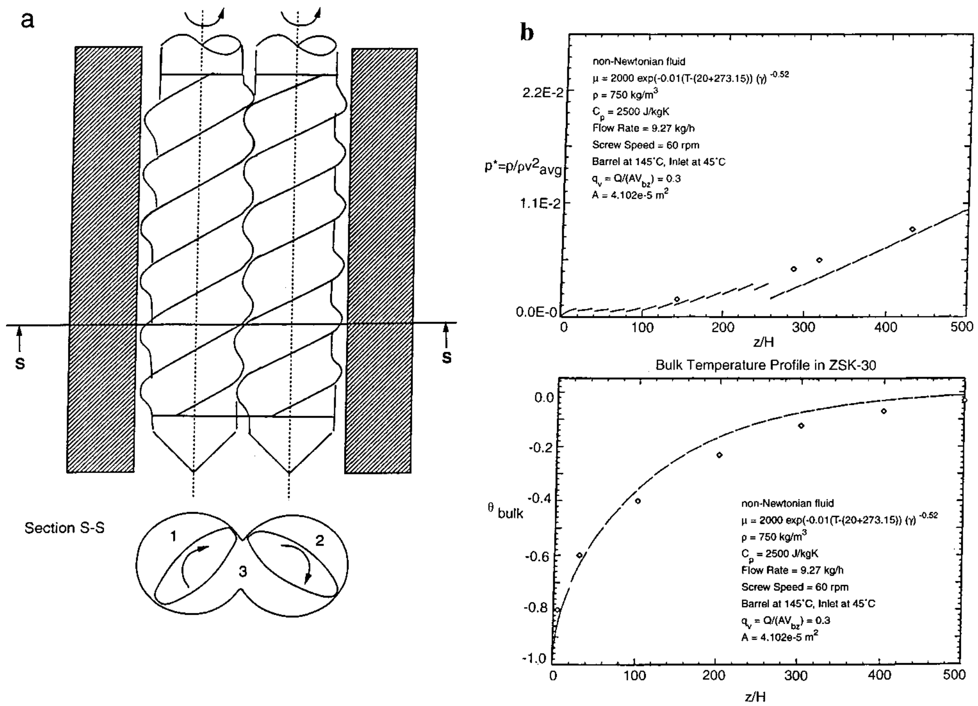

Fig. 19 (*a*) A corotating twin screw extruder with a self-wiping screw profile; (*b*) comparison between the results obtained from finite volume and finite element approaches, the latter being shown as points, for a corotating, self-wiping, twin screw extruder

tially full or containing powder which cannot be treated as a fluid. Further work is needed on chemical kinetics and on micro-structural changes in such problems.

Powder Flow. In the processing of plastics and food, the material is generally fed into the extruder as solid pieces or as powder. This material is conveyed by the rotating screw, compacted and then melted or chemically converted due to the thermal and mechanical energy input. Figure 22(*a*) shows a schematic of the overall process for food extrusion. The solid conveying region is generally modeled as a plug flow with friction and slip at the boundaries, as sketched in Fig. 22(*b*). Friction factors have been measured for different materials and are available in the literature. The force balance yields the pressure variation in this region [38,72]. This material is compacted due to the increase in pressure downstream. For modeling the compaction process, information is needed on the variation of density or porosity of the material with pressure. Also, accurate friction factors are needed for the given powder and barrel and screw materials. Very little work has been done on powder flow and compaction, even though it is expected that this process will have a substantial effect on the flow, heat transfer and conversion processes downstream [72]. Clearly, further detailed work is needed on this problem.

Additional Aspects. The preceding presentation on polymer extrusion brings out the major concerns and complexities in this important area. However, there are many additional aspects that arise in practical circumstances. These include melting and solidification of the material, different screw configurations, leakage across screw flights, flow stability, process feasibility, and the conjugate transport due to conduction in the barrel. Transient effects are particularly important, both for the start-up of the process and for changes in the operating conditions. The feasibility of the process is determined largely by the pressure and temperature rise in the extruder and, therefore, by the flow. Many of these aspects have been considered in detail in the literature and the references given in this section may be used for additional information.

Summary. The processing of polymers and other similar materials like food, rubber and pharmaceutical materials is used extensively in a wide variety of industries. Extrusion also frequently precedes injection molding, another important processing method for plastics. Composite materials are also generally produced by reinforcing polymers with a variety of fibers made of metals, ceramics, glass, etc., to obtain the desired characteristics. Again, extrusion and injection molding are important processing techniques for such materials. The fluid flow strongly affects the mixing process, as well as the residence time, which influences the physical and chemical changes in the material. The flow also affects the thermal transport, which determines the temperature field, the fluid viscosity, and the pressure rise. These variables and the flow determine the characteristics of the final product.

Optical Fiber Drawing. Another important manufacturing process, which was considered in the preceding discussion and which has become critical for advancements in telecommunications and networking, is optical fiber drawing, sketched in Fig. 1(*a*). In this process, the viscosity of glass, which is a supercooled liquid at room temperature, is a very strong function of temperature. At its softening point, the viscosity is still very high, being of the same order as that of polymer melts considered in the previous subsection. Thus, viscous dissipation is important and the momentum and energy equations are coupled. The analytical/numerical treatment is thus similar to that described in the previous section. Even small temperature differences are important because of the effect on the viscosity and thus on the flow field. However, glass flow may be treated as Newtonian at typical draw speeds.

In optical fiber drawing, the diameter of the cylindrical rod, which is specially fabricated to obtain a desired refractive index variation and is known as a preform, changes substantially, from 2–10 cm to about 125 μm, in a distance of only a few centimeters. This places stringent demands on the grid, shown in Fig. 5, as well as on the numerical scheme because of the large change in the surface velocity. The radiative transport within the glass is

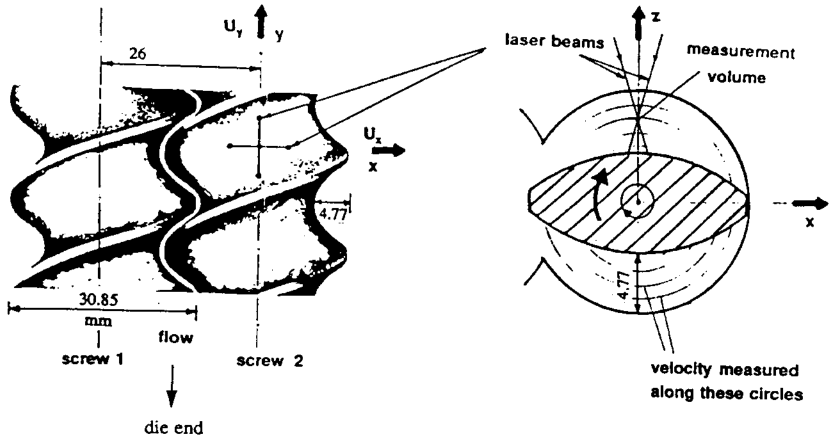

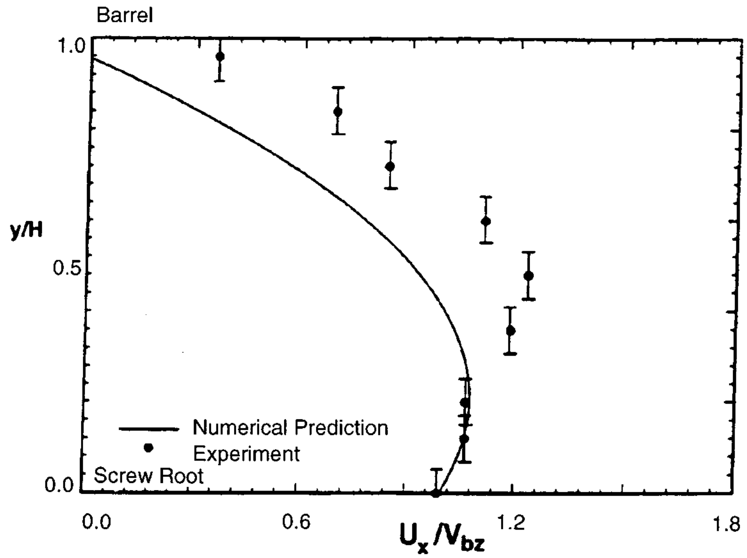

(b)

Fig. 20 (*a*) Experimental arrangement for velocity measurements in the flow of corn syrup in a twin-screw extruder; (*b*) comparison between calculated and measured tangential velocity U_x profiles for isothermal heavy corn syrup at 26.5°C, with mass flow rate of 6 kg/h and screw speed of 30 rpm

determined using the optically thick medium approximation or improved models such as the zonal method [73]. The main interest in this process lies in obtaining high quality optical fibers, as indicated by low concentration of process-induced defects, desired variation of refractive index, low tension, strength, and other important measures, at high draw speeds.

Typical computed results in the neck-down region, for a specified profile, are shown in Fig. 23, indicating the streamfunction, vorticity, viscous dissipation and temperature contours. The flow is smooth and well-layered because of the high viscosity. A typical temperature difference of 50–100°C arises across the fiber for preform diameters of around 2.0 cm. As mentioned earlier, even this small difference is an important factor in fiber quality and characteristics. Larger temperature differences obviously arise for larger preform diameters. Viscous dissipation, though relatively small, is mainly concentrated near the end of the neck-down, in the small diameter region, and plays an important role in maintaining the temperatures above the softening point. Further details on this problem may be obtained from [14,17,18,41,74].

Neck-Down. The simulation of the free surface is another difficult problem, as discussed earlier. Several studies in the literature have considered fiber formation from the melt, particularly for polymers, and jets and other free surface flows [75–78]. Optical fiber drawing involves modeling the free surface flow of glass under large temperature differences and large changes in viscosity and cross-sectional area. Several simple models have been employed to study the flow in this region, known as the neck-down region [74]. In a recent study, a combined analytical and numerical approach, based on the transport equations and surface force balance, was developed for the generation of the neck-down profile of an optical fiber during the drawing process [41]. An axisymmetric, laminar flow was assumed in the glass and in the circulating inert gases. The governing transport equations were solved employing a finite difference method. The radially lumped axial velocity, the normal force balance and the vertical momentum equations were used to obtain a correction scheme for the neck-down profile. After a new corrected profile is obtained, the full governing equations are solved for the flow and heat trans-

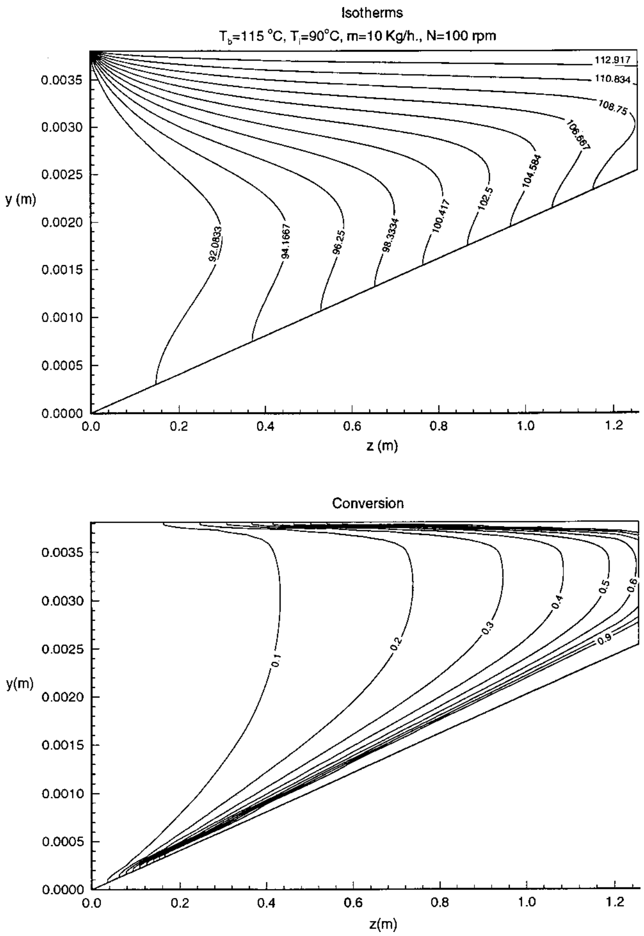

Fig. 21 Isotherms and conversion contours while extruding amioca in a tapered single screw extruder, with $T_b=115°C$, $T_i=90°C$, $N=100$ rpm, mass flow rate $\dot{m}=10$ kg/h, moisture $=30$ percent

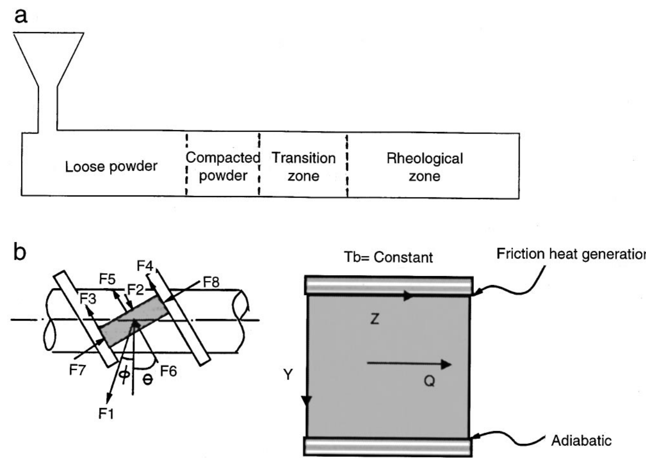

Fig. 22 (*a*) **Schematic of the various regions in food extrusion; (*b*) modeling of powder flow in a single screw extruder**

fer, considering both radiation and convection transport. This process is continued until the neck-down shape does not change from one iteration to the next. It was found that viscous and gravitational forces are dominant in the determination of the profile. Surface tension effects are small even though they are important in many other free boundary flows [79]. The external shear and inertial effects are small, as expected.

A typical example of the numerical generation of neck-down profile with a cosinusoidal starting profile is shown in Fig. 24(*a*). From the figure it is seen that during the first few iterations, the neck-down profile is quite unrealistic, with a flat region and an abrupt change in radius around where the starting polynomial profile ends. But after a few iterations the shape becomes smooth and monotonically decreasing, eventually reaching a steady, converged, profile, indicated by the invariance of the profile with further iterations. It must be mentioned here that the radius approaches the dimensionless fiber radius as the axial distance approaches the furnace exit. However, because of the small value of dimensionless fiber radius, the graphs seem to show that the value

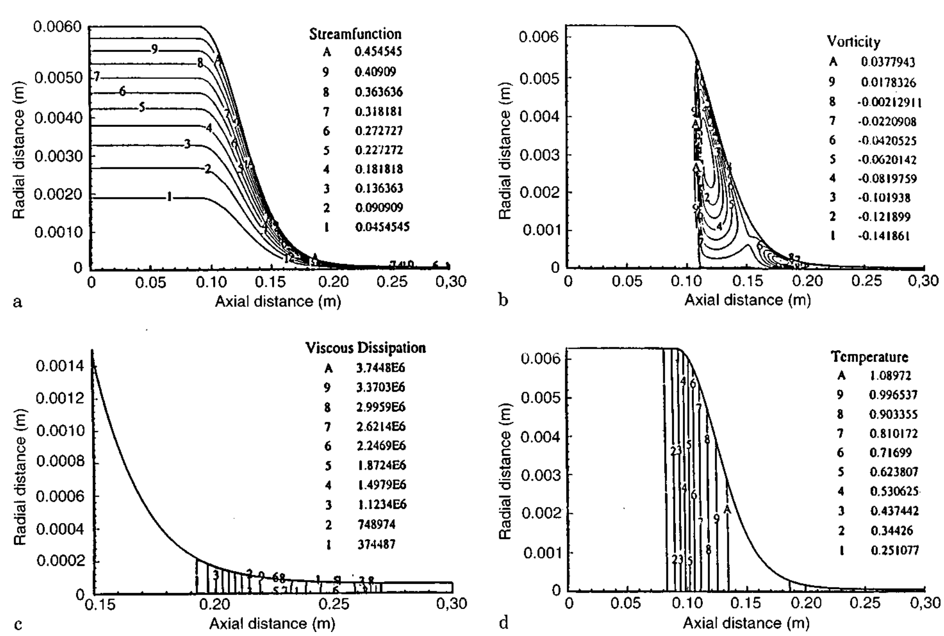

Fig. 23 Calculated (*a*) streamfunction, (*b*) vorticity, (*c*) viscous dissipation, and (*d*) temperature contours in the optical fiber drawing process for typical drawing conditions

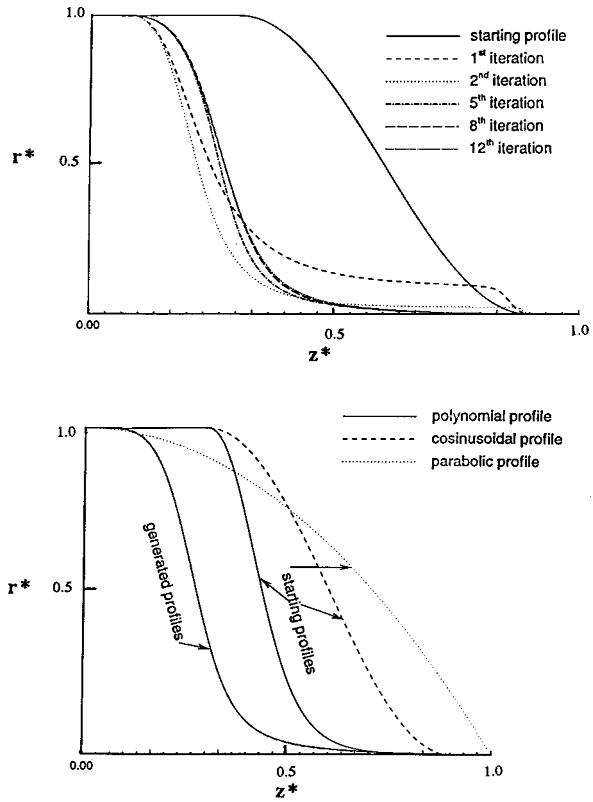

Fig. 24 Iterative convergence of the neck-down profile in optical fiber drawing. Here, $r^*=r/R$ and $z^*=z/L$, where R is the preform radius and L the furnace length.

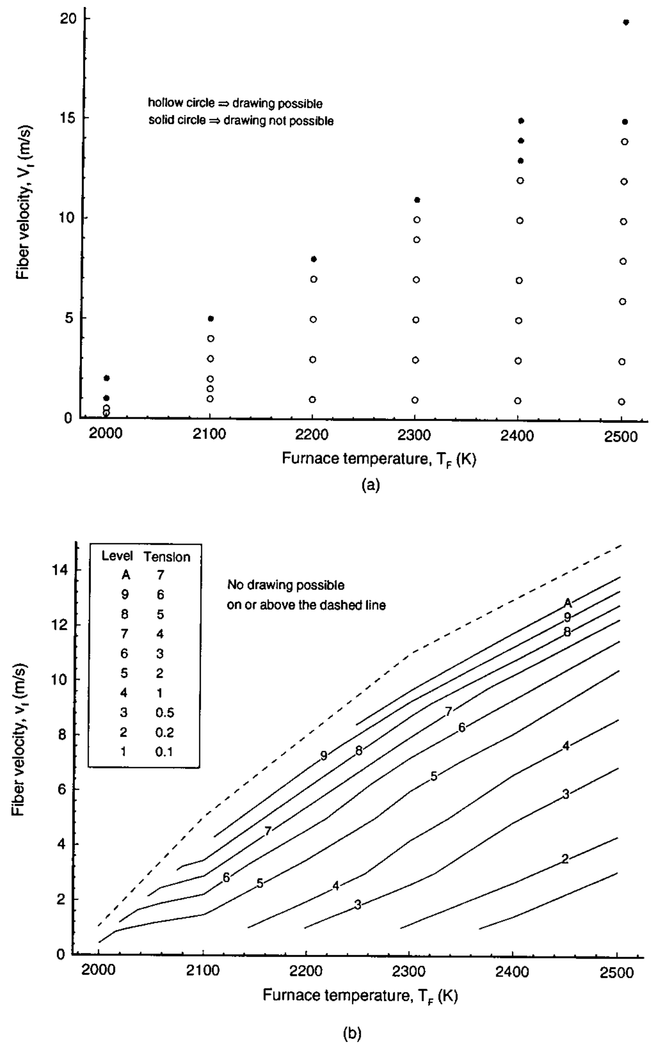

Fig. 25 Results obtained from a feasibility study of the fiber drawing process: (*a*) different cases studied, showing both feasible and infeasible combinations of parameters and (*b*) "iso-tension" contours for the feasible range of fiber drawing

approached is zero. For convergent cases, perturbations to the initial profile and different starting shapes lead to the converged neck-down profile, as seen in Fig. 24(*b*), indicating the robustness of the scheme and the stability of the drawing process. The force balance conditions were also closely satisfied if the iterations converged. However, convergence does not occur in every case, leading to a feasible domain, as discussed below.

Feasible Domain. It was shown by Roy Choudhury et al. [41] that, for given fiber and preform diameters and for a given draw speed, the fiber cannot be drawn at any arbitrary furnace wall temperature distribution. If the furnace temperature is not high enough, the iterative radius correction shows that the fiber breaks due to lack of material flow, a phenomenon that is known as viscous rupture [80]. Similarly, it can be shown that for a particular furnace temperature and fiber speed, the fiber can be drawn only if it is above a certain diameter. It can also be shown that for a given preform and fiber size, and with a given furnace temperature, there is a limit on the speed beyond which no drawing is possible, as this leads to rupture. Figure 25(*a*) shows the different cases studied, including the cases where drawing was feasible and the cases when it was not. From this figure, a region can be identified beyond which drawing is not possible. For the region where drawing is feasible, the draw tension is calculated. The "iso-tension" contours are shown in Fig. 25(*b*). As expected, the draw tension is low at higher temperatures and lower speeds, which explains the positive slope of the iso-tension contours. For a realistic fiber-drawing operation, these results are very important, since the operating parameters (such as furnace temperature and draw-down speed) can be identified so that a fiber of desired diameter can be drawn at the applied tension [81,82]. It must be pointed out that only a combination of fiber speed and furnace temperature has been considered here. It is possible to obtain similar results for different combination of other physical and process variables such as the external gas, flow velocity, flow configuration, furnace temperature profile, furnace size, etc. Thus, feasibility of the process is determined largely by fluid flow, as was the case in polymer processing.

Experiments. Experimental work on the flow and thermal transport in the optical fiber drawing is very complicated because of the high temperatures, high draw speeds and difficult accessibility into the furnace [74]. Most measurements have focused on the characteristics of the fiber for different operating conditions such as furnace wall temperature, draw speed and applied tension. Relatively few results are available that may be used for comparisons with numerical predictions. A comparison with the profile experimentally obtained by Paek and Runk [83] has been carried out. For the heat transfer coefficient distribution given by Paek and Runk, a parabolic furnace temperature profile has been used by Lee and Jaluria [17,18] to predict the maximum temperature in the preform/fiber and its location. The same parabolic furnace temperature profile, with a maximum temperature of 3000 K and minimum temperature of 2300 K, was used for obtaining the neck-down profiles [41]. From the analytical results obtained by Paek et al. [84], the draw tension plotted on a logarithmic scale is expected to vary linearly with the inverse of the furnace temperature. A comparison of the computed results with the experimental

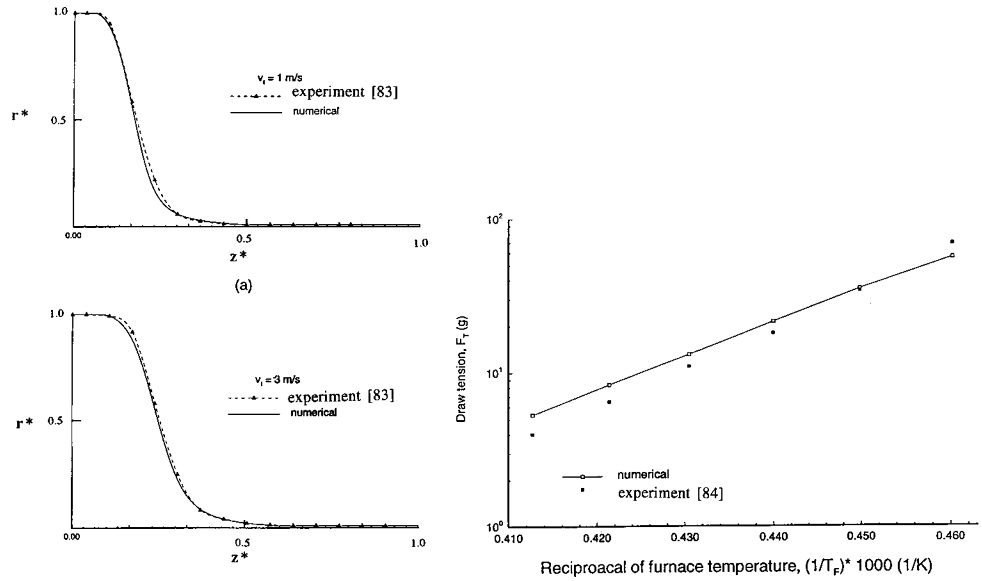

Fig. 26 Comparison of the numerical predictions of neck-down profile and draw tension with experimental results

data show good agreement, as seen in Fig. 26. The quantitative trend is reasonably good, even though the furnace temperature profile, except for the maximum value, is guessed, and all properties for fused silica are taken from the literature. These comparisons with experimental results lend strong support to the approach outlined here for determining the neck-down profile.

A study of the flow and thermal transport associated with the draw furnace require accurate knowledge of the furnace wall temperature distribution. An experimental procedure involving mounting rods of different materials and diameters and feeding them axially within the furnace cavity was employed for this purpose, see Fig. 27(*a*). Each rod was instrumented with thermocouples inserted through an axial hole along the centerline. The temperature measurements were used along with a numerical model for the flow and heat transfer in the furnace in order to obtain the furnace wall temperature profile [85]. This is an inverse problem since the centerline temperature in the rod is known whereas the furnace thermal conditions are not known. The results obtained using the graphite rods suggest that the furnace temperature is not affected by rod size. Figure 27(*b*) shows the computed temperature distribution along the graphite heating element. The dashed lines represent the water cooled portion of the furnace cavity. The convergence of the optimization method used for deriving the heating element temperature distribution is demonstrated by the agreement between the predicted and measured rod temperatures. The computed maximum element temperatures were in good agreement with the furnace sensor temperature at the hot zone centerline, lending support to the model for the flow and thermal transport in the furnace. The small difference between the computed element temperatures for the two rod sizes is in support of the previous statement that there was a small influence of rod size on the furnace temperature distribution. However, the effect of larger than the presently used rod sizes on furnace temperature needs further investigation. Similar results were obtained for the other furnace temperatures and for other materials, including silica glass [86].

Coating. As shown in the schematic diagram of the typical fiber drawing process in Fig. 1(*a*), the fiber is cooled as it moves toward the coating section where it is coated with a jacketing material for protection against abrasion, to reduce stress induced microbending losses, and for increased strength. The upper temperature at the coating section is limited by the properties of the coating material used. For commercial curable acrylates, this tem-

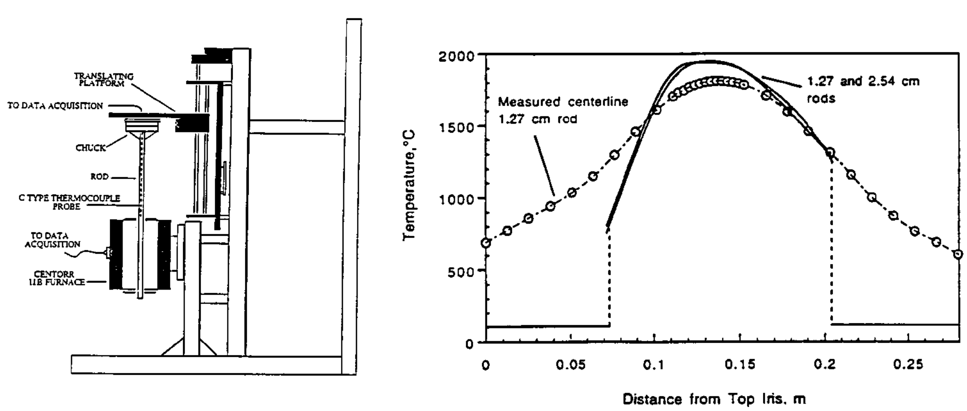

Fig. 27 (*a*) Schematic of an experimental system for measuring the temperature distribution in a rod located in an optical fiber drawing furnace; (*b*) computed furnace temperature distributions (solid line) from graphite rod data. Experimental points are from the 1.27 cm diameter rod.

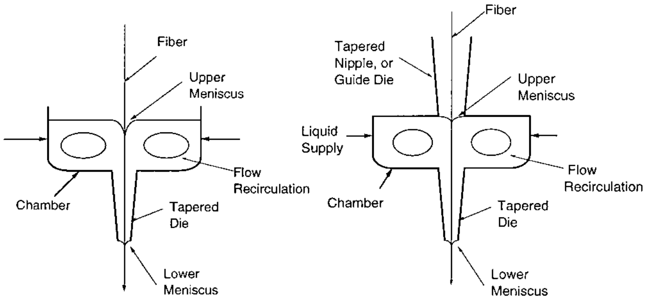

Fig. 28 Sketch of the flow in the chamber and the die for (*a*) an open cup, and (*b*) a pressurized coating applicator, showing the upper and lower menisci

perature generally cannot exceed 150°C. The wet coating is then cured by ultra-violet radiation as it passes through the curing station, and finally the fiber is spooled around a takeup drum at the base of the tower.

The basic coating process involves drawing the fiber through a reservoir of coating fluid from where it is passed through a die that may be used to control the thickness and the concentricity of the coating layer. Coating thickness may also be controlled by ''metering'' the flow rate, while a flexible exit die may be used for centering the fiber. This is immediately followed by a curing process that results in solidification of the coating material around the fiber. Figure 28 shows schematic diagrams of typical coating applicator and die systems. Viscous shear due to the moving fiber results in a circulatory fluid motion within the fluid. This problem is very similar to polymer flow in a channel or die, as discussed earlier. A balance between surface tension, viscous, gravitational, and pressure forces results in an upstream meniscus at the cup entrance [87–90]. This consideration is similar to that employed for determining the neck-down profile in fiber drawing and a similar approach may be used in this case too. A downstream meniscus at the die exit results primarily from a balance between viscous and inertia forces, the surface tension being a relatively small effect. Centering forces within the tapered die contribute to the positioning of the fiber at the die exit center. Successful coatings are concentric, of uniform thickness, and free of particle inclusions or bubbles. Excellent reviews of much of the earlier investigations on fiber coatings have been presented by Blyler et al. [91], Li [14], and Paek [92].

The use of high draw rates requires consideration of alternate pressurized applicator designs, where pressure induced motion of the coating material is used to reduce the shear at the fiber surface and probably results in the establishment of a stable free surface flow, though this aspect needs further investigation. An additional benefit resulting with such pressurized dies has been the incorporation of gas bubble reducing, or bubble stripping, designs which have resulted in minimizing gas bubbles entrained at the coating cup entrance and then trapped within the coating layer. The physical and rheological properties of coating materials and their temperature dependence are particularly important for the flow within the applicator. However, accurate property data are generally not available. Coating layer thicknesses range between 30 and 300 μm.

Several investigators have focused their attention on air entrapment by the moving fiber and the resulting deterioration of the coating. The characteristics of the meniscus, particularly its stability, have been studied in detail. Ejection of air bubbles by tip streaming from interface cusps near the fiber was investigated [93]. The dynamic meniscus in pressurized and unpressurized fiber coating applicators was studied in detail, experimentally and numerically, by Ravinutala et al. [94], following an experimental study by Abraham and Polymeropoulos [95]. Figure 29 shows images of the meniscus formed with the fiber moving into an unpressurized open cup applicator, as well as inside a micropipette tube with a pressurized applicator. The fiber speed was 20 m/min. In both cases, the dynamic contact angle was near 180 deg. Figure 29 A clearly shows the breakdown of the meniscus into saw tooth patterns and tip streaming as previously observed. On the other hand, the pressurized applicator meniscus image, Fig. 29 B, appears to be smooth, suggesting suppression of large scale breakdown at the same fiber speed. Figures 29 C and D are low magnification images clearly demonstrating that the unpressurized meniscus generates a large number of relatively large air bubbles compared to the pressurized meniscus in Fig. 29 D where air bubbles are probably too small to be detected. Comparison of the shape of the menisci in Figs. 29 A and 29 B shows that the effects of pressure and geometry are to flatten the meniscus and to increase the slope of the liquid-air interface near the fiber compared to those for an unpressurized meniscus. This probably results in a smaller air volume available for entrainment accounting for the difference between Figs. 29 C and 29 D. Numerical modeling results were found to agree closely with the experimental observations on the flow and pressure distributions. However, further investigation is clearly needed to understand the effect of pressure on air entrainment and to design applicators and dies to obtain high-quality fiber coatings.

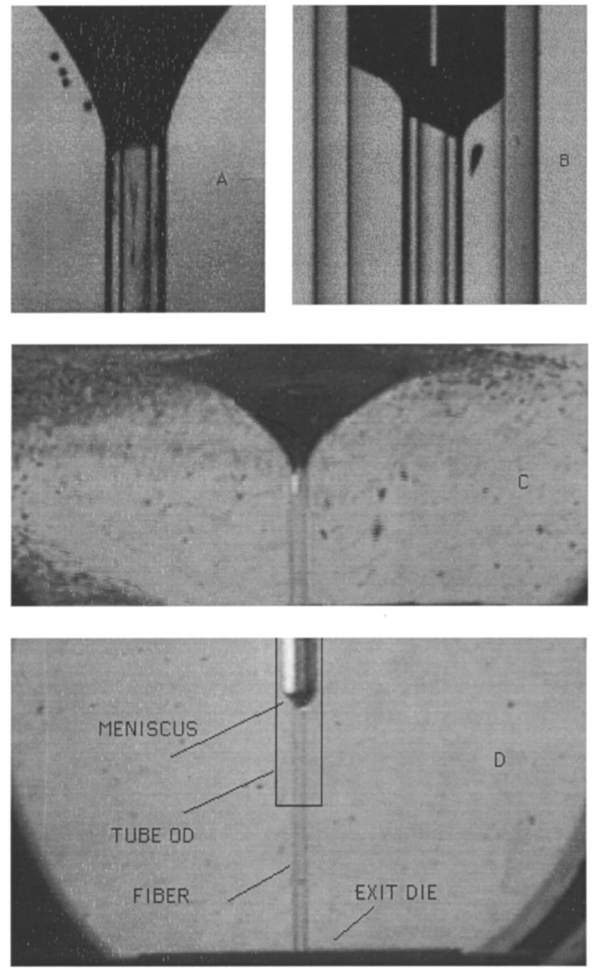

Fig. 29 (A, C) Unpressurized test section; (B, D) Meniscus in 630 μm diameter tube, test section pressurized. Fiber speed =20 m/min.

Additional Aspects. The main considerations that arise in the drawing of optical fibers are outlined in this section. The problem is an extremely complex one, though it is also a very important material processing technique because of the tremendous worldwide demand for optical fibers. This has led to increasing draw

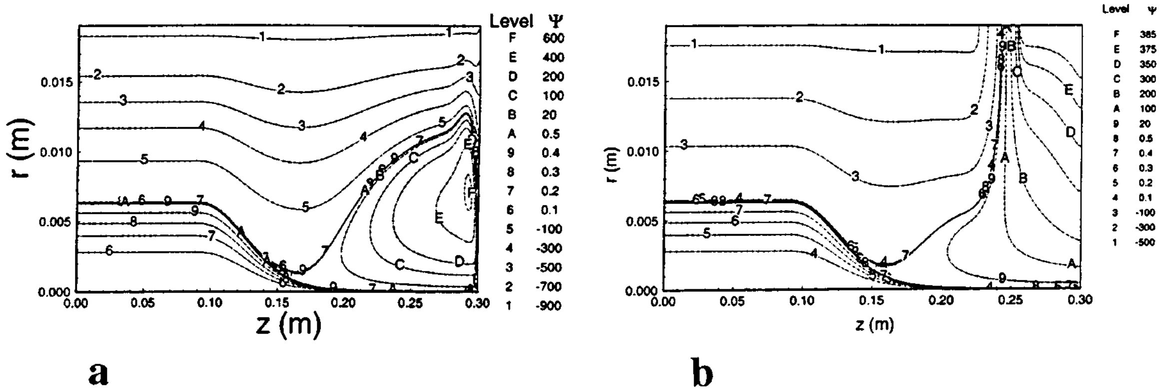

Fig. 30 Inert gas flow field in the optical fiber drawing furnace for two geometrical configurations: inlet flow in opposite direction to fiber motion and side entry

speeds and preform diameters, resulting in stringent requirements being applied to both the process and to its modeling. The fiber has to be cooled rapidly in order to reach appropriate temperature levels before coating is applied. Substantial work has been done on the flow in the forced cooling process, considering laminar and turbulent flow in the cooling section [74,96]. This is similar to the continuous processing problem, considered later in this paper.

The flow of inert gases in the draw furnace plays a very important role in the transport processes within the furnace and thus in the flow and heat transfer in the glass. However, the flow is a strong function of the geometry, particularly the locations of the inlet/outlet channels, and of the flow rate. The flow can affect local transport rates and thus cause local hot or cold spots. Figure 30 shows the calculated flows for two different configurations. The side inlet, though more convenient to design and operate [81], directs the cold fluid at the fiber, causing possible local cooling and breakage. Similarly, flows that aid or oppose fiber motion respectively increase or decrease the heat transfer, significantly affecting the process.

Defects are another important consideration, because these affect the quality of transmission in the fiber and the distance one could go without enhancing the signal. Many defects are generated by the thermal field and the flow, and enhanced cooling could affect the distribution and retention of these defects. The glass flow also affects the distribution of these defects, as well as of dopants put into the preform to obtain specialized fibers. Several studies have considered the kinetics of thermally induced defects [97,98]. Yin and Jaluria [82] used the equation for the kinetics of these defects to obtain their concentrations as functions of location and operating conditions. The approach is similar to that for the inclusion of chemical kinetics in other materials processing cases, such as in food and reactive polymer extrusion considered earlier.

Summary. The flow of glass and inert gases in the furnace affect the heating up of the glass preform and the neck-down profile, which in turn affect the temperature field, the generation of defects, the tension in the fiber, and the distribution of impurities and dopants. Similarly, the flow in the coating process affects the menisci, which determine the entrapment of bubbles and the uniformity, thickness and concentricity of the coating. Thus, the flow strongly affects fiber quality as well as the stability and feasibility of the process.

Casting. Solidification and melting processes have been studied extensively because of their importance in a wide variety of processes such as casting, crystal growing, welding, and polymer injection molding, considering pure materials as well as mixtures such as alloys [99–103]. As mentioned earlier, the natural convection flow in the liquid or melt region is solved and coupled with the transport in the solid. The location of the moving boundary is not known and must be obtained from the solution, as is the case for mold casting shown in Fig. 1(*c*). A coordinate transformation, such as the Landau transformation, which was also used for the neck-down region in optical fiber drawing, may be employed to make the computational domains rectangular or cylindrical, from the complicated ones shown [24,104,105]. This considerably simplifies the numerical procedure by allowing a regular rectangular or cylindrical mesh to be used. Several other techniques have been developed to treat such moving boundary problems and the complicated domains that arise. For the continuous casting problem of Fig. 1(*b*), the interface between the solid and the liquid is not known at the onset and an iterative procedure may be adopted to determine its shape and location. Again, body fitted coordinates may be employed to approximate the irregular shaped computational domains. Of course, if the enthalpy model is employed, the entire region is treated as one, considerably simplifying the computational procedure. Interest lies in obtaining high quality castings, with few voids and defects, good grain structure and low stresses, at high production rates.

Figure 31 shows the numerical results for melting in an enclosed region using the enthalpy model. Streamlines and isotherms are shown for four different times during the melting of pure Gallium. This is a benchmark problem in which melting is initiated by a step change in the temperatures at the left and right boundaries, the left being at temperature higher than the melting point and the right lower. The streamlines indicate the effect of thermal buoyancy which causes the interface between the solid and the liquid to bend, rather than remain parallel to the vertical boundaries. The amount of material melted increases with time till it reaches a steady state for this problem. The recirculation in the liquid is clearly seen. These results are found to agree well with experimental results available in the literature [16]. The two-region approach can also be used for modeling this problem. For pure metals, the two-phase, two-region, approach leads to more accurate results, whereas the enthalpy method is more useful for alloys and mixtures. A lot of work has been done on such melting and solidification problems, as reviewed by Viskanta [16,100].

Conjugate transport is also important in these problems, as was also the case in polymer extrusion and optical fiber drawing. Figure 32 shows typical numerical results when conduction in the mold is coupled with heat transfer in the liquid and the solid [106]. With increasing time, the liquid region shrinks due to solidification, whereas the solidified region increases. The effect of the imposed conditions at the outer surface of the mold on the solidification process can be investigated by solving this conjugate problem, which yields the temperature field in the mold along with that in the solid and the liquid, as shown. Banaszek et al. [107] carried out experiments and numerical simulations to demonstrate the importance of conduction in the wall, as shown in Fig. 33. Such numerical and experimental studies can be used to

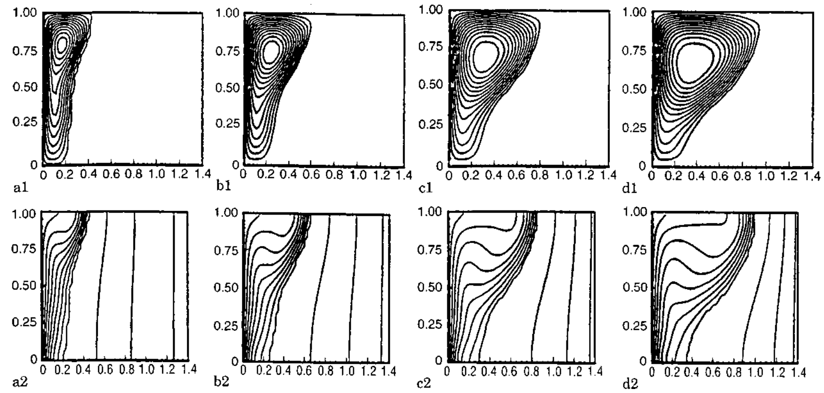

Fig. 31 Streamlines (1) and isotherms (2) for melting of Gallium in an enclosed region, with the left vertical boundary at a temperature higher than melting point, the right vertical boundary at a temperature lower than melting point and the remaining two boundaries insulated. The enthalpy method is used and results are shown at different dimensionless time t following the onset of melting. (*a*) t=0.5248, (*b*) t=1.0416, (*c*) t=1.5622, (*d*) t=1.9789.

determine the progression of the solidification front and thus monitor the generation of voids and other defects in the casting.

Experimental studies have been relatively few because of the complexity of the process arising from a moving interface and time-dependent flow [108,109]. However, detailed experimental results are needed to critically evaluate the various models employed for simulation as well as to provide information on the characteristics of the interface for development of microscale models. Figure 34 shows typical experimental results, along with numerical predictions, for the melting and solidification of pure tin [110,111]. The comparisons are fairly good, though the differences at small time indicate the need to improve the model to more closely approximate the experimental conditions.

Alloys. There has been a growing interest in the basic characteristics of solidification for mixtures, particularly alloys, as reviewed by Prescott and Incropera [103]. Combined heat and mass transfer processes arise in this case and significantly affect the flow. Figure 35 shows a schematic of the double-diffusive convective flow that arises and increases in intensity with time. The left wall is heated and solidification occurs on the right wall. As the salt-enriched liquid is ejected from the mushy zone, it forms a layer at the bottom and subsequently additional layers arise, with recirculation in each layer driven by horizontal temperature gradients. Lower heat transfer at the bottom results in larger mushy region thickness [112]. Many interesting experiments on the solidification of aqueous NH_4Cl solutions and other such fluids have been carried out to study the flow structure [101–103]. Similarly, interest lies in understanding microscopic phenomena associated with solidification. This is an area of intense current research work. The solidification front can be divided into various morphological forms such as planar, cellular and dendritic. Various mod-

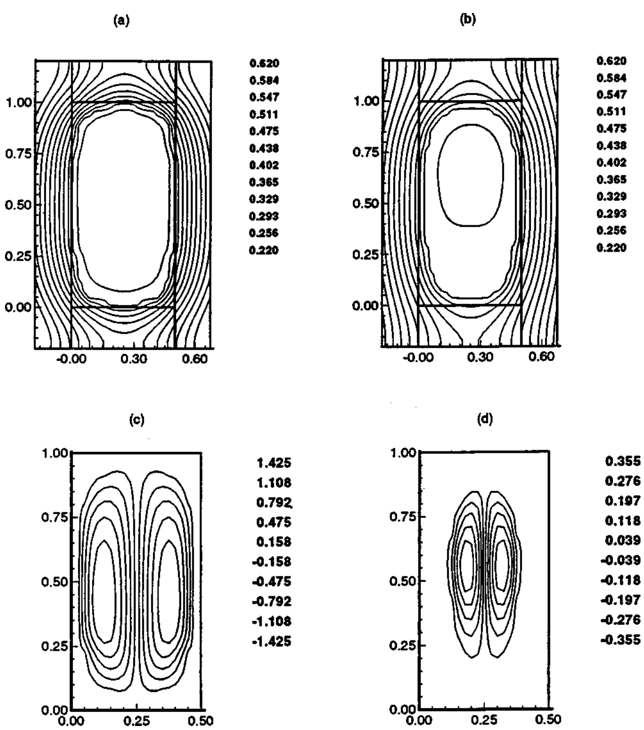

Fig. 32 Isotherms (*a,b*) and streamlines (*c,d*) for solidification in a cavity with conjugate transport to the mold. (*a, c*) t=0.05, and, (*b, d*) t=0.1.

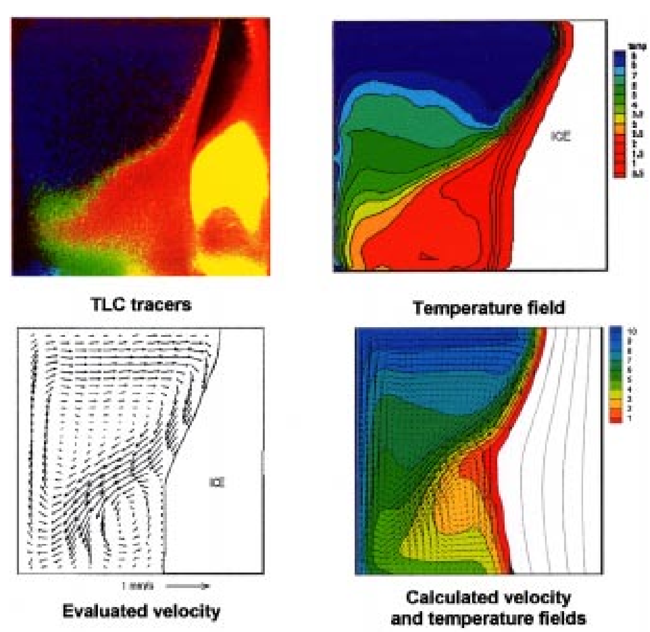

Fig. 33 Experimental and numerical results for water solidification driven by convection and conduction

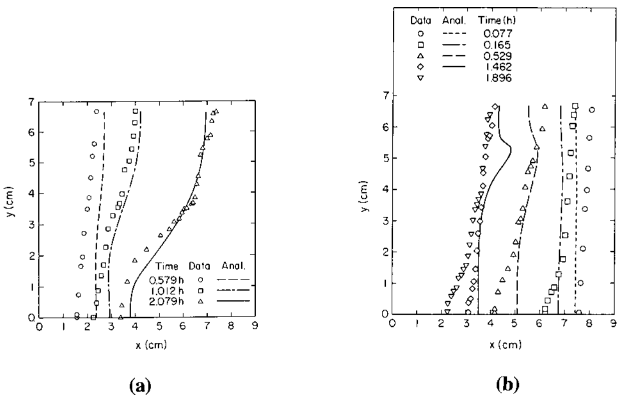

Fig. 34 Comparison between measured and predicted interface locations during (*a*) melting, and (*b*) solidification of pure tin from a vertical surface [110,111]

els have been proposed and experiments carried out to characterize such structures and growth [113,114]. For instance, Fig. 36 shows equiaxed and columnar denritic crystals. Averaging volumes and dendrite envelopes that may be used for modeling of the microscopic phenomena are shown.

The numerical results for continuous casting are shown in terms of isotherms in Fig. 37, again using the enthalpy method [115]. The material is *n*-octadecane which starts as a liquid at the top and solidifies as it flows through a mold. The buoyancy effects in the flow are found to be small in this case. The shaded region indicates the demarcation between pure liquid and pure solid. Therefore, the liquid fraction f_1 is 1.0 at the top of the shaded region and zero at the bottom of this region. A value of 0.5 may be taken to represent the liquid-solid interface, but the enthalpy method yields a finite region over which solidification is predicted to occur. It is seen that the material solidifies over a shorter distance at a larger value of the heat transfer rate, indicated by the Biot number, as expected.

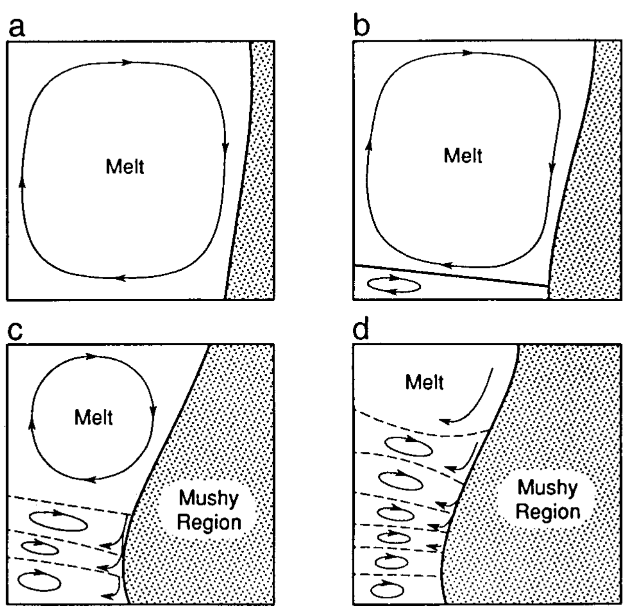

Fig. 35 Schematic of double-diffusive convection during solidification of aqueous Na_2CO_3 solution at various times following start of the solidification process. (*a*) 10 min; (*b*) 30 min; (*c*) 75 min, and (*d*) 150 min [112].

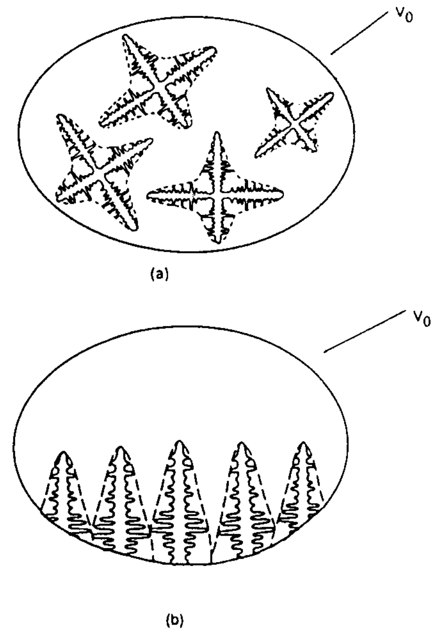

Fig. 36 Schematic illustration of the averaging volume and the dendrite envelopes for (*a*) equiaxed growth and (*b*) columnar growth [113]

Polymer Melting and Solidification. In many polymer processing applications, the melting and solidification of the material is an important consideration. In injection molding, for instance, the molten polymer is injected under pressure in a mold and, after the mold is filled, the material is allowed to cool and thus solidify. Solidification in extrusion dies and in channels leading to a mold is not desirable since it affects the flow and the pressure due to the resulting blockage. The basic flow configuration is shown in Fig. 38(*a*), indicating a solidified layer near the boundaries and flow in the central core. Work has been done on this problem using the enthalpy approach discussed earlier. The interface between the solid and melt regions, and the velocity and temperature distributions are computed [116]. Some typical results are shown in Figs.

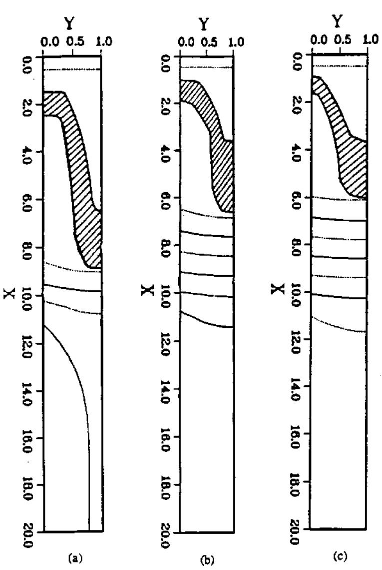

Fig. 37 Effect of cooling rate at the mold in terms of the Biot number Bi on the solidification in vertical continuous casting of n-octadecane, using the enthalpy method. (*a*) Bi=0.05, (*b*) Bi=0.1, (*c*) Bi=0.15.

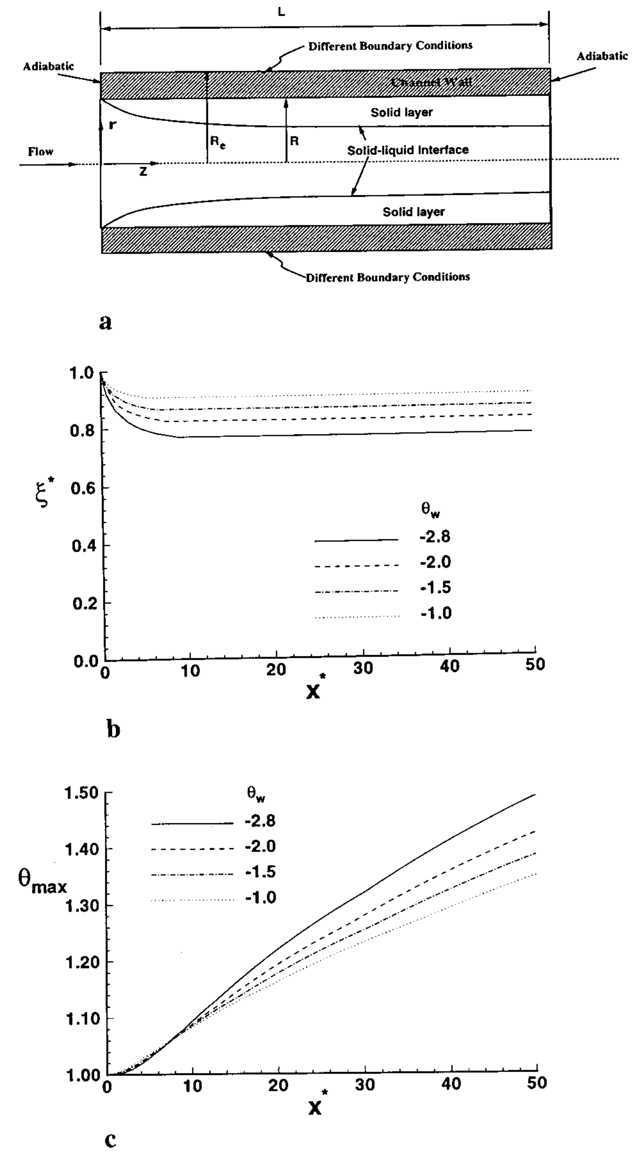

Fig. 38 (*a*) Schematic of polymer solidification in a channel; (*b*) dimensionless solid-liquid interface ξ^*; and (*c*) maximum temperature $\theta_{\max}$ in the melt, for different outer wall temperatures θ_w

38(*b*) and (*c*). It is interesting to note that as the temperature at the boundary is decreased, the thickness of the solidified layer increases, resulting in greater blockage to the flow. This, in turn, causes increased viscous dissipation, which heats up the fluid flowing in the central region. Thus, lowering the wall temperature ends up increasing the fluid temperature over the parametric ranges considered here. Complete blockage is not found to occur because of increased viscous dissipation effects with greater blockage.

Summary. The preceding discussion outlines only a few important aspects in the modeling of material processing techniques based on phase change. More work is clearly needed on coupling microscale phenomena with the overall macro-model of the process and the system. However, recent studies have led to a much better understanding of the solidification process than what was available before. The flow affects the heat and mass transfer processes, which in turn influence the characteristics of the melt-solid interface and the rate of melting/solidification. The flow also affects the quality of the product because of undesirable oscillations, generation of voids, and distribution of impurities.

Continuous Processing. A continuously moving material undergoing processing results in another important complication in the numerical simulation and experimentation of manufacturing processes. The cooling of the moving optical fiber before coating is an example of such processing. If the location of the moving surface is known, as is the case for the circumstance of Fig. 7(*b*), the continuous movement of the boundary may be replaced by steps, so that the length L is held constant over a time increment Δt and the transient conduction problem is solved over this interval. The length L is then taken at the increased value for the next time interval, with the additional finite region adjacent to the base taken at temperature T_0, and the computation is carried out for this interval. The procedure is carried out until results are obtained over a given time interval or until the steady state circumstance is obtained [20]. The corresponding initial and boundary conditions are

$$t=0:\ L(t)=0$$

$$t>0:\ \text{at}\ x=0,\ \ T=T_0;\ \ \text{at}\ \ x=L(t), -k\frac{\partial T}{\partial x}=h_L(T-Ta) \tag{38}$$

where h_L is the heat transfer coefficient at the end of the moving rod. The problem may be solved analytically [49] or numerically, with the latter approach more appropriate for two- and three-dimensional problems. As time increases, the length of the rod L increases and the temperature at the end decreases. At large time, a steady-state distribution arises over the rod and the temperature at the moving end reaches the ambient temperature. The problem may then be solved as a steady, continuously moving, infinite rod case.

Conjugate conditions are very frequently encountered in manufacturing processes like hot rolling, extrusion, metal forming and fiber drawing, which was discussed earlier. Conjugate conditions arise at the surface and the convective transport in the fluid must be solved in conjunction with conduction in the moving solid [117]. The region near the point of emergence of the material has large axial gradients and require the solution of the full equations. However, far downstream, the axial diffusion terms are small and a parabolic, marching, scheme may be adopted. This reduces the computational time, as compared to the solution of the elliptic problem over the entire computational domain. In continuous processing, interest lies in controlling the local and global processing of the material to obtain uniformity, high productivity, and desired product characteristics.

Figure 39 shows the typical streamlines for a plate moving in a quiescent medium. The ambient fluid is drawn toward the moving surface. Large pressure gradients directed towards the origin give rise to a small reverse flow in this region. Farther downstream, this effect dies down and the flow approaches the characteristics of a boundary-layer flow, with its thickness growing in the direction of motion. The inclusion of buoyancy effects due to a heated plate increases the maximum velocity in the boundary layer, beyond the plate speed U_s, if the buoyancy and the plate motion are both directed upward, as shown in the figure. This, in turn, increases the heat transfer from the plate. Similarly, other orientations have been investigated.

The time-dependent flow that arises at the initial stages of the process is also important. Figure 40 shows the numerical results for an aluminum plate moving vertically upward in water. A long plate is assumed to start moving at time $t=0$, when the upstream temperature is also raised to a temperature T_0 which is higher than the ambient temperature T_a. The flow is seen to start near the moving boundary due to the no-slip conditions. A recirculating flow region appears near the heated end, gradually moves downstream, and is finally swept away by the flow. The boundary layer thickness grows along the direction of motion. The heat transfer

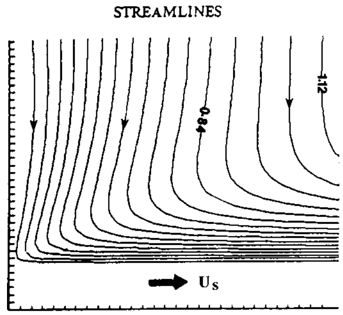

(a)

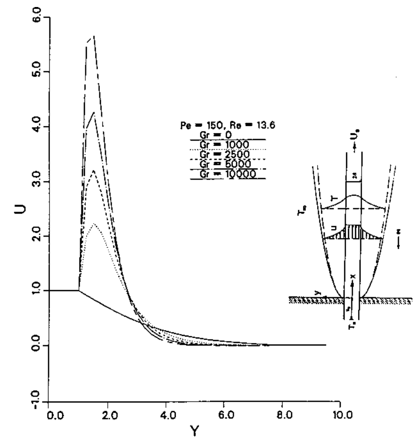

(b)

Fig. 39 (*a*) Flow in the ambient fluid due to a continuously moving material; (*b*) dimensionless velocity (u/U_s) distribution in the fluid due to a vertically moving heated plate with aiding buoyancy effects

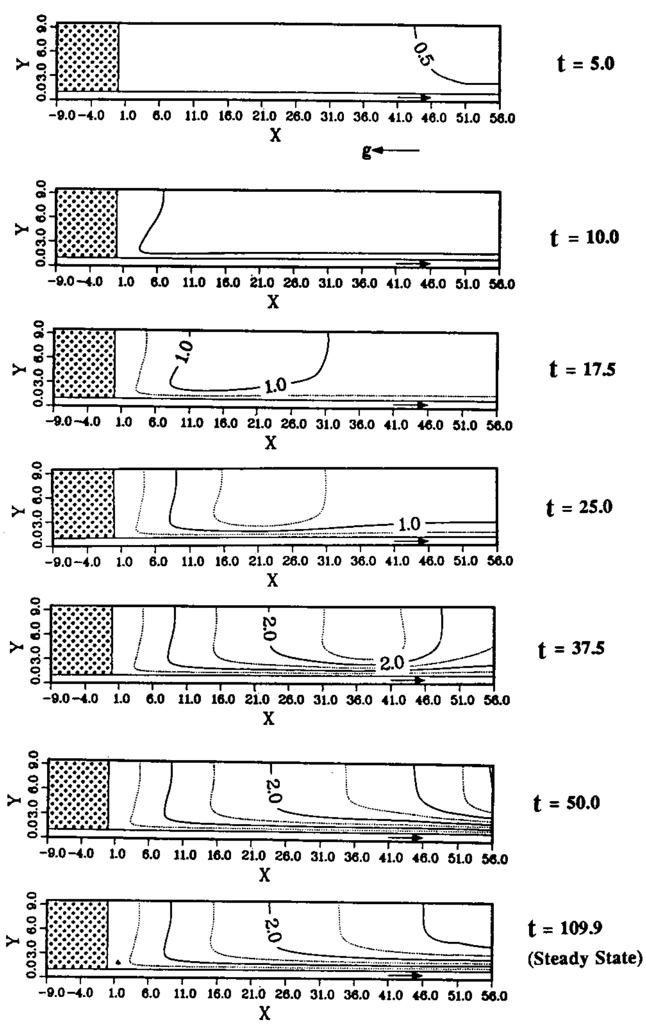

Fig. 40 Calculated time-dependent streamlines for a heated aluminum plate moving vertically in water at Pr=7.0, Re=25, and Gr=1000

coefficient from the plate was found to reach a minimum near the recirculation region. Local hot spots can thus arise in this region. Buoyancy effects were found to increase with time as the fluid temperature rises. Therefore, the transient flow and the heat transfer rates can be substantially different from steady state conditions which are eventually reached and which agree well with experimental results. Many different fluids, materials, and flow condi-

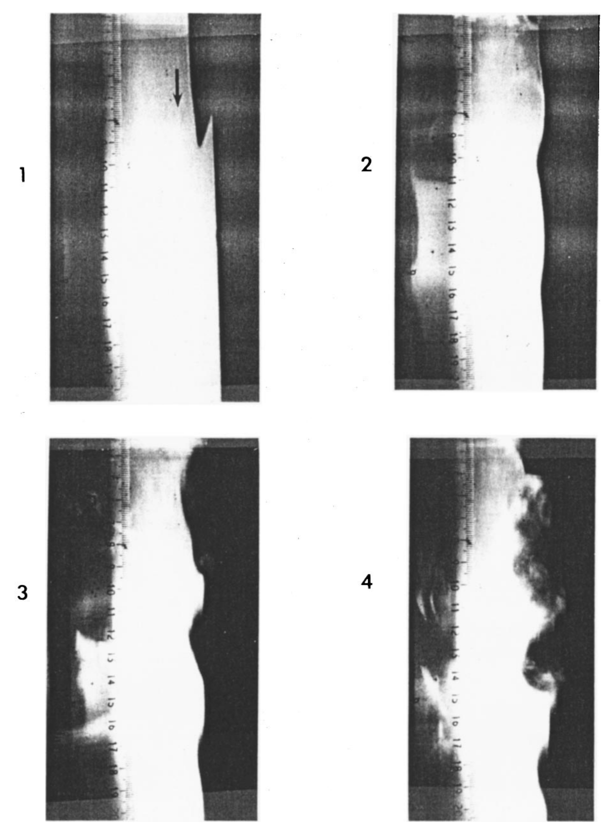

Fig. 41 Sequence of shadowgraph photographs showing the flow near the surface of an aluminum plate moving vertically downward in water at a speed of 3.7 cm/s, at Re=140.36 and Gr/Re^2=0.45

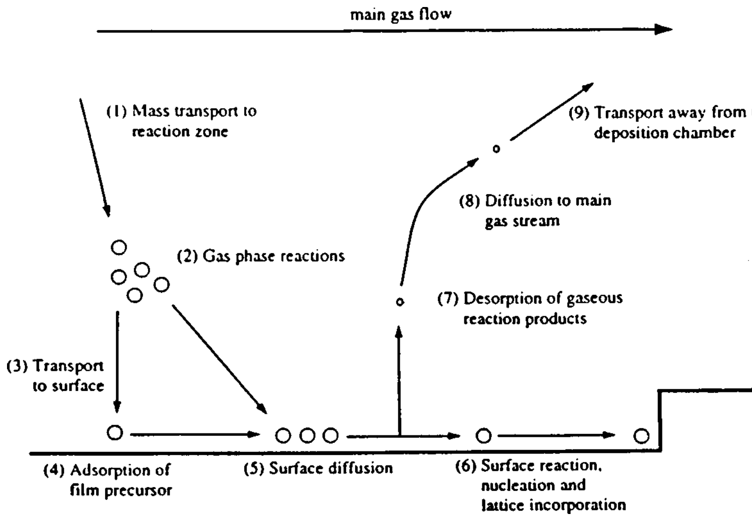

Fig. 42 Schematic of steps in a chemical vapor deposition process [34]

tions, including channel flows and the effect of buoyancy, have been considered for a wide variety of applications in materials processing [20].

A few experimental investigations have also been carried out on this problem and provide the results that can be used for the validation of the mathematical/numerical model [118–120]. Generally, good agreement has been obtained between numerical and analytical predictions and experimental results for a wide range of materials, geometries and speeds. However, the occurrence of instability, transition and turbulence at large speeds or at large temperature differences has been found to increase the difference between numerical and experimental results, indicating the need for better modeling of these flows. Figure 41 shows a sequence of shadowgraph photographs of the flow near the surface of an aluminum plate moving vertically downward. As time increases, a large disturbance leading to flow separation is seen to arise. The flow under consideration is an opposing buoyancy circumstance, which could lead to flow separation downstream [22]. The disturbance was found to remain largely at one location and not move downstream, indicating that the observed phenomenon is due to opposing buoyancy and not transient effects. The effect is governed by the local mixed convection parameter $Gr_x/Re_x^2 = g\beta\Delta Tx/\nu^2$, and the effect was found to be larger at larger values of this parameter. Such disturbances in the flow affect the local transport at the surface and thus the local characteristics of the product. It is important to understand and control these effects for better consistency in the processed material.

Summary. The flow is driven by forced flow mechanisms, due to the moving surface and external pressure field, as well as by buoyancy effects. Thus orientation and geometry are often important considerations in determining the flow. The flow field influences the thermal transport that can affect the local and average processing undergone by the material. Transient effects are important at the initial stages of the process and also if changes occur in the operating conditions.

Chemical Vapor Deposition. The deposition of thin films on- to a solid substrate has become an important technique for materials processing and is of interest in a wide variety of applications such as those involved with the fabrication of microelectronic circuits, optical and magnetic devices, high performance cutting and grinding tools, and solar cells. Though a relatively new method for materials processing, thin film deposition has attracted the interest of many researchers because of its relevance to many important areas, high quality of material generated, good control of the process and overall efficiency of the process.

Thin films are generally deposited from a gas phase onto a solid surface. A chemical reaction takes place during the deposition process and this is referred to as chemical vapor deposition (CVD). The products of the reactions form a solid crystalline or amorphous layer on the substrate. The activation energy needed for the numerous chemical reactions is provided by an external heat source. After material deposition on the surface, the byproducts of the reactions are removed by carrier gases [34]. The sequence of events involved in a CVD process are shown schematically in Fig. 42. Film thicknesses range from a few nanometers to tens of microns. The quality of the film deposited is characterized in terms of its purity, composition, thickness, adhesion, surface morphology and crystalline structure. The level of quality needed depends on the intended application, with electronic and optical materials imposing the most stringent demands. In order to improve the quality of the film deposited, it is necessary to understand the basic mechanisms that govern the access of the appropriate chemical species to the substrate. This in turn depends on the flow, the associated heat and mass transfer in the flow region and at the surface, and chemical reactions that arise. Large area

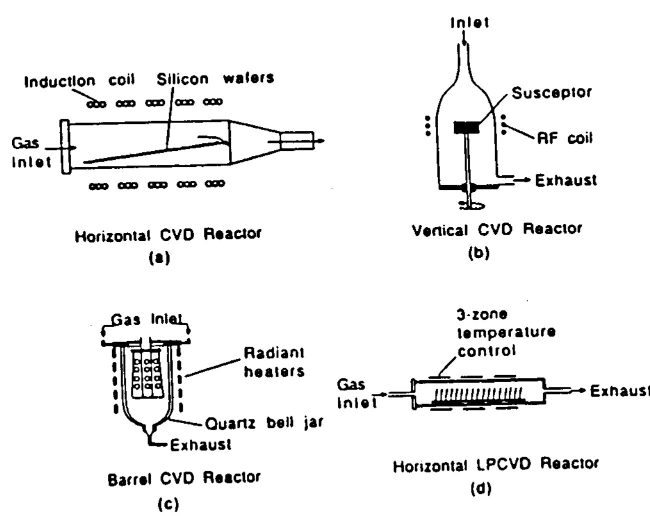

Fig. 43 Practical CVD reactor configurations: (*a*) horizontal reactor, (*b*) vertical reactor, (*c*) barrel reactor, (*d*) conventional multiple-wafer-in-tube low-pressure reactor [33]

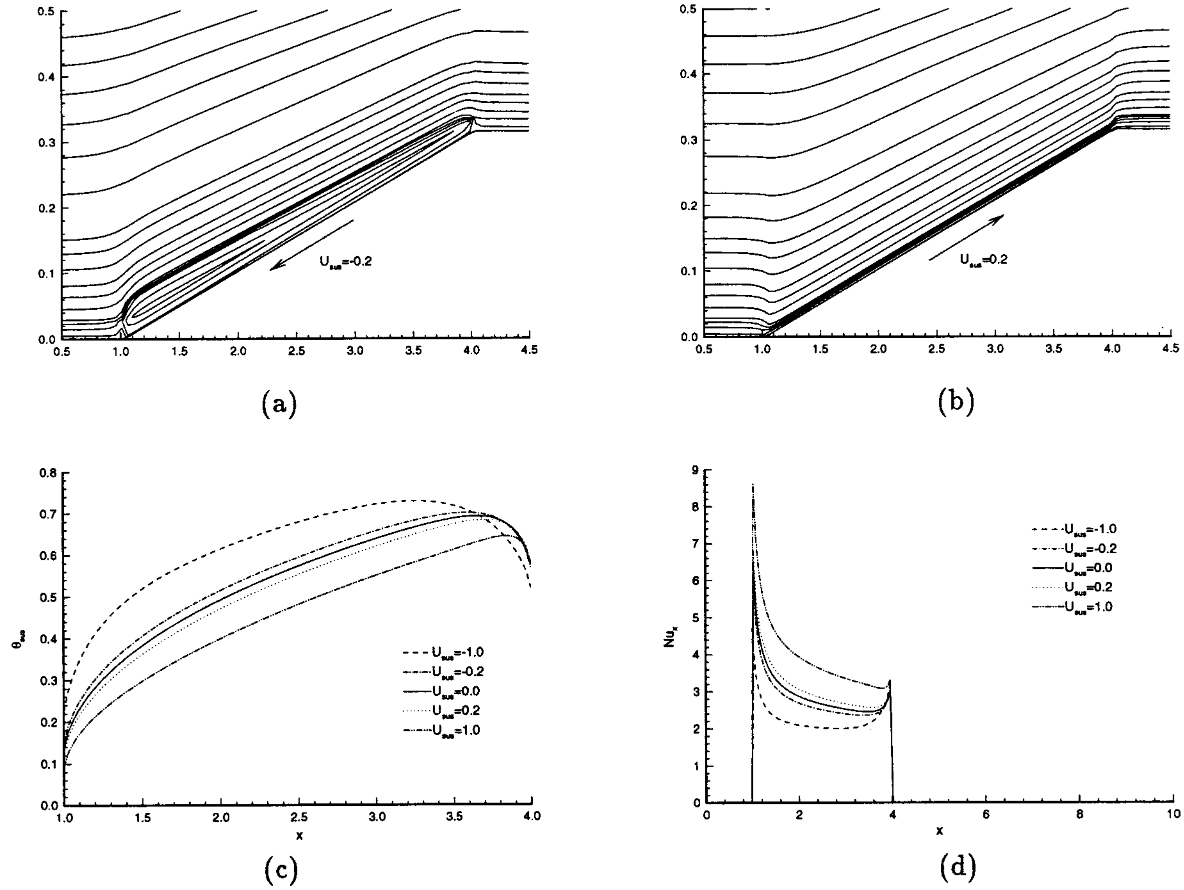

Fig. 44 Computed streamlines, temperature distribution, and Nusselt number for different values of dimensionless susceptor velocity U_{sus}

film thickness and composition uniformity are achieved by proper control of the governing transport processes [33,34].

Many different types of CVD reactors have been developed and applied for different applications. Most reactor configurations can be classified into two general classes; the horizontal and the vertical reactor. In the horizontal reactor, the heated susceptor on which deposition is to be obtained is placed at an angle to the incoming horizontal flow. The vertical flow reactor has the susceptor positioned perpendicular to the downward flow. Both types of reactors are commonly used. A few practical CVD reactor configurations are shown in Fig. 43. In most cases, a batch process is used, with the susceptor stationary or rotating, and after the process is completed the susceptor is removed and a new charge undertaken. Though much of the initial effort was directed at silicon deposition because of its relevance to the semiconductor industry, much of the recent interest is directed at the deposition of materials such as titanium nitride, silicon carbide, diamond, and metals like titanium, tungsten, aluminum, and copper.

The quality, uniformity, and rate of deposition are dependent on the fluid flow in a CVD reactor, on the heat and mass transfer, and on the chemical reactions that are themselves strongly influenced by temperature and concentration levels. Mahajan [34] has presented an excellent review on CVD for materials processing. The flow and heat transfer in CVD reactors were investigated by Evans and Greif [121], Fotiadis et al. [122] and Karki et al. [123]. These studies used numerical models based on parabolic governing equations along with experimental data to verify numerical predictions. Analytical models using similarity variables had been used in earlier work, followed by numerical models using boundary layer approximations. One and two dimensional studies were carried out by Fotiadis et al. [122] using finite element methods (FEM). This is appropriate for complex geometries encountered in some CVD processing systems. Rotating susceptor, three dimensional flow, and experimental measurements have also been considered in various investigations.

Figure 44 shows some typical results obtained with a moving susceptor by Chiu and Jaluria [124]. Both analysis and experimen-

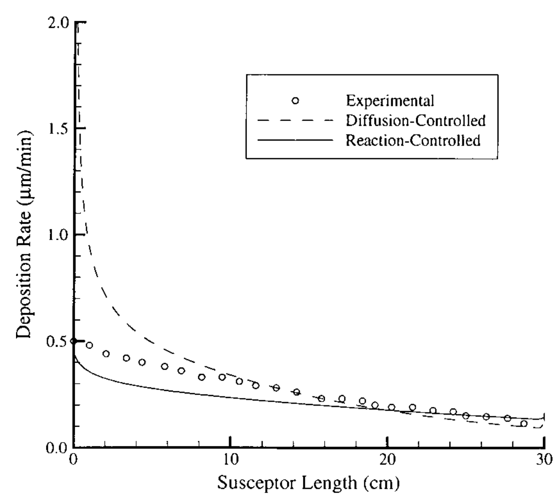

Fig. 45 Comparison between numerical predictions, using the diffusion-controlled approximation and the reaction-controlled chemical modeling, and experimental results of Eversteyn et al. [125]

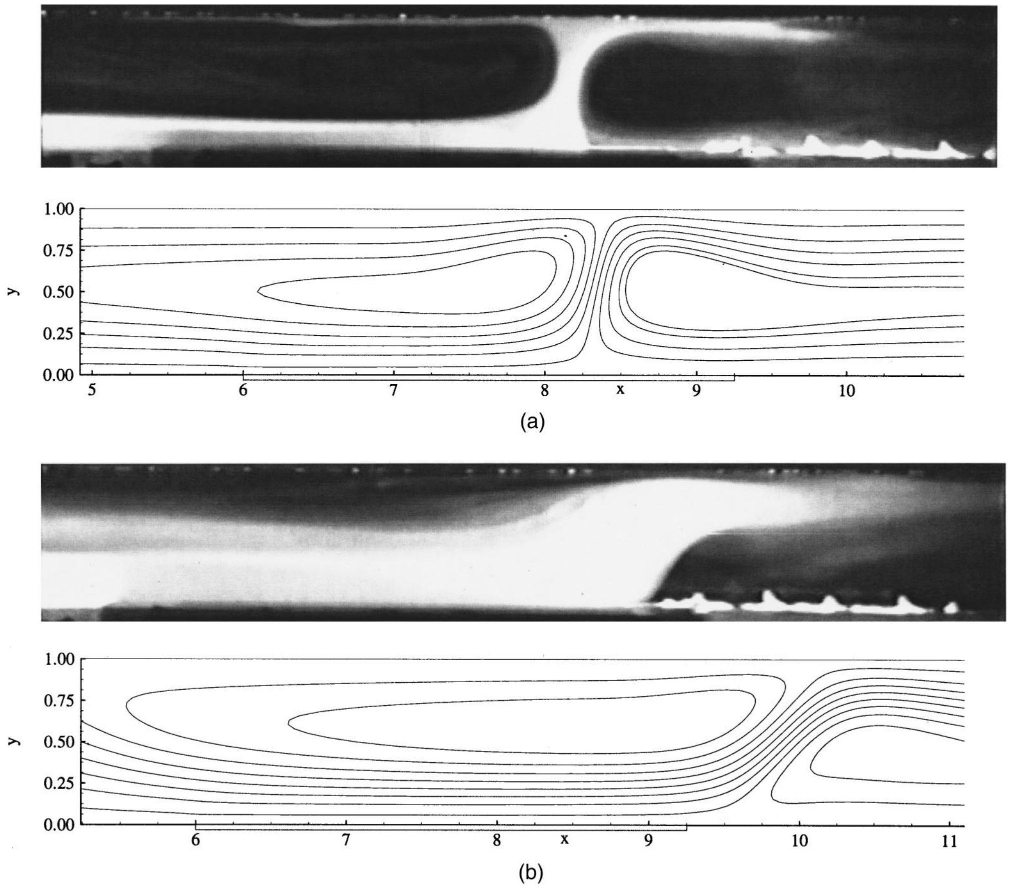

Fig. 46 Comparison between experimental observations and numerical predictions of streamlines at Re=9.48 and Re=29.7 for a ceramic susceptor

tal studies have indicated the feasibility of such continuous motion. Clearly, continuous processing is a very desirable feature since it will impact positively on production rates of the processed materials. It is seen that, at small susceptor speeds, the effect on the flow and the temperature field is relatively small, making it possible to use a continuous process. Also, the speed and direction of motion may be used advantageously to affect the film quality. Conjugate transport at the heated surface is also an important consideration, since in actual practice thermal energy is supplied to the susceptor, often at a constant rate, and the temperature distribution at the surface depends on the transport processes that arise. An isothermal condition is an idealization and is rarely obtained.

Experimental Results. Figure 45 shows a comparison between the silicon deposition rate computed using the chemical kinetics expression given by Eq. (17) with the measurements of Eversteyn et al. [125]. A fairly good agreement is observed. This model assumes chemical kinetics limited deposition. Similarly, a diffusion limited case was considered where the deposition is largely restricted by the transport process. A large discrepancy is seen near the susceptor's leading edge in this case. The reaction-controlled deposition model thus yields much better agreement with experimental results. The reaction-controlled deposition model accounts for the deposition rate dependence on temperature and species concentration at the deposition surface. Depending on the materials involved, the deposition characteristics may be taken as diffusion or kinetics limited. Of course, the problem is fairly complicated and the transport processes as well as the chemical reactions must be considered at the surface and in the gas phase to satisfactorily model the overall deposition process. Even though kinetics results are available for common materials like silicon, lack of accurate data for deposition of metals and other materials is a major problem in accurate prediction of the deposition rate.

Experimental studies have also been carried out on the flow in channels, such as those shown in Fig. 2(*e*), for CVD applications [33,126,127]. Predicted streamlines are compared to experimental observations in Fig. 46 for flow of air in a straight horizontal channel over a susceptor heated by a uniform heat flux source, for two flow rates. As the gas travels over the heated susceptor, gas heating gives rise to buoyancy effects. In the case of the lower Re, a plume develops above the susceptor. This flow pattern generates two transverse rolls, with their axis of rotation perpendicular to the flow direction. The upstream roll produces a recirculation region, while the downstream roll entrains flow from outside. These

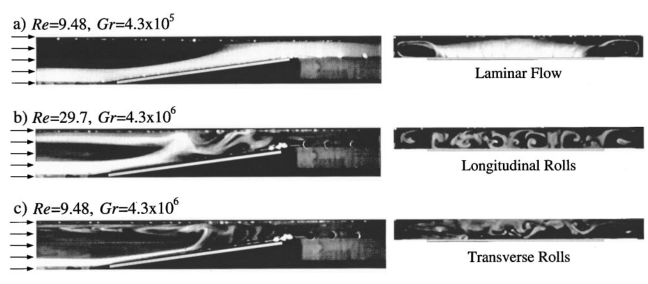

Fig. 47 Side view and tail view of the flow pattern in a converging channel with 8 deg tilt. Tail views are located at the end of the heated section with a light sheet oriented perpendicular to the main flow.

rolls can have significant effect on the deposition rate and film uniformity due to the convective displacement of reactants and effect on heat transfer rates. As Re is increased, the plume shifts downstream due to greater bulk gas flow. Consequently, the two transverse rolls become smaller and flow entrainment from the outside is reduced. The appearances of oscillatory flow, turbulent flow, transverse and longitudinal rolls are found to be dependent on the channel cross-sectional aspect ratio, flow rate and heating rate.

Significantly different flow regimes are observed when the same parametric space is examined for a converging channel with an 8 deg tilted heating section. The flow remains steady and laminar over a larger range of conditions, as compared to a straight channel, since the reduction in channel height increases the local gas velocity and diminishes the relative effect of the buoyancy force. When the flow rate and heating rate are increased, the transition to a new flow regime, composed of longitudinal rolls with the axis of rotation parallel to the main flow, occurs. The side view of this regime shows oscillatory flow. The tail view reveals the presence of rolls along the heated plate. These rolls are unsteady in nature and their presence promotes mixing within the channel. Buoyancy effects increase as Re is decreased or as Gr is increased, and a thermal plume appears above the heated plate, as shown in Fig. 47. The corresponding side view shows the breakup of longitudinal roll structures. When this condition occurs, the flow shifts to a regime dominated by transverse rolls. The plume generated above the heated plate creates an upstream transverse roll which is observed to be two-dimensional near the center of the channel. Near the exit, the flow structure breaks up into turbulent flow. The transition from longitudinal rolls to transverse rolls is defined by fitting a curve across the transition zone, yielding a critical mixed convection parameter of $Gr/Re^2=6000$. The effect on the temperature field and on the heat transfer is also studied. In the design of CVD reactors, entrainment at the exit and transverse rolls are undesirable. Flow entrainment introduces byproducts and other forms of contaminants onto the deposition surface, thereby lowering product quality. Rolls may act like stagnation zones, preventing the desired species from migrating to the deposition surface. These issues must be considered in detail when CVD reactors are designed.

Summary. The flow in the CVD reactor affects the temperature and concentration fields, which determine the local and average deposition rates. Instability and oscillations in the flow can affect the film quality, particularly its uniformity. The flow depends on the geometry, operating conditions like flow rate, temperature, and inlet species concentration, and the fluids involved. Detailed investigations are needed on the chemical kinetics, the associated flow and the resulting deposition for a variety of new and emerging materials.

Additional Flows. The preceding discussion has presented several important materials processing techniques and outlined the present state of the art in analysis, numerical simulation and experimentation of the fluid flows associated with these. However, as mentioned earlier, materials processing is a vast field and it is not possible to cover all the different techniques and systems used for fabricating new, advanced or traditional materials. The preceding discussion presents just a few important processes. There are many more processes in which fluid flow is of critical importance and which have seen intense research activity in recent years. Three such processes are outlined below to bring out some additional concerns and to link these with the flows considered earlier.

Crystal Growing. This is a very important area since most semiconductor devices are fabricated from single crystals grown from the vapor phase or from the melt. The former generally involves sublimation and chemical transport in a sealed enclosure [128]. The latter was mentioned earlier and sketches of two important techniques, Czochralski and floating zone, were shown in Fig. 2. Several other crystal growth techniques, such as Bridgman crystal growth in which the furnace has an upper zone at temperature above the melting point and a lower zone at temperature below the melting point, have been developed [47,129]. The Czochralski method has dominated the production of single crystals for microelectronics and has been the subject of considerable research interest [129,130]. The fluid flow phenomena involves buoyancy-driven convection due to temperature and concentration gradients, forced and mixed convection because of moving surfaces and materials, thermocapillary flows because of surface tension gradients, phase change, and thermal and mass transport processes. The main concerns are very similar to those in casting and other phase-change processes. The flow affects the quality of the crystal through oscillations, instability, effect on local and average transport rates, and distribution of impurities.

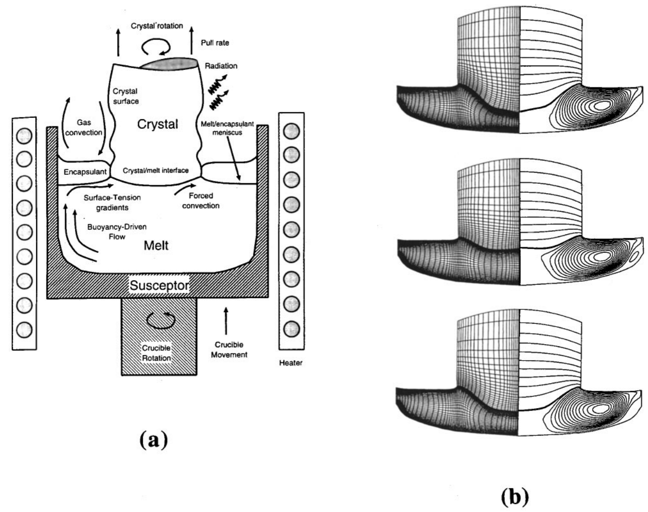

Fig. 48 (*a*) Schematic of the high-pressure liquid-encapsulated Czochralski crystal growing system; (*b*) grid distribution, flow field and melt-crystal interface at three instants of time showing strong oscillatory behavior which damps out at large time [130]

Though Silicon crystals have been of particular interest in the fabrication of electronic devices, there has been growing interest in GaAs, InP and other such compounds because of their use in various electro-optic applications. An encapsulant layer of a very viscous melt such as boric oxide is placed over the melt to curb escape of volatiles in these cases. Figure 48(*a*) shows a schematic of the high pressure liquid-encapsulated Czochralski process, indicating various mechanisms that arise [130, 131]. The flow in the melt arises under the combined effects of buoyancy, surface tension and rotation. Similar mechanisms arise for the process shown in Fig. 2(*a*). Several studies have considered these mechanisms separately, as well as together, to determine the dominant ones and to develop methods to control undesirable flow-induced effects. The flow due to the combined effects of these mechanisms is shown in Fig. 48(*b*), indicating oscillatory behavior of the flow and of the melt-crystal interface. Oscillations damp out at large time. However, at higher rotational speeds, the oscillatory behavior increases and the process is difficult to simulate due to thin boundary layers. An applied magnetic field has been found to suppress oscillations and result in a flat interface [130]. Various other aspects, such as three-dimensional effects, continuous growth system, thermal boundary conditions, and convection in high-pressure liquid-encapsulated Czochralski crystal growth, have been investigated.

Microgravity Materials Processing. Over the past two decades, there has been considerable interest in materials processing under microgravity conditions. Such an environment would be obtained, for instance, in laboratories orbiting in space and would allow the processing of materials to be carried out with reduced effects of the terrestrial gravitational field. As discussed earlier, buoyancy-driven flows in the melt of a crystal growing system affect the quality and characteristics of the crystal by impacting on the solidification process, local transport rates and the nature of the liquid-solid interface. Similarly, gravity plays an important role in the shape of the meniscus in the fiber coating process and in the neck-down profile in optical fiber drawing. Thus, by controlling the gravitational force, we could influence the resulting flow and thus the process and the final product [132,133]. Consequently, substantial research effort is being directed in this area by NASA, the European Space Agency, and other space organizations.

The gravitational force is reduced to much smaller amounts in space. However, it is not zero and buoyancy-driven flows, though substantially reduced, are still present. Similarly, other effects due to gravity are present in reduced form. Also, several other effects and mechanisms that are relatively small on the Earth become much more important. These include thermocapillarity, orbital rotation which gives rise to the Coriolis force, disturbances and fluctuations. Detailed investigations have been carried out on thermocapillarity since this is often the dominant mechanism for flow under microgravity conditions. Attention has been directed at the resulting steady flows that would affect the solidification process and the solid-liquid interface. Since instabilities and oscillations are not desirable for a uniform, defect-free, crystal of high purity, extensive work has been done on the onset of instability, nature of oscillatory flows that arise and the different flow regimes that result for various governing parameters such as Prandtl, Marangoni, and Biot numbers [134–137]. The nature of flow under specified conditions, the critical Marangoni numbers, and the stability diagrams have been determined. Both numerical and experimental studies have been carried out, including experiments under microgravity. Many papers have focused their attention on crystal growing processes like floating zone and Czochralski methods. Many other aspects of materials processing under microgravity, such as bubble migration, film deposition and deforming interfaces, have also been investigated [138,139]. Such efforts continue and are expected to lead to a much better understanding of the fluid flow for materials processing under microgravity conditions.

Thermal Sprays. This is another area which has received considerable attention as a viable process for manufacturing near-net shape structured materials. Sprays containing droplets of the desired deposition material are directed at a chosen substrate and deposited by rapid solidification. The process is fast since many processing steps are eliminated and rapid solidification eliminates macro-segregation which weakens traditionally cast materials [140]. Superior properties associated with fine-grained microstructures and non-equilibrium phases are usually obtained. A wide variety of materials, such as aluminum, tin, and various alloys have been employed in the droplet-based manufacturing process. This process involves generating the droplets, the convective flow in the spraying process, droplet impact and deformation, and rapid solidification [140–144]. Plasma spraying is used for fabricating ceramics, particularly nanostructured ceramics, and various other materials [145,146].

Much of the effort in these and other papers has focused on rapid solidification because the properties of the final product are strongly dependent on this process. Various models have been developed and carefully conducted experimental data have been used for validating and improving the models. The impact of the droplet on the surface, its deformation and spread, and the solidification time are determined. The velocity field inside the spreading droplet is computed and the free surface is tracked. The solidification process is then treated with multi-dimensional models to determine pores, cavities and other defects. The stagnation-flow problem is investigated to model the spray and its impingement on a substrate, involving solidification of liquid in motion. In-flight behavior of droplets, particularly with respect to nucleation and solidification, are also considered. The overall problem is obviously very complicated since it involves complex flows with free boundaries, moving surfaces, phase change, and rapid changes with time. However, because of the advantages it offers in material fabrication, in terms of speed and quality, substantial research effort is directed at the thermal spray process at present.

System Simulation, Design and Optimization. Another important aspect that must be mentioned here is the numerical simulation of the overall system, since the process undergone by the material is a consequence of the flow and energy exchange with the various components of the system. The numerical simulation of the system refers to the use of the numerical model to obtain a quantitative representation of the physical system and to characterize its behavior for a given design or set of operating conditions and for variations in these. Consider, for instance, a typical electrical furnace, which consists of the heater, walls, insulation, inert gas environment and the material undergoing heat treatment. The transport mechanisms in all these components are coupled through the boundary conditions. The gas flow is driven by an externally imposed pressure difference, such as that due to a fan or a blower, by moving materials in continuous processing, and by buoyancy. Each individual component may first be numerically simulated as uncoupled from the others, by employing prescribed boundary conditions. Then, these individual simulations are combined, employing the appropriate coupling through the boundary conditions. This procedure provides a systematic approach to the numerical simulation of the system, which may be a simple one or a complicated practical one [23,43]. Once the simulation of the system is achieved, with satisfactory experimental validation, the design and optimization of the process as well as of the system may be undertaken. The results obtained from the simulation provide the necessary inputs for improving existing designs and developing new ones for improving the productivity and the product quality for a given manufacturing process [1].

Present State-of-the-Art

It is obvious from the preceding review that the fluid flow phenomena associated with a wide variety of materials processing techniques have been investigated in detail. Mathematical models of various complex circumstances that arise in materials processing have been developed and applied to practical systems and processes. Some of the common situations are:

1 Moving and free boundaries
2 Combined transport mechanisms
3 Conjugate conditions that couple different regions
4 Mechanisms occurring at different length and time scales
5 Flows with phase change and chemical reactions
6 Large material property changes
7 Non-Newtonian flows
8 Particulate flows

Though numerical approaches have been most extensively used to solve the governing equations, analytical solutions have also been obtained for certain simplified and idealized cases. These have been mainly used for validating numerical models and for providing physical insight into underlying mechanisms. Experimental results have also been obtained in a limited number of flows in order to validate the numerical models and to provide guidelines for model development by increasing the basic understanding of the process.

Much of the effort in this area has been directed at the numerical modeling and simulation of processing. Using advances in computational fluid dynamics, many specialized techniques have been developed to simulate the complexities that typically arise in materials processing. These include

1 Coordinate transformations for grid generation in complex domains
2 Coupling of different regions and mechanisms
3 Finite difference, finite element and other approaches
4 Simulation of deforming materials
5 Solution of inverse problems
6 Modeling complicated boundary conditions
7 Solution of time-dependent problems
8 Other complications mentioned earlier

Advantage has been taken of advances in computational hardware and software for visualization, improving accuracy, and for reducing computational storage and time. Similarly, experimental work has relied heavily on the techniques developed for flow visualization and measurement, such as laser Doppler anemometry, particle image velocimetry, infra-red, laser and video imaging, high-speed photography, as well as traditional methods of measuring flow, temperature, pressure and other variables. Specialized techniques for measuring, for instance, temperature and velocity in a rotating screw extruder, have been developed to investigate flow phenomena in materials processing. The preceding review has presented several analytical, numerical and experimental methods that have been employed to investigate these flows.

Future Research Needs

Our understanding of flow phenomena in materials processing has grown significantly over the last three decades. However, there are still many areas that need detailed and concentrated further investigation. These are considered in terms of separate categories in the following.

Critical Areas. The three main areas that are in critical need of further study are:

1. *Material properties*. In many of the simulations and experiments, the material properties available in the literature have been used. Frequently, data are available only under standard conditions, even though the processes occur at much higher temperature and pressure. Equations for chemical kinetics are often not available or only a few data points are available. Therefore, the measurement and availability of accurate material properties are crucial to a study in this area.

2. *Experimentation*. It has been mentioned that experimental results are very sparse because of the time and effort needed for accurate data. However, experiments are strongly needed for validation of models and for providing inputs and insight for future model development.

3. *Coupling of micro/macro scales*. It is very important to satisfactorily link the transport mechanisms at the microscale where material processing generally occurs with those at the macro or engineering scale where the appropriate boundary conditions are imposed. A few studies have considered this aspect, as mentioned earlier. But much more needs to be done in order to link material quality with the operating and design conditions.

Additional Topics. Besides these three major areas that need further investigation, work is needed on several other topics. Some of the main ones are:

1 New and innovative experimental techniques for realistic materials which are often opaque and for measurements under high temperature and pressure.
2 Numerical techniques for very large material property changes and for coupling the transport equations with the chemical kinetics which may involve several different reactions, with different reaction rates, activation energy, and other constants.
3 Flow circumstances involving complex materials such as powders, particulates, granules, and highly porous materials.
4 Accurate numerical modeling of combined mechanisms, multiple domains, multiphase flows, and conjugate conditions.
5 Instability of the process due to underlying flow instability mechanisms. Effect of these instabilities on process feasibility.
6 Characteristics of free surfaces and interfaces.
7 Effect of flow on product characteristics and thus on the operation and optimization of the process and system.
8 Development of new products, processes and systems on the basis of underlying fluid phenomena.

Important Processes for Future Study. Several important materials processing techniques and systems have been considered in this review and their future reseach needs have been outlined. However, there are many others that need careful detailed investigation because of their growing importance. Some of the important processes that are expected to be important in the future and that should be targeted for research are:

1 Chemical reaction based processing
2 Biological systems and biomaterials
3 Droplet-based manufacturing: rapid solidification, thermal and plasma sprays
4 Advanced polymers and composites
5 Crystal growth
6 Space-based materials processing
7 High speed coating
8 Processing of ceramics, glass, nanostructured ceramics
9 Laser processing
10 Solidification of alloys and mixtures
11 Power processing

Concluding Remark

Finally, It must be stressed that fluids engineering research can impact on the growing and important field of materials processing only if significant effort is also directed at understanding the basic mechanisms and processes that govern changes in the material. It is not enough to use available kinetics or information on material behavior to model the relevant fluid flow phenomena. One must understand how the observed phenomena affect the material properties, structure and characteristics. This makes the study of fluid flow phenomena in materials processing challenging, interesting and useful.

Acknowledgments

This review was made possible by the Freeman Scholar Program in Fluids Engineering of ASME. The author is grateful to the Program and the Standing Committee of C. T. Crowe (Chair), R. A. Bajura and M. L. Billet for providing him this opportunity. The support of the National Science Foundation, of the industry, and of the New Jersey Commission on Science and Technology through various Centers for much of the work reported here and for the preparation of this paper is gratefully acknowledged. The author also acknowledges the work done by several students, as referenced here, that made it possible to present this review. Figure 6 was provided by Prof. S. Kou and is gratefully acknowledged.

Nomenclature

b, b_m, B = constants, Eqs. (20), (22), and (23)
Bi = Biot number, $\mathrm{Bi} = hL/k_s$
c_m = species concentration
C = specific heat
C_p = specific heat at constant pressure
$\underline{e}$ = unit vector in the direction of gravitational force
E = activation energy
Ec = Eckert number, Eq. (35)
f_1 = liquid mass fraction
$F(t)$ = cumulative residence time function, Eq. (37)
$\underline{F}$ = body force vector
g = magnitude of gravitational acceleration
Gr = Grashof number, Eq. (35)
h = convective heat transfer coefficient
H = enthalpy

H^o = enthalpy at 0 K
$\overline{i}$ = unit vector in x-direction
k = thermal conductivity
K = bulk viscosity, reaction rate
K_c = consistency index for non-Newtonian fluid, Eq. (19)
L = characteristic length
L_h = latent heat of fusion
$\dot{m}$ = mass flow rate
Ma = Marangoni number
n = power-law fluid index
N = speed in revolutions/min (rpm)
p = local pressure
p_a = hydrostatic pressure
p_d = dynamic pressure due to fluid motion
Pr = Prandtl number, Eq. (35)
q = heat flux
q_v = dimensionless volume flow rate in an extruder
$\dot{Q}$ = volumetric source
R = universal gas constant, radius
Re = Reynolds number, Eq. (35)
Sr = Strouhal number, Eq. (35)
t = time
T = temperature
u,v,w = velocity components in x, y, and z directions, respectively
U, U_S = speed of a moving solid or source
$\overline{V}$ = velocity vector
We = Weber number
$\tilde{x}$ = position vector
x, y, z = coordinate distances
X,Y,Z = dimensionless coordinate distances

Greek Symbols

α = thermal diffusivity
β = coefficient of thermal expansion
$\dot{\gamma}$ = strain rate
δ = location of interface between solid and liquid
ε = surface emissivity
λ = second viscosity coefficient
μ = dynamic viscosity of fluid
ν = kinematic viscosity
Φ = viscous dissipation function
ρ = density
σ = surface tension
θ = dimensionless temperature
τ = shear stress

Subscripts

a = ambient
b = barrel, wall
i = initial, inlet
l = liquid
m = melting point
o = reference
s = solid, surface

References

[1] Jaluria, Y., 1998, *Design and Optimization of Thermal Systems*, McGraw-Hill, New York.
[2] Doyle, L. E., Keyser, C. A., Leach, J. L., Scharder, G. F., and Singer, M. B., 1987, *Manufacturing Processes and Materials for Engineers*, Prentice-Hall, Englewood Cliffs, NJ.
[3] Schey, J. A., 1987, *Introduction to Manufacturing Processes*, 2nd Ed., McGraw-Hill, New York.
[4] Kalpakjian, S., 1989, *Manufacturing Engineering and Technology*, Addison-Wesley, Reading, MA.
[5] Szekely, J., 1979, *Fluid Flow Phenomena in Metals Processing*, Academic Press, New York.
[6] Ghosh, A., and Mallik, A. K., 1986, *Manufacturing Science*, Ellis Horwood, Chichester, U.K.
[7] Avitzur, B., 1968, *Metal Forming: Processes and Analysis*, McGraw-Hill, New York.
[8] Altan, T., Oh, S. I., and Gegel, H. L., 1971, *Metal Forming: Fundamentals and Applications*, Amer. Soc. Metals, Metals Park, OH.
[9] Fenner, R. T., 1979, *Principles of Polymer Processing*, Chemical Publishing, New York.
[10] Easterling, K., 1983, *Introduction to Physical Metallurgy of Welding*, Butterworths, London, U.K.
[11] Hughel, T. J., and Bolling, G. F., eds., 1971, *Solidification*, Amer. Soc. Metals, Metals Park, OH.
[12] Kuhn, H. A., and Lawley, A., eds., 1978, *Powder Metallurgy Processing, New Techniques and Analysis*, Academic Press, New York.
[13] Chen, M. M., Mazumder, J., and Tucker, C. L., eds., 1983, ''*Transport Phenomena in Materials Processing*,'' HTD Vol. 29, Amer. Soc. Mech. Engrs., New York.
[14] Li, T., ed., 1985, *Optical Fiber Communications, Vol. 1: Fiber Fabrication*, Academic Press, New York.
[15] Poulikakos, D., ed., 1996, *Transport Phenomena in Materials Processing*, Adv. Heat Transfer, Academic Press, San Diego, CA **18**.
[16] Viskanta, R., 1988, ''Heat Transfer During Melting and Solidification of Metals,'' ASME J. Heat Transfer, **110**, pp. 1205–1219.
[17] Lee, S. H.-K., and Jaluria, Y., 1996, ''Effect of Variable Properties and Viscous Dissipation During Optical Fiber Drawing,'' ASME J. Heat Transfer, **118**, pp. 350–358.
[18] Lee, S. H.-K., and Jaluria, Y., 1996, ''Simulation of the Transport Processes in the Neck-Down Region of the Furnace Drawn Optical Fiber,'' Int. J. Heat Mass Transf., **40**, pp. 843–856.
[19] Jaluria, Y., 1996, ''Heat and Mass Transfer in the Extrusion of Non-Newtonian Materials,'' Adv. Heat Transfer, **28**, pp. 145–230.
[20] Jaluria, Y., 1992, ''Transport from Continuously Moving Materials Undergoing Thermal Processing,'' Annu. Rev. Heat Transfer, **4**, pp. 187–245.
[21] Jaluria, Y., 1980, *Natural Convection Heat and Mass Transfer*, Pergamon Press, Oxford, UK.
[22] Gebhart, B., Jaluria, Y., Mahajan, R. L., and Sammakia, B., 1988, *Buoyancy-Induced Flows and Transport*, Taylor and Francis, Philadelphia, PA.
[23] Jaluria, Y., and Torrance, K. E., 1986, *Computational Heat Transfer*, Taylor and Francis, Philadelphia, PA.
[24] Ramachandran, N., Gupta, J. P., and Jaluria, Y., 1982, ''Thermal and Fluid Flow Effects During Solidification in a Rectangular Enclosure,'' Int. J. Heat Mass Transf., **25**, pp. 187–194.
[25] Bennon, W. D., and Incropera, F. P., 1988, ''Developing Laminar Mixed Convection with Solidification in a Vertical Channel,'' ASME J. Heat Transfer, **110**, pp. 410–415.
[26] Viswanath, R., and Jaluria, Y., 1993, ''A Comparison of Different Solution Methodologies for Melting and Solidification Problems in Enclosures,'' Numer. Heat Transfer, Part B, **24B**, pp. 77–105.
[27] Prescott, P. J., and Incropera, F. P., 1996, ''Convection Heat and Mass Transfer in Alloy Solidification,'' Adv. Heat Transfer, **28**, pp. 231–338.
[28] Harper, J. M., 1981, *Extrusion of Foods: Volume I*, CRC Press, Boca Raton, FL.
[29] Kokini, J. L., Ho, C.-T., and Karwe, M. V., eds., 1992, *Food Extrusion Science and Technology*, Marcel Dekker, New York.
[30] Wang, S. S., Chiang, C. C., Yeh, A. I., Zhao, B., and Kim, I. H., 1989, ''Kinetics of Phase Transition of Waxy Corn Starch at Extrusion Temperatures and Moisture Contents,'' J. Food. Sci., **54**, pp. 1298–1301.
[31] Abib, A. H., Jaluria, Y., and Chiruvella, R. V., 1993, ''Thermal Processing of Food Materials in a Single Screw Extruder,'' *Heat Transfer in Food Processing*, ASME Heat Transfer Div., Vol. 254, ASME, New York, pp. 57–67.
[32] Chiruvella, R. V., Jaluria, Y., and Karwe, M. V., 1996, ''Numerical Simulation of Extrusion Cooking of Starchy Materials,'' J. Food. Eng., **30**, pp. 449–467.
[33] Jensen, K. F., Einset, E. O., and Fotiadis, D. I., 1991, ''Flow Phenomena in Chemical Vapor Deposition of Thin Films,'' Annu. Rev. Fluid Mech., **23**, pp. 197–232.
[34] Mahajan, R. L., 1996, ''Transport Phenomena in Chemical Vapor-Deposition Systems,'' Adv. Heat Transfer, **28**, pp. 339–425.
[35] Jensen, K. F., and Graves, D. B., 1983, ''Modeling and Analysis of Low Pressure CVD Reactors,'' J. Electrochem. Soc., **130**, pp. 1950–1957.
[36] Jaluria, Y., 1996, *Computer Methods for Engineering*, Taylor and Francis, Washington, DC.
[37] Chiu, W. K.-S., Jaluria, Y., and Glumac, N. C., 2000, ''Numerical Simulation of Chemical Vapor Deposition Processes Under Variable and Constant Property Approximations,'' Numer. Heat Transfer, **37**, pp. 113–132.
[38] Tadmor, Z., and Gogos, C., 1979, *Principles of Polymer Processing*, Wiley, New York.
[39] Pearson, J. R. A., and Richardson, S. M., eds., 1983, *Computational Analysis of Polymer Processing*, Appl. Sci. Pub., London, UK.
[40] Karwe, M. V., and Jaluria, Y., 1990, ''Numerical Simulation of Fluid Flow and Heat Transfer in a Single-Screw Extruder for Non-Newtonian Fluids,'' Numer. Heat Transfer, **17**, pp. 167–190.
[41] Choudhury, S. Roy, Jaluria, Y., and Lee, S. H.-K., 1999, ''Generation of neck-down profile for furnace drawing of optical fiber,'' Numer. Heat Transfer, **35**, pp. 1–24.
[42] Jaluria, Y., 1976, ''Temperature Regulation of a Plastic-Insulated Wire in Radiant Heating,'' ASME J. Heat Transfer, **98**, pp. 678–680.
[43] Jaluria, Y., 1988, ''Numerical Simulation of the Transport Processes in a Heat Treatment Furnace,'' Int. J. Numer. Methods Eng., **25**, pp. 387–399.
[44] Siegel, R., 1978, ''Shape of Two-Dimensional Solidification Interface During

Directional Solidification by Continuous Casting,'' ASME J. Heat Transfer, **100**, pp. 3–10.
[45] Siegel, R., 1984, ''Two-Region Analysis of Interface Shape in Continuous Casting with Superheated Liquid,'' ASME J. Heat Transfer, **106**, pp. 506–511.
[46] Chu, T. Y., 1975, ''A Hydrostatic Model of Solder Fillets,'' The Western Electric Engineer, **19**, No. 2, pp. 31–42.
[47] Kou, S., 1996, *Transport Phenomena and Materials Processing*, Wiley, New York.
[48] Jaluria, Y., and Singh, A. P., 1983, ''Temperature Distribution in a Moving Material Subjected to Surface Energy Transfer,'' Comput. Methods Appl. Mech. Eng., **41**, pp. 145–157.
[49] Choudhury, S. Roy, and Jaluria, Y., 1994, ''Analytical Solution for the Transient Temperature Distribution in a Moving Rod or Plate of Finite Length with Surface Heat Transfer,'' Int. J. Heat Mass Transf., **37**, pp. 1193–1205.
[50] Kwon, T. H., Shen, S. F., and Wang, K. K., 1986, ''Pressure Drop of Polymeric Melts in Conical Converging Flow: Experiments and Predictions'' Polym. Eng. Sci., **28**, pp. 214–224.
[51] Lin, P., and Jaluria, Y., 1997, ''Conjugate Transport in Polymer Melt Flow Through Extrusion Dies,'' Polym. Eng. Sci., **37**, pp. 1582–1596.
[52] Patankar, S. V., 1980, *Numerical Heat Transfer and Fluid Flow*, Taylor and Francis, Philadelphia, PA.
[53] Mallinson, G. D., and de Vahl Davis, G., 1973, ''The Method of False Transient for the Solution of Coupled Elliptic Equations,'' J. Comput. Phys., **12**, pp. 435–461.
[54] Leonard, B. P., 1997, ''Bounded Higher-Order Upwind Multidimensional Finite-Volume Convection-Diffusion Algorithms,'' *Advances in Numerical Heat Transfer*, Minkowycz, W. J. and Sparrow, E. M., eds., Vol. 1, Taylor and Francis, Philadelphia, PA, pp. 1–57.
[55] Peaceman, D. W., and Rachford, H. H., 1955, ''Numerical Solution of Parabolic and Elliptic Differential Equations,'' J. Soc. Ind. Appl. Math., **3**, pp. 28–41.
[56] Acharya, S., 1994, ''Solution-Adaptive Techniques in Computational Heat Transfer and Fluid Flow,'' Springer, Heidelberg, Germany **14**, pp. 447–467.
[57] Sastrohartono, T., Esseghir, M., Kwon, T. H., and Sernas, V., 1990, ''Numerical and Experimental Studies of the Flow in the Nip Region of a Partially Intermeshing Co-Rotating Twin Screw Extruder,'' Polym. Eng. Sci., **30**, pp. 1382–1398.
[58] Sastrohartono, T., and Kwon, T. H., 1990, ''Finite Element Analysis of Mixing Phenomena in Tangential Twin Screw Extruders for Non-Newtonian Fluids,'' Int. J. Numer. Methods Eng., **30**, pp. 1369–1383.
[59] Kwon, T. H., Joo, J. W., and Kim, S. J., 1994, ''Kinematics and Deformation Characteristics as a Mixing Measure in the Screw Extrusion Process,'' Polym. Eng. Sci., **34**, pp. 174–189.
[60] Kalyon, D. M., Gotsis, A. D., Yilmazer, U., Gogos, C., Sangani, H., Aral, B., and Tsenoglou, C., 1988, ''Development of Experimental Techniques and Simulation Methods to Analyze Mixing in Co-Rotating Twin Screw Extrusion,'' Adv. Polym. Technol., **8**, pp. 337–353.
[61] Rauwendaal, C., 1986, *Polymer Extrusion*, Hanser Pub., New York.
[62] Esseghir, M., and Sernas, V., 1991, ''A Cam-Driven Probe for Measurement of the Temperature Distribution in an Extruder Channel,'' *SPE ANTEC Tech. Papers*, Vol. 37, pp. 54–57.
[63] Esseghir, M., and Sernas, V., 1992, ''Experiments on a Single Screw Extruder with a Deep and Highly Curved Screw Channel,'' *Food Extrusion Science and Technology*, J. L. Kokini, C. T. Ho, and M. V. Karwe, eds., Marcel Dekker, New York, pp. 21–40.
[64] Sastrohartono, T., Jaluria, Y., Esseghir, M., and Sernas, V., 1995, ''A Numerical and Experimental Study of Three-Dimensional Transport in the Channel of an Extruder for Polymeric Materials,'' Int. J. Heat Mass Transf., **38**, pp. 1957–1973.
[65] Wang, Y., and White, J. L., 1989, ''Non-Newtonian Flow Modeling in the Screw Region of an Intermeshing Co-rotating Twin Screw Extruder,'' J. Non-Newtonian Fluid Mech., **32**, pp. 19–38.
[66] Kwon, G. H., Jaluria, Y., Karwe, M. V., and Sastrohartono, T., 1991, ''Numerical Simulation of the Transport Processes in a Twin screw Polymer Extruder,'' *Prog. Modeling Polymer Processing*, A. I. Isayev, ed., Ch. 4, Hanser Pub., New York, pp. 77–115.
[67] Sastrohartono, T., Jaluria, Y., and Karwe, M. V., 1994, ''Numerical Coupling of Multiple Region Simulations to Study Transport in a Twin Screw Extruder,'' Numer. Heat Transfer, **25**, pp. 541–557.
[68] Chiruvella, R. V., Jaluria, Y., Karwe, M. V., and Sernas, V., 1996, ''Transport in a Twin-Screw Extruder for the Processing of Polymers,'' Polym. Eng. Sci., **36**, pp. 1531–1540.
[69] Zhu, W., and Jaluria, Y., 2001, ''Transport Processes and Feasible Operating Domain in a Twin-Screw Polymer Extruder,'' Polym. Eng. Sci., **41**, pp. 107–117.
[70] Karwe, M. V., and Sernas, V., 1996, ''Application of Laser Doppler Anemometry to Measure Velocity Distribution Inside the Screw Channel of a Twin Screw Extruder,'' Journal of Food Process Engineering, **19**, pp. 135–152.
[71] Bakalis, S., and Karwe, M. V., 1997, ''Velocity Field in a Twin Screw Extruder'' Int. J. Food Sci. Technol., **32**, pp. 241–253.
[72] Jaluria, Y., Liu, Y., and Chiruvella, R. V., 1999, ''Modeling and Simulation of the Solids Conveying and Unfilled Regions in Polymer Extrusion,'' J. Reinf. Plast. Compos., **18**, pp. 15–26.
[73] Yin, Z., and Jaluria, Y., 1997, ''Zonal Method to Model Radiative Transport in an Optical Fiber Drawing Furnace,'' ASME J. Heat Transfer, **119**, pp. 597–603.
[74] Paek, U. C., 1999, ''Free Drawing and Polymer Coating of Silica Glass Optical Fibers,'' ASME J. Heat Transfer, **121**, pp. 775–788.
[75] Goren, S. L., and Wronski, S., 1966, ''The Shape of Low-Speed Jets of Newtonian Liquids,'' J. Fluid Mech., **25**, pp. 185–198.
[76] Nickell, R. E., Tanner, R. I., and Caswell, B., 1974, ''The Solution of Viscous Incompressible Jet and Free-Surface Flows using Finite-Element Methods,'' J. Fluid Mech., **65**, pp. 189–206.
[77] Lewis, J. A., 1977, ''The Collapse of a Viscous Tube,'' J. Fluid Mech., **81**, pp. 129–135.
[78] Gifford, W. A., 1982, ''A Finite Element Analysis of Isothermal Fiber Formation,'' Phys. Fluids, **25**, pp. 219–225.
[79] Levich, V. G., and Krylov, V. S., 1969, ''Surface-Tension Driven Phenomena,'' Annu. Rev. Fluid Mech., **1**, pp. 293–316.
[80] Dianov, E. M., Kashin, V. V., Perminov, S. M., Perminova, V. N., Rusanov, S. Y., and Sysoev, V. K., 1988, ''The Effect of Different Conditions on the Drawing of Fibers from Preforms,'' Glass Technol., **29**, No. 6, pp. 258–262.
[81] Choudhury, S. Roy, and Jaluria, Y., 1998, ''Practical Aspects in the Thermal Transport During Optical Fiber Drawing,'' J. Mater. Res., **13**, pp. 483–493.
[82] Yin, Z., and Jaluria, Y., 2000, ''Neck Down and Thermally Induced Defects in High Speed Optical Fiber Drawing,'' ASME J. Heat Transfer, **122**, pp. 351–362.
[83] Paek, U. C., and Runk, R. B., 1978, ''Physical Behavior of the Neck-down Region during Furnace Drawing of Silica Fibers,'' J. Appl. Phys., **49**, pp. 4417–4422.
[84] Paek, U. C., Schroeder, C. M., and Kurkjian, C. R., 1988, ''Determination of the Viscosity of High Silica Glasses During Fibre Drawing,'' Glass Technol., **29**, No. 6, pp. 263–266.
[85] Issa, J., Yin, Z., Polymeropoulos, C. E., and Jaluria, Y., 1996, ''Temperature Distribution in an Optical Fiber Draw Tower Furnace,'' J. Mater. Process. Manuf. Sci., **4**, pp. 221–232.
[86] Liu, Y., and Polymeropoulos, C. E., 1998, ''Measurement and Prediction of Thermocouple Probe Temperatures Within Glass Rods Subjected to Radiative Heating,'' *Proc. 11th Int. Heat Transfer Conf.*, Kyongju, Korea, Taylor and Francis, Philadelphia, Vol. 4, pp. 27–32.
[87] Christodoulou, K. N., and Scriven, L. E., 1989, ''The Fluid Mechanics of Slide Coating,'' J. Fluid Mech., **208**, pp. 321–354.
[88] Dussan, E. B., Rame, E., and Garoff, S., 1991, ''On Identifying the Appropriate Boundary Conditions at a Moving Contact Line: an Experimental Investigation,'' J. Fluid Mech., **230**, pp. 97–116.
[89] Chen, Q., Rame, E., and Garoff, S., 1997, ''The Velocity Field Near Moving Contact Lines,'' J. Fluid Mech., **337**, pp. 49–66.
[90] Quere, D., 1999, ''Fluid Coating on a Fiber,'' Annu. Rev. Fluid Mech., **31**, pp. 347–384.
[91] Blyler, L. L., and DiMarcello, F. V., 1980, ''Fiber Drawing, Coating and Jacketing,'' *Proc. IEEE*, **68**, pp. 1194–1198.
[92] Paek, U. C., 1986, ''High Speed High Strength Fiber Coating,'' J. Lightwave Technol., **LT-4**, pp. 1048–1059.
[93] Simpkins, P., and Kuck, V., 2000, ''Air Entrapment in Coatings Via Tip Streaming Meniscus,'' Nature (London), **403**, pp. 641–643.
[94] Ravinutala, S., Rattan, K., Polymeropoulos, C., and Jaluria, Y., 2000, ''Dynamic Menisci in a Pressurized Fiber Applicator,'' *Proc. 49th Int. Wire Cable Symp.*, Atlantic City, NJ.
[95] Abraham, A., and Polymeropoulos, C. E., 1999, ''Dynamic Menisci on Moving Fibers,'' *Proc. 48th Int. Wire Cable Symp.*, Atlantic City, NJ.
[96] Vaskopulos, T., Polymeropoulos, C. E., and Zebib, A., 1995, ''Cooling of Optical Fibers in Aiding and Opposing Forced Gas Flow,'' Int. J. Heat Mass Transf., **18**, pp. 1933–1944.
[97] Hanafusa, H., Hibino, Y., and Yamamoto, F., 1985, ''Formation Mechanism of Drawing-Induced E' Centers in Silica Optical Fibers,'' J. Appl. Phys., **58**, No. 3, pp. 1356–1361.
[98] Hibino, Y., Hanafusa, H., and Sakaguchi, S., 1985, ''Formation of Drawing-Induced E' Centers in Silica Optical Fibers,'' Jpn. J. Appl. Phys., **24**, No. 9, pp. 1117–1121.
[99] Flemings, M. C., 1974, *Solidification Processing*, McGraw-Hill, New York.
[100] Viskanta, R., 1985, ''Natural Convection in Melting and Solidification,'' *Natural Convection: Fundamentals and Applications*, S. Kakac, W. Aung, and R. Viskanta, eds., Hemisphere Pub. Co., Washington, DC, pp. 845–877.
[101] Huppert, H. E., 1990, ''The Fluid Mechanics of Solidification,'' J. Fluid Mech., **212**, pp. 209–240.
[102] Davis, S. H., 1990, ''Hydrodynamic Interactions in Directional Solidification,'' J. Fluid Mech., **212**, pp. 241–262.
[103] Prescott, P. J., and Incropera, F. P., 1996, ''Convection Heat and Mass Transfer in Alloy Solidification,'' Adv. Heat Transfer, **28**, pp. 231–338.
[104] Sparrow, E. M., Patankar, S. V., and Ramadhyani, S., 1977, ''Analysis of Melting in the Presence of Natural Convection in the Melt Region,'' ASME J. Heat Transfer, **99**, pp. 520–526.
[105] Voller, V. R., 1997, ''An Overview of Numerical Methods for Solving Phase Change Problems,'' *Advances in Numerical Heat Transfer*, Minkowycz, W. J., and Sparrow, E. M., eds., Vol. 1, Taylor and Francis, Philadelphia, PA, pp. 341–380.
[106] Viswanath, R., and Jaluria, Y., 1995, ''Numerical Study of Conjugate Transient Solidification in an Enclosed Region,'' Numer. Heat Transfer, **27**, pp. 519–536.
[107] Banaszek, J., Jaluria, Y., Kowalewski, T. A., and Rebow, M., 1999, ''Semi-implicit FEM Analysis of Natural Convection in Freezing Water,'' Numer. Heat Transfer, **36**, pp. 449–472.
[108] Bathelt, A. G., Viskanta, R., and Leidenfrost, W., 1979, ''An Experimental

Investigation of Natural Convection in the Melted Region Around a Heated Horizontal Cylinder,'' J. Fluid Mech., **90**, pp. 227–240.
[109] Gau, C., and Viskanta, R., 1986, ''Melting and Solidification of a Pure Metal on a Vertical Wall,'' ASME J. Heat Transfer, **108**, pp. 174–181.
[110] Wolff, F., and Viskanta, R., 1987, ''Melting of a Pure Metal from a Vertical Wall,'' Exp. Heat Transfer, **1**, pp. 17–30.
[111] Wolff, F., and Viskanta, R., 1988, ''Solidification of a Pure Metal at a Vertical Wall in the Presence of Liquid Superheat,'' Int. J. Heat Mass Transf., **31**, pp. 1735–1744.
[112] Thompson, M. E., and Szekely, J., 1988, ''Mathematical and Physical Modeling of Double-Diffusive Convection of Aqueous Solutions Crystallizing at a Vertical Wall,'' J. Fluid Mech., **187**, pp. 409–433.
[113] Beckermann, C., and Wang, C. Y., 1995, ''Multiphase/-Scale Modeling of Alloy Solidification,'' Annu. Rev. Heat Transfer, **6**, pp. 115–198.
[114] Wang, C. Y., and Beckermann, C., 1993, ''A Unified Solute Diffusion Model for Columnar and Equiaxed Dendritic Alloy Solidification,'' Mater. Sci. Eng., **A171**, pp. 199–211.
[115] Kang, B. H., and Jaluria, Y., 1993, ''Thermal Modeling of the Continuous Casting Process,'' J. Thermophys. Heat Transfer, **7**, pp. 139–147.
[116] Lin, P., and Jaluria, Y., 1997, ''Heat Transfer and Solidification of Polymer Melt Flow in a Channel,'' Polym. Eng. Sci., **37**, pp. 1247–1258.
[117] Kang, B. H., Jaluria, Y., and Karwe, M. V., 1991, ''Numerical Simulation of Conjugate Transport from a Continuous Moving Plate in Materials Processing,'' Numer. Heat Transfer, **19**, pp. 151–176.
[118] Arridge, R. G. C., and Prior, K., 1964, ''Cooling Time of Silica Fibers,'' Nature (London), **203**, pp. 386–387.
[119] Tsou, F. K., Sparrow, E. M., and Godstein, R. J., 1967 ''Flow and Heat Transfer in the Boundary Layer on a Continuous Moving Surface,'' Int. J. Heat Mass Transf., **10**, pp. 219–235.
[120] Karwe, M. V., and Jaluria, Y., 1992, ''Experimental Investigation of Thermal Transport from a Heated Moving Plate,'' Int. J. Heat Mass Transf., **35**, pp. 493–511.
[121] Evans, G., and Greif, R., 1987, ''A Numerical Model of the Flow and Heat Transfer in a Rotating Disk Chemical Vapor Deposition Reactor,'' ASME J. Heat Transfer, **109**, pp. 928–935.
[122] Fotiadis, D. I., Boekholt, M., Jensen, K. F., and Richter, W., 1990, ''Flow and Heat Transfer in CVD Reactors: Comparison of Raman Temperature Measurements and Finite Element Model Predictions,'' J. Cryst. Growth, **100**, pp. 577–599.
[123] Karki, K. C., Sathyamurthy, P. S., and Patankar, S. V., 1993, ''Three-Dimensional Mixed Convection in a Chemical Vapor Deposition Reactor,'' ASME J. Heat Transfer, **115**, pp. 803–806.
[124] Chiu, W. K. S., and Jaluria, Y., 2000, ''Continuous Chemical Vapor Deposition Processing with a Moving Finite Thickness Susceptor,'' J. Mater. Res., **15**, pp. 317–328.
[125] Eversteyn, F. C., Severin, P. J. W., Brekel, C. H. J., and Peek, H. L., 1970, ''A Stagnant Layer Model for the Epitaxial Growth of Silicon from Silane in a Horizontal Reactor,'' J. Electrochem. Soc., **117**, pp. 925–931.
[126] Chiu, W. K.-S., Richards, C. J., and Jaluria, Y., 2000, ''Flow Structure and Heat Transfer in a Horizontal Converging Channel Heated From Below,'' Phys. Fluids, **12**, pp. 2128–2136.
[127] Chiu, W. K. S., and Jaluria, Y., 1997, ''Heat Transfer in Horizontal and Vertical CVD Reactors,'' *ASME Heat Transfer Div.*, Vol. 347, Amer. Soc. Mech. Engrs., New York, pp. 293–311.
[128] Rosenberger, F., 1980, ''Fluid Dynamics in Crystal Growth from Vapors,'' PhysicoChem. Hydrodyn., **1**, pp. 3–26.
[129] Ostrach, S., 1983, ''Fluid Mechanics in Crystal Growth—The 1982 Freeman Scholar Lecture,'' ASME J. Fluids Eng., **105**, pp. 5–20.
[130] Prasad, V., Zhang, H., and Anselmo, A. P., 1997, ''Transport Phenomena in Czochralski Crystal Growth Processes,'' Adv. Heat Transfer, **30**, pp. 313–435.
[131] Brown, R. A., 1988, ''Theory of Transport Processes in Single Crystal Growth from the Melt,'' AIChE J., **43**, pp. 881–911.
[132] Ostrach, S., 1982, ''Low-Gravity Fluid Flows,'' Annu. Rev. Fluid Mech., **14**, pp. 313–345.
[133] Guyene, T. D., and Hunt, J., eds., 1983, ''Materials Sciences Under Microgravity,'' *European Space Agency*, Rep. ESA-SP-191.
[134] Kamotani, Y., Ostrach, S., and Pline, A., 1994, ''Analysis of Velocity Data Taken in Surface Tension Driven Convection Experiment in Microgravity,'' Phys. Fluids, **6**, pp. 3601–3609.
[135] Xu, J., and Zebib, A., 1998, ''Oscillatory Two- and Three-Dimensional Thermocapillary Convection,'' J. Fluid Mech., **364**, pp. 187–209.
[136] Le Cunff, C., and Zebib, A., 1999, ''Thermocapillary-Coriolis Instabilities in Liquid Bridges,'' J. Phys. Fluids, **11**, pp. 2539–2545.
[137] Schwabe, D., 1999, ''Microgravity Experiments on Thermocapillary Flow Phenomena: Examples and Perspectives,'' Journal of Japanese Society of Microgravity Applications, **16**, pp. 1–6.
[138] Balasubramaniam, R., and Lavery, J. E., 1989, ''Numerical Simulation of Thermocapillary Bubble Migration Under Microgravity for Large Reynolds and Marangoni Numbers,'' Numer. Heat Transfer, **16**, pp. 175–187.
[139] Mundrane, M., Xu, J., and Zebib, A., 1995, ''Thermocapillary Convection in a Rectangular Cavity with a Deformable Interface,'' Adv. Space Res., **16**, pp. 41–53.
[140] Wang, G. X., and Prasad, V., 2000, ''Rapid Solidification: Fundamentals and Modeling,'' Annu. Rev. Heat Transfer, **11**, pp. 207–297.
[141] Bian, X., and Rangel, R. H., 1996, ''The Viscous Stagnation-Flow Solidification Problem,'' Int. J. Heat Mass Transf., **39**, pp. 3581–3594.
[142] Delplanque, J. P., and Rangel, R. H., 1998, ''A Comparison of Models, Numerical Simulation, and Experimental Results in Droplet Deposition Processes,'' Acta Mater., **46**, pp. 4925–4933.
[143] Bussmann, M., Mostaghimi, J., and Chandra, S., 1999, ''On a Three-Dimensional Volume Tracking Method of Droplet Impact,'' Phys. Fluids, **11**, pp. 1406–1417.
[144] Pasandideh-Fard, M., Bhola, R., Chandra, S., and Mostaghimi, J., 1998, ''Deposition of Tin Droplets on a Steel Plate: Simulations and Experiments,'' Int. J. Heat Mass Transf., **41**, pp. 2929–2945.
[145] Delplanque, J. P., Cal, W. D., Rangel, R. H., and Lavernia, E. J., 1997, ''Spray Atomization and Deposition of Tantalum Alloys,'' Acta Mater., **45**, pp. 5233–5243.
[146] Ahmed, I., and Bergman, T. L., 1999, ''Thermal Modeling of Plasma Spray Deposition of Nanostructured Ceramics,'' Journal of Thermal Spray Technology, **8**, pp. 315–322.